SAIMM URANIUM CONFERENCE 2026

19-20 AUGUST 2026
SWAKOPMUND HOTEL AND ENTERTAINMENT CENTRE, SWAKOPMUND, NAMIBIA

Langer Heinrich Uranium

Harmony Gold mining company – South Uranium plant, ion-exchange plant

18 August 2026 – Workshop
19-20 August 2026 – Conference
21 August 2026 – Technical Visit

ECSA and SACNASP Validated CPD Activity Credits = 0.1 per hour attended

SAIMM
THE SOUTHERN AFRICAN INSTITUTE OF MINING AND METALLURGY

Proceeding Book

SAIMM
THE SOUTHERN AFRICAN INSTITUTE OF MINING AND METALLURGY

THE SOUTHERN AFRICAN INSTITUTE OF MINING AND
METALLURGY JOHANNESBURG 2026

SAIMM Uranium Conference 2026

19-20 August 2026
SWAKOPMUND HOTEL AND ENTERTAINMENT
CENTRE, SWAKOPMUND, NAMIBIA

SAIMM PUBLICATIONS

THE MONOGRAPH SERIES

M1 Lognormal-De Wijsian Geostatistics for Ore Evaluation
(2nd ed 1981) D.G. Krige

M2 An Introduction to Geostatistical Methods of Mineral Evaluation
(2nd ed 1981) J.-M.M. Rendu

M3 Principles of Flotation
(1982) (3rd imp. 1986) Edited by R.P. King

M4 Increased Underground Extraction of Coal
(1982) Edited by C.J. Fauconnier and R.W.O. Kersten

M5 Rock Mechanics in Mining Practice
(1983) (3rd imp. 1986) Edited by S. Budavari

M6 Assay and Analytical Practice in the South African Mining Industry
(1986) W.C. Lenahan and R. de L. Murray-Smith

M7 The Extractive Metallurgy of Gold in South Africa,
2 volumes (1987) Edited by G.G Stanley

M8 Mineral and Metal Extraction — An Overview
(1994) L.C. Woollacott and R.H. Eric

M9 Rock Fracture and Rockbursts—an illustrative study
(1997) Edited by W.D. Ortlepp

THE SPECIAL PUBLICATIONS SERIES

SP1 Proceedings, Underground Transport Symposium
(1986) Edited by R.C.R. Edgar

SP2 Backfill in South African Mines (1988)

SP3 Treatment and Re-use of Water in the Minerals Industry (1989)

SP4 COREX Symposium 1990
(1990) Edited by H.M.W. Delport and P.J. Holaschke

SP5 Measurement, Control, and Optimization in Mineral Processing
(1994) Edited by H.W. Glen

SP6 Handbook on Hard-rock Strata Control
(1994) A.J.S. Spearing

SP7 Rock Engineering for underground coal mining
(2002) J. Nielen van der Merwe and Bernard J. Madden

SP8 Second Edition: Rock Engineering for underground coal mining
(2010) J. Nielen van der Merwe and Bernard J. Madden

SP9 Theoretical Rock Mechanics for Professional Practice
(2016) M. Handley

SP10 Johannesburg and its Holey Mining Heritage 2021
(2021) T.R. Stacey

SP11 Mineral and Metal Extraction — An Overview
(2021) L.C. Woollacott and R.H. Eric

SP12 The Fall of a Giant: The story of the disintegration of the South African Mining Industry
(2022/2023) Dr I. Robinsoin

SP13 COMRO's Legacy: Research and Development of Stoping Mining Machinery and Technologies
(2023) B. Protheroe

SUPPLEMENT TO THE SAIMM JOURNAL

The Metals and Minerals Industry in South Africa - Part 1 (1989)
Edited by H.W. Glen

THE SYMPOSIUM SERIES

S1 Mathematical Statistics and Computer Applications in Ore Valuation (1966)

S2 Planning Open Pit Mines (1970) (4th imp.)
Edited by P.W.J. van Rensburg

S3 Application of Computer Methods in the Mineral Industry (APCOM 1973) Edited by M.D.G. Salamon

S4 Infacon 1974 Edited by H.W. Glen

S5 Proceedings of the 12TH CMMI Congress 2 volumes (1982)
Edited by H.W. Glen

S6 Rockbursts and Seismicity in Mines (1984)
Edited by N.C. Gay and E.H. Wainwright

S7 The Planning and Operation of Open Pit and Strip Mines (1986) Edited by J.P. Deetlefs

S8 GOLD 100: Proceedings of the International Conference on Gold (1986)
Volume 1: Gold Mining Technology
Edited by H. Wagner and R.P. King
Volume 2: Extractive Metallurgy of Gold
Edited by C.E. Fivaz and R.P. King
Volume 3: Industrial Uses of Gold
Edited by G. Gafner and R.P. King

S9 APCOM 87: Proceedings of the Twentieth International Symposium on the Application of Computers and Mathematics in the Mineral Industries (1987)
Volume 1: Mining
Edited by L. Wade, R.W.O. Kersten and J.R. Cutland
Volume 2: Metallurgy
Edited by R.P. King and I.J. Barker
Volume 3: Geostatistics
Edited by I.C. Lemmer, H. Schaum and F.A.G.M. Camisani-Calzolari

S10 International Deep Mining Conference (1990)
Volume 1: Innovations in Metallurgical Plant
Edited by G.A. Brown and P. Smith
Application of Materials Engineering in the Mining Industry
Edited by B. Metcalfe
Volume 2: Technical Challenges in Deep Level Mining
Edited by D.A.J. Ross-Watt and P.D.K. Robinson

S11 Infacon 6 (Incorporating Incsac) (1992)
Edited by H.W. Glen

S12 Massmin 92
Edited by H.W. Glen (out of print)

S13 Minefill 93
Edited by H.W. Glen

S14 XVTH CMMI Congress Publications (1994)
Volume 1: Mining
Edited by H.W. Glen
Volume 2: Metals Technology and Extractive Metallurgy (1994) Edited by H.W. Glen

S15 Surface Mining 1996
Edited by H.W. Glen

S16 Hidden Wealth (1996)
Edited by H.W. Glen

S17 Heavy Minerals 1997
Edited by R.E. Robinson

S18 The 8TH International Platinum Symposium (1998)

S19 Mining in Africa '98

S20 Extraction Metallurgy Africa '98

S21 Sixth International Symposium for Rock Fragmentation by Blasting (1999)

S22 Metallurgy Africa '99

S23 Heavy Minerals 1999
Edited by R.G. Stimson

S24 Tunnels under Pressure
Technical Editor T.R. Stacey

S25 Mine Hoisting 2000

S26 Coal–The Future (2000)

S27 The Fifth International Symposium on Rockburst and Seismicity in Mines (RaSim 5) (2001)

S28 6TH International Symposium on Mine Mechanization and Automation (2001)

S29 XIV International Coal Preparation Congress and Exhibition

S30 Surface Mining 2002—Modern Developments for the New Millennium

S31 IFSA 2002, Industrial Fluidization South Africa

S31a APCOM 2003—Application of Computers and Operations Research in the Minerals Industries

S32 ISSA/Chamber of Mines Conference—Mines and Quarries: Prevention of Occupational Injury and Disease

S33 ISRM—Technology Roadmap for Rock Mechanics

S34 Heavy Minerals Conference 2003

S35 Safety in Mines Research Institutes (2003)

S36 VII International Conference on Molten Slags, Fluxes & Salts (2004)
Tenth International Ferroalloys Congress INFACONX 2004

S37 Deep and high stress mining 2004

S38 'Platinum adding value' 2004

S39 Base Metals—Southern Africa's response to changing global base metals market dynamics 2005

S40 Strategic versus Tactical approaches in mining 2005

S41 Best practices in rock engineering SARES 2005

S42 IFSA 2005, Industrial Fluidization South Africa

S43 Southern African Pyrometallurgy 2006 International Conference

S44 Stability of rock slopes in open pit mining and civil engineering situations

S45 'Platinum Surges Ahead' 2006

S46 Hydraulic Transport of Solids - Hydrotransport 17 (2007)

S47 Fourth Southern African Base Metals Conference 'Africa's base metals resurgence'

S48 Heavy Minerals Conference, 2007

S49 Cave Mining Conference, 2007

S50 International Symposium on Lead and Zinc processing – Lead & Zinc 2008

S51 Surface Mining 2008

S52 Platinum in transformation 2008

S53 IFSA 2008, Industrial Fluidization South Africa

S54 Hydrometallurgy Conference 2009

S55 Shotcrete for Africa 2009

S56 Base Metals Conference 2009

S57 Heavy Minerals Conference, 2009

S58 Hard Rock Safe—Safety Conference 2009

S59 Sampling and Blending 2009

S60 World Gold 2009 Conference

S61 Physical Beneficiation Conference 2010

S62 Second Hardrock Safe—Safety Conference 2010

S63 Platinum in Transition 'Boom or Bust' 2010

S64 South African Pyrometallurgy 2011 International Conference

S65 Minefill 2011 (10TH International Symposium on Mining with Backfill)

S66 Base Metals Conference 2011

S67 MineSafe 2011 Conference

S68 Iron Ore and Manganese Ore Metallurgy 2011

S69 Percolation leaching: The status globally and in Southern Africa 2011

S70 IFSA 2011, Industrial Fluidization South Africa

S71 Southern Hemisphere International Rock Michanics Symposium 2012

S72 Platinum Conference 'A catalyst for change' 2012

S73 Ferrous 2012—Ferrous and Base Metals Development Network Conference

S74 Diamonds - Source to use 2013

S75 Sampling and analysis: Best-practice in African mining 2013

S76 Base Metals Conference 2013

S77 Precious Metals 2013 Conference—The Precious Metals Development Network (PMDN)

S78 Physical Beneficiation 2013 Conference

S79 21st Century challenges to the southern African coal sector 2014

S80 Furnace Tapping Conference 2014

S81 Platinum Conference 'Platinum—Metal for the Future' 2014

S82 IFSA 2014, Industrial Fluidization South Africa

S83 Copper Cobalt Africa 2015

S84 The Danie Krige Geostatistical Conference 2015 - Vol. 1

The Danie Krige Geostatistical Conference 2015 - Vol. 2

S85 World Gold Conference 2015

S86 Slope Stability 2015

S87 2nd Annual Young Professionals Conference 2015

S88 AMI–Nuclear Materials Development Network 2015

S89 MPES–23rd International Symposium on Mine Planning & Equipment Selection 2015

S90 Diamonds still Sparkling Conference 2016

S91 The SAMREC/SAMVAL Companion Volume Conference 2016

S92 New Technology and Innovation in the Minerals Industry Colloquium 2016

S93 Theoretical Rock Mechanics for Professional Practice (Special Publications Series 9) by M. Handley - 2016

S94 Hydrometallurgy Conference 2016

S95 10TH Heavy Minerals Conference 2016

S96 MineSafe Conference 2016

S97 AMI-Ferrous and Base Metals Development Conference 2016

S98 3rd Young Professionals Conference 2017

S99 Proximity Detection and Collosion Avoidance Systems in Mining Colloquium 2017

S100 6TH Sulphur and Sulphuric Acid Conference 2017

S101 Mine Planning Colloquium 2017

S102 Chrome Colloquium 2017

S103 4TH Mineral Project Valuation Colloquium 2017

S104 Water Conference 2017

S105 Rapid Underground Mine and Civil Access Engineering 2017

S106 MineSafe Conference 2017

S107 Uranium 2017 International Conference 2017

S108 IFSA 2017–Industrial Fluidization Conference 2017

S109 AfriRock 2017–ISRM International Symposium 2017

S110 AMI Precious Metals 2017–The Precious Metals Development Network (PMDN) Symposium

S111 7TH International Platinum Conference 2017

S112 Infacon XV: International Ferro-Alloys Conrgress 2018

S113 SOMP–Society of Mining Professors 6TH Regional Conference 2018

S114 Digitalization in Mining Conference 2018

S115 Diamonds – Source to Use 2018 Conference 2018

S116 The 9TH Southern African Base Metals Conference 2018

S117 Geometallurgy Conference 2018

S118 Mine Safe Technical Conference and Industry Day 2018

S119 ASM Conference 2018

S120 4TH Young Professionals Conference 2018

S121 Furnace Tapping 2018 Conference 2018

S122 7TH Sulphur and Sulphuric Acid Conference 2019

S123 Mine Planner's Colloquium 2019

S124 9TH International Conference on Deep & High Stress Mining 2019

S125 New Technology Conference and Trade Show 2019

S126 Smart Mining Smart Environment Smart Society Conference 2019

S127 The Eleventh International Heavy Minerals Conference 2019

S128 Surface Mining Masterclass 2019

S129 International Mine Health and Safety Conference 2019

S130 Tailings Storage Conference 2020

S131 IMPC2020 XXX International Mineral Processing Congress

S132 Johannesburg and its Holey Mining Heritage (Special Publications Series 10) by T.R. Stacey - 2021

S133 Mineral and Metal Extraction – An Overview (Special Publications Series 11) by L.C. Woollacott and R.H. Eric - 2021

S134 Diamonds - Source to Use - 2021 Online Conference 2021

S135 WorldGold Online Conference 2021

S136 APCOM 2021 Minerals Industry4.0-The next digital transformation in mining

S137 5TH Young Professionals Online Conference 2021

S138 Southern African Rare Earths International Online Conference 2021

S139 SAMCODES Conference 2021

S140 Global Tailings Standards and Opportunities`For the Mine of the Future Conference 2022

S141 The Fall of a Giant: The story of the disintegration of the South African Mining Industry (Special Publications Series 12) by I. Robinson - 2022/2023

S142 Battery Materials Conference 2022

S143 32ND SOMP Annual Meeting and Conference 2022

S144 SDIMI (Sustainable Development in the Minerals Industry) 10TH International Conference 2022

S145 THANOS International Conference 2022

S146 Mine Impacted Water Online Conference 2022 (Abstract Book Only)

S147 8TH International PGM Conference 2022

S148 SANCOT Symposium 2022

S149 8TH Sulphur and Sulphuric Acid Conference 2023

S150 Southern African Hydrogen and Fuel Cell Conference 2023

S151 COMRO's Legacy: Research and Development of Stoping Mining Machinery and Technologies (Special Publications Series 13) by B. Protheroe - 2023

S152 Copper Cobalt Africa in Association with The 10TH Southern African Base Metals Conferenc 2023

S153 Digital Transformation in Mining Conference 2023

S154 Diamonds Source to Use 2023 Online Conference

S155 12TH International Heavy Minerals Conference 2023

S156 Geometallurgy Conference 2023

S157 Next Generation Tailings Opportunitiy or Risk? Conference 2023

S158 6TH Young Professionals Conference 2023

S159 Southern African Pyrometallurgy 2024 International Conference

S160 The 11TH World Conference of Sampling and Blending 2024

S161 SANIRE Symposium 2024 Technical Applications in Rock Engineering

S162 2ND International Conference 2024 Southern African Rare Earths

S163 2ND Battery Materials Conference 2024

S164 Hydrometallurgy Conference 2024

S165 Environmental Social Governance Sustainability Conference 2024

S166 MineSafe Mine Health and Safety Conference 2024

S167 Mintek@90 Conference 2024

S168 Mine Closure Conference 2025

S169 2ND Southern African Hydrogen and Fuel Cell Conference 2025

S170 9TH Sulphur and Sulphuric Acid Conference 2025

S171 4TH Digital Transformation in Mining Conference 2025

S172 AfriRock 2025 Pioneering Progress Conference

S173 Thirteen International Heavy Minerals Conference 2025

S174 International Mineral Asset Valuation Conference 2025

S175 Geometallurgy Conference 2025

S176 9TH International PGM Conference 2025

S177 MineSafe Conference 2025

S178 Tailings Conference 2026 - Where to Now?

S179 SANCOT SYMPOSIUM Conference 2026

S180 Pyrometallurgy International Conference 2026

S190 SANIRE SYMPOSIUM 2026

S200 Critical Minerals Conference 2026

Published by The Southern African Institute of Mining and Metallurgy
Minerals Council South Africa, 7th Floor, Rosebank Towers, 19 Biermann Avenue,
Rosebank, 2196, Republic of South Africa

ISBN 978-0-6398821-2-3

The abstracts in this volume have been for the most part prepared from Word documents supplied by the authors, with additional typesetting and formatting by The Southern African Institute of Mining and Metallurgy.

Organising Committee

J. van Deventer-Conference Chair
S. Archer
D. Auerswald
O. Bazhko
J. Brown
T. Kotze
E. Pobe

Reviewers

O. Bazhko
M. Bower
J. Brown
S. Burelli
A. Lombard
W. Marx
G. Ndlovu
S. Scott
A. Tapfuma
J. van Deventer
P. van Staden
K. Voogt
O. Yahorava

Desktop prepared by SAIMM

FOREWORD

It is my great pleasure and privilege to introduce the proceedings of the Southern African Institute of Mining and Metallurgy (SAIMM) Uranium Conference 2026.

Uranium already forms part of a reliable and low-emission energy mix in many countries, contributing significantly to global decarbonisation efforts. With demand for clean and dependable energy expected to increase in the coming decades, nuclear energy is poised to assume an even more important role. This is the perfect time to bring together professionals from across the uranium value chain to exchange ideas, share experiences and discuss the future of the industry.

Namibia is one of the world's leading uranium-producing nations and it is thus only fitting to have this conference in the beautiful town of Swakopmund – the heart of Namibia's uranium mining industry. Speakers and delegates from all corners of the world contributed, emphasising the truly global nature of the industry.The papers and presentations in these proceedings cover a wide range of topics relevant to uranium exploration, mining, processing and environmental stewardship.

Starting with a sound understanding of the geology of any deposit is critical to the success of the project. Equally important is the effective management of radioactivity, both during mining and processing, to ensure the safety of personnel and equipment. Continuous improvement of existing processes is essential, and it is good to see that there is no shortage of innovation in this area. Topics range from optimising the productivity of the haul-truck fleet, to minimising reagent consumption, increasing the understanding of each unit operation to allow tweaking of the flowsheet, and improving the purity of the final product.

I would like to thank everyone who has contributed to the success of this event. My sincere appreciation goes to our sponsors, for their invaluable support. Thank you also to the SAIMM team, for their organisational skills and dedication. And a huge thank you to every speaker and delegate, without whom events like these would not be possible.

On behalf of the organising committee, I wish you a great conference.

Johanna van Deventer,
Chairperson: Organising Committee,
SAIMM Uranium Conference 2026

Contents

Page No

The organizers of the event wish to thank the following sponsors for their support

AECI MINING

ALS
right solutions.
right partner.

bme

CM solutions
metallurgical consultancy & laboratories

CYMOT
SINCE 1948

ECOLAB
Purolite™ Resins

EKATO

HATCH

Köppern

LANGER HEINRICH URANIUM

Paterson & Cooke
KNOWLEDGE | EXPERIENCE | PASSION

CNNC
Rössing Uranium
Working for Namibia

50
1976 - 2026

SCANMIN
ONLINE ANALYSERS

SGS

SkyGeo

wood.
a Sidara company

verni
speciality construction products

Management of iron level in yellow cake during uranium processing

M. Ramabulana, O. Bazhko

Mintek, South Africa

Mintek has conducted comprehensive research on uranium extraction to develop advanced processes and identify potential future developments. The primary aim of this research is to meet the increasing demand for uranium processing, which is driven by both current and future energy requirements. This initiative places a significant emphasis on evaluating existing methodologies for the extraction of uranium ores. Furthermore, an in-depth understanding of contaminant behaviour is critical for nuclear reactor performance and for ensuring the purity of final products, given the inherent challenges associated with uranium processing.

Iron is one of the most common impurities encountered in the uranium circuit. It can be separated through a range of processing techniques, including solvent extraction, ion exchange, nanofiltration, and precipitation. This impurity may originate from the ore itself or be introduced during various stages of processing. This paper aims to examine the behaviour of iron at each stage of uranium processing, as well as the operational techniques designed to reduce its concentration to acceptable levels in the final concentrate.

Keywords: Ion exchange, Iron impurity, Membrane technology, Precipitation, Solvent extraction, Yellow cake

INTRODUCTION

The final product of uranium metallurgical processing is known as yellow cake, a concentrate with high uranium content and high purity, suitable to meet the requirements of the nuclear fuel industry. This is because the efficiency of nuclear fuel operation decreases if the fuel contains impurities that capture neutrons. Impurity levels in yellow cake are regulated by ASTM standards and converter specifications. According to ASTM C 967-20, the maximum allowable concentration of Fe in the concentrate is 1%. ConverDyn only accepts material with ≤0.5% Fe.

The process flowsheets for yellow cake production and iron behaviour during each processing step are discussed in this paper. In addition, various strategies to minimise the iron level in the final product are investigated.

Uranium processing

The typical flowsheet for uranium processing from ore comprises comminution, leaching, solid/liquid separation, purification via ion exchange and/or solvent extraction, and precipitation of the final product, as indicated in Figure 1.

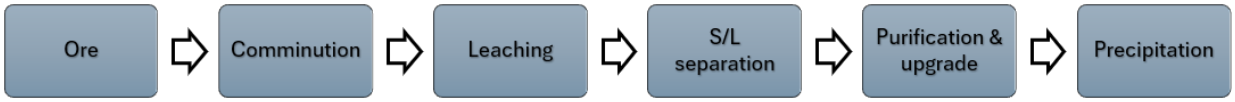

Figure 1. Typical uranium processing flowsheet.

Leaching

Uranium mineralisation varies significantly from deposit to deposit, and each operation is designed to fit the specific characteristics of its ore. Nevertheless, the most common leaching technique for uranium extraction is acidic leaching with sulfuric acid used as lixiviant. The presence of tetravalent uranium with a low solubility in diluted acid requires oxidation to the hexavalent state (Lunt, 2007).

Iron is generally present as a common constituent in the ore present in the form of carbonates, oxides, partially soluble silicates, and sulfide minerals. It can be introduced as metallic iron because of wear and abrasion in the grinding circuit. Iron can also be added on demand, such as in acidic leach, where ferric iron acts as the principal oxidant of tetravalent uranium (Venter & Boylett, 2009).

The mechanism for the dissolution of uranium in sulfuric acid is based on the Fe^{3+}/Fe^{2+} couple, facilitating the leach process by acting as the electron transfer agent during oxidation according to the following reaction. The ferric oxidises the tetravalent uranium to the soluble hexavalent uranium while being reduced to ferrous:

$$U^{4+} + 2\ Fe^{3+} \rightarrow U^{6+} + 2\ Fe^{2+} \qquad (1)$$

With MnO_2 added as an oxidant, ferric is regenerated:

$$2\ Fe^{2+} + MnO_2 + 4\ H^{+} \rightarrow 2\ Fe^{3+} + Mn^{2+} + 2\ H_2O \qquad (2)$$

A ferric concentration of approximately 1 to 2 g/L is usually considered adequate for the effective dissolution of uranium. A minimum requirement of 0.5 g/L was suggested by Merritt (1971).

Iron concentration in the pregnant leach solution (PLS) is typically between 1 and 4 g/L, but can reach 10-12 g/L and higher, due to recirculation. Ferric in the sulfuric acid pregnant leach solution exists in the form of an anionic $Fe(SO_4)_2^-$ species, like uranium, and can follow uranium in different processing steps, contaminating the final product.

Purification and upgrade

The leached solution composition will essentially be determined by the mineralogy of the ore and the leaching medium. Depending on the solution composition, several upgrade and purification combinations may be applicable. For example, the alternatives can include the processing steps shown in Figure , selected based on the feed solution analyses and grade of product required (Uranium extraction technology, 1993).

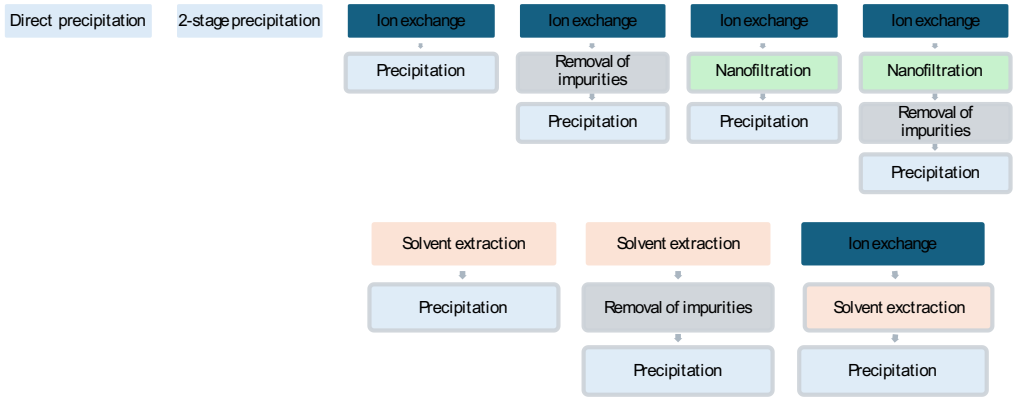

Figure 2: U downstream processing.

The composition of the uranium concentrate produced using various approaches can vary significantly.

Ion exchange

A significant amount of uranium has been produced using strong-base ion-exchange as the primary method of upgrade and purification. Prior to 1980, the plants in South Africa and Canada mainly used strong-base ion-exchange in fixed-bed downflow column contactors to treat semi-clarified sulfuric acid leach liquor (Boydell, 1980). Resin-in-pulp systems are also utilised by the uranium industry; these systems require a large-size resin bead to facilitate resin/pulp separation, but the resins have the same functionality as those used in fixed-bed applications, and purification available from RIP systems is essentially the same as that offered by conventional means.

Strong base Type I resins with quaternary ammonium groups were the first ion exchange resins used for uranium recovery and remain the resin of choice in the industry (Bibler, 1990). Adsorption of uranium from an acidic sulfate solution is based on the following reactions (where R depicts the backbone of the resin):

$$R_2SO_4 + UO_2(SO_4)_2^{2-} = R_2UO_2(SO_4)_2 + SO_4^{2-} \quad (3)$$

$$2\ R_2SO_4 + UO_2(SO_4)_3^{4-} = R_4UO_2(SO_4)_3 + 2\ SO_4^{2-} \quad (4)$$

From diluted sulfate solutions at pH < 2, uranium is adsorbed as $UO_2(SO_4)_3^{4-}$ (McGarvie, 1981). An increase in pH to the value of 3-3.5 results in improved uranium extraction due to loading of $[UO_2(SO_4)_2]^{2-}$, $[U_2O_5(SO_4)_3]^{4-}$ and $[U_2O_5(SO_4)_2]^{2-}$ (Zontov, 2006).

The selectivity with which strong-base anion exchange resins absorb uranyl sulfate complexes from solution is well documented. A typical affinity series is given below for the acid leach process (McGarvye, 1981):

$$V_2O_7^{4-} > MO_8O_{26}^{4-} > UO_2(SO_4)_3^{4-} > UO_2(SO_4)_2^{2-} > Fe(OH)(SO_4)_2^{2-} > SO_4^{2-} > Fe(SO_4)_2^{-} > NO_3^{-} > HSO_4^{-} > CI^{-}$$

Ferrous is not loaded onto the uranium resins, while ferric can be adsorbed in the form of an anionic species. Ferric loading onto the resin depends on its concentration in solution relative to other ions as well as pH (Nascimento, 2004). Sharafutdinov (2024) evaluated ferric loading onto anion exchanger BO 020. The loading increased with an increase in Fe concentration in the liquid phase. At pH 1.2, the resin loaded 4 mg/g Fe from the solution containing 18 g/L Fe. Work conducted at Mintek (Yahorava, 2010) showed that A 4400 resin was loaded with 28 g/L U and 5.3 g/L Fe after batch contact with the liquor containing 0.51 g/L U and 2.1 g/L Fe at pH 1.8 and a solution:resin ratio of 1:100.

Loaded resin is typically eluted with 1 M to 2 M acid (sulfuric, nitrate, chloride), or carbonate (McGarvye, 1981). Iron follows uranium in the elution process.

To decrease the iron content in the eluate, a split elution can be applied. The iron-rich first fraction of the eluate can be removed and returned to the leach circuit. However, a significant amount of uranium can also report to this fraction. Work was done at Mintek, eluting A4400 resin pre-loaded to 41.2 g/L U, 0.43 g/L Fe using 110 g/L H_2SO_4. It showed that only 40% Fe can be removed with 1 bed volume (BV) of the elunt without losing U, while 84% Fe removal was accomplished with 2.5 BVs of the elunt, but also stripping 32% of the U in the same fraction.

Another approach is ferric scrubbing with diluted acid before uranium stripping. Scrubbing can be done in a batch or column. Alfredson (1980) reported that at the Mary Kathleen operation, an initial flush with 1.25 BVs of dilute sulfuric acid (pH 1), which targeted the removal of the adsorbed rare earths, also removed some of the absorbed ferric iron. Peganov reported that column treatment of the resin loaded with 6.9 % U and 0.62 % Fe using x BVs of 3% H_2SO_4 resulted in the removal of 60-63% Fe with U loss to the scrub liquor of 0.5%; after this pre-treatment, the U eluate contained less than 20 mg/L Fe (Peganov, 2014).

Mintek conducted a test work programme targeting the optimisation of scrubbing conditions. Figure 3 shows results for the A500 resin, pre-loaded to 20 g/L U and 0.7 g/L Fe, scrubbed in a column using a liquor with 2, 5, 15, 20, and 25 g/L H_2SO_4. As the acid concentration increased, more Fe was scrubbed per BV of acid, but at 2 g/L H_2SO_4, the acid was too weak to have a significant impact on the removal of Fe. The highest Fe peak achieved was at an acid concentration of 10 g/L.

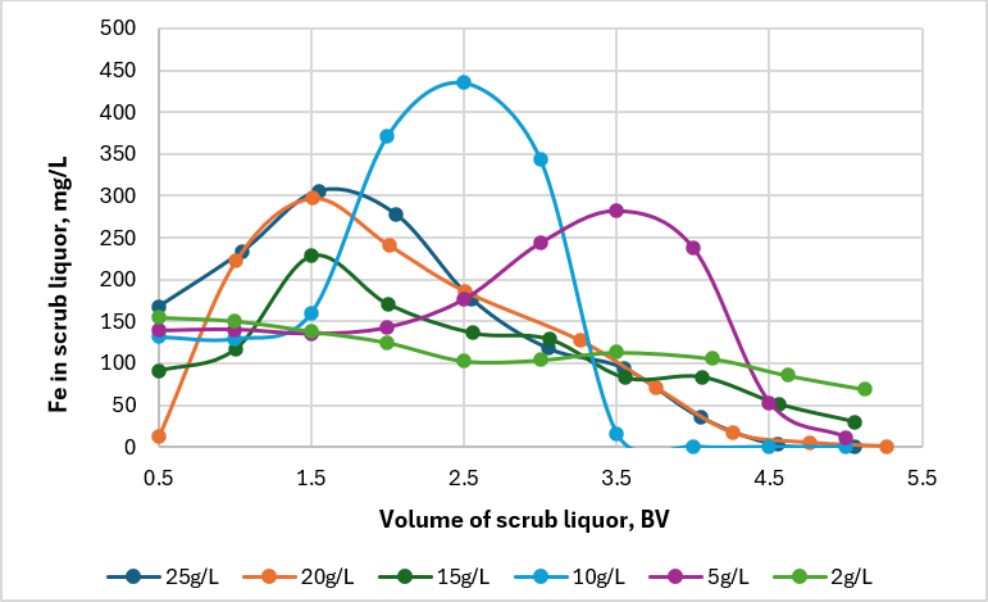

Figure 3: Fe scrub results for A500 macroporous resin.

Table I shows the percentage of uranium and iron stripped at the different acid concentrations tested on A500 resin pre-loaded to 20 g/L U and 0.7 g/L Fe, and A600 resin pre-loaded to 14.3 g/L U and 1.4 g/L. The tests were performed under ambient conditions in fixed-bed columns using H_2SO_4 at concentrations of 2, 5, 10, 15, 20, and 25 g/L as the eluent. The acid was passed through the resin bed at a flow rate of ±2 BV/h using a peristaltic pump. Samples of the eluate were taken every 0.5 BV for analysis. Once 5 BV of the H_2SO_4 eluate had passed through the resin bed, the test was stopped, and the resin was washed with de-ionised water.

The scrubbing of Fe from the macroporous A500 resin appeared to be more efficient than for the gel type A600 resin. Although an increase in acid concentration increased the amount of Fe scrubbed from the resin, the amount of uranium that was eluted in the process also increased.

Table I: Uranium stripped during Fe scrub tests

Resin	**Gel type A600**		**Macroporous A500**	
H_2SO_4 concentration, g/L	Uranium	Ferric	Uranium	Ferric
	stripped			
2	0.13%	36%	0.25%	85%
5	0.35%	47%	1%	98%
10	**1.1%**	**67%**	**2%**	**96%**
15	1.4%	70%	4%	97%
20	3%	83%	9%	99%
25	4%	79%	13%	99%

More uranium was co-eluted together with iron from the Macroporous resin in comparison to the gel type; however, its scrubbing efficiency was much higher. The optimum H_2SO_4 concentration necessary for the removal of Fe from uranium-loaded resin was 10 g/L, as the maximum amount of Fe was stripped with minimal uranium losses.

The HIMIX process was developed for impurity removal from the loaded uranium resin. The process included contacting resin with a portion of high-grade eluate that has been pretreated to adjust the pH to around 3.5. During this prior adjustment of the eluate with lime or powdered limestone, some sulfates were precipitated as gypsum, while iron and other contaminants precipitated as hydroxides. Purified eluate effectively displaced impurities from the loaded resin. The process also enabled the resin to load uranium to a very high level (90-120 g/L) due to the formation of uranium ions such as $UO_2(SO_4)_2^{2-}$ and $U_2O_5(SO_4)_3^{4-}$ (Himsley, 1980).

A set of conditioning tests was conducted at Mintek to remove impurities and load additional uranium. A solution containing 31.2 g/L U and ~0.1 M sulfate at pH 3.5 was contacted with resin that had been preloaded with 28 g/L U and 5.3 g/L Fe (U/Fe ratio on the resin of 5.3) at different solution-to-resin ratios. Figure 4 shows uranium and iron loading at different solution/resin ratios and pH behaviour. Uranium adsorption onto the resin and the final pH increased with an increase in the ratio of solution/resin , while iron was displaced by uranium from the resin. The best iron displacement (the main impurity in uranium plants) was achieved at a solution/resin ratio of 2, bringing the U/Fe ratio on the resin to 78.5. Poorer iron displacement with a larger volume of conditioning liquor could be due to its precipitation inside the resin bead at relatively high pH (Yahorava, 2010). A combination of scrubbing and conditioning can produce an eluate with only traces of Fe (Peganov, 2014).

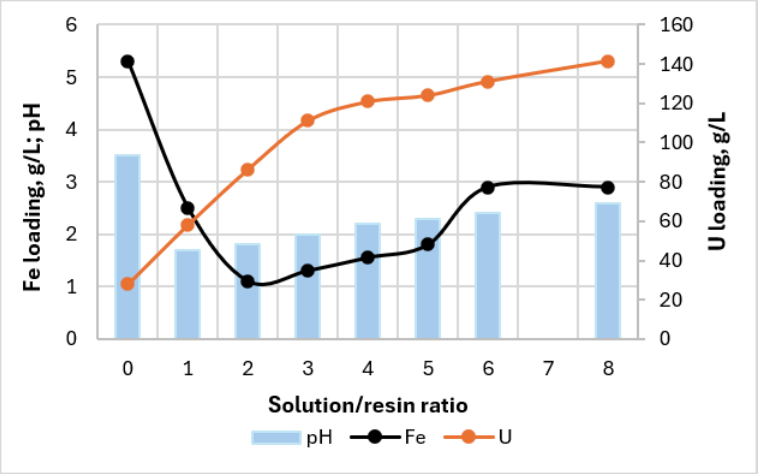

Figure 4: Pre-conditioning based on a Himsley process.

Solvent extraction

Solvent extraction is also often used in uranium processing for U upgrade and purification. Tertiary amines, such as Alamine 336, have been the most widely used anion extractants for the recovery of uranium from sulfuric acid leach liquors. Figure 5 shows the mixer-settlers operated for uranium extraction at Mintek.

Figure 5: Mintek SX mini-plant.

The equation describing the extraction of uranium by protonated tertiary amines is (where R_3N depicts the structure of the organic):

$$2(R_3NH)_2SO_{4\ or} + UO_2(SO_4)_3^{4-}{}_{aq} \rightarrow (R_3NH)_4UO_2(SO_4)_{3\ org} + 2SO_4^{2-}{}_{aq} \qquad (5)$$

The impurities can be transferred from the PLS into the final product by either physical entrainment of the PLS (and crud) in the organic phase, and/or chemical transfer. Tertiary amines are relatively selective for uranium. The selectivity order reported by Fleming (1981) is:

$$UO_2(SO_4)_n^{(2n-2)-} > NO_3^- >> Cl^- > HSO_4^- > SO_4^{2-} >> Fe(SO_4)_2^-$$

this is not an equation and therefore has no a number.

Iron contamination of the loaded organic is mainly due to entrainment and typically occurs in small quantities. Crane (2010) reported that from a PLS containing 0.42 g/L U and 5 g/L Fe (U/Fe ratio of 0.084), the loaded organic contained 16.95 g/L U and 0.05 g/L Fe (U/Fe ratio of 339). Khanramaki (2018) reported that from a PLS with 0.24 g/L U and 1.1 g/L Fe (U/Fe ratio of 0.218), the loaded organic contained 0.23 g/L U and 0.15 g/L Fe (U/Fe ratio of 1.53).

Stripping with sodium chloride and ammonium chloride, carbonate or sulfate is often used for U removal from the organic phase (Boydell, 1980). Before stripping, the loaded organic can be subjected to scrubbing to remove impurities that are less strongly held than uranium, such as iron. Diluted acid scrub at pH 1.5-1.8 is effective for iron removal.

Nanofiltration

A nanofiltration (NF) step can be introduced to concentrate uranium and recover sulfuric acid from an ion exchange eluate solution. The application of NF for acid recovery in uranium processing is a relatively new development (Cameron & Edwards, 2012). An acid recovery of 35% was obtained in their study due to osmotic pressure limiting the overall recovery (concentrations as high as 85 g/L U were reached). Recently, many more studies were conducted in this field.

NF membranes restrict the transport of multivalent ions by taking advantage of the Donnan (charge) exclusion and size exclusion properties (molecular weight cutoff, MWCO = 80–2000 Da). Thus, it is expected that Fe will also report to the U concentrate. NanoPro A–30121 membrane with 180 Dalton cut-off weight, stable in high acid environment (pH 1–14), was tested on different U streams. The treatment goal was to concentrate uranium and recover acid. Nano filtration of the PLS from a heap leach operation containing 809 mg/L U and 19910 mg/L Fe resulted in a reporting of 98.5% U and 99.4% Fe to the retentate, at 60% volume collected. Using NF to treat the raffinate from a uranium solvent extraction operation, a major part of the U (97.6%) and Fe (99.1%) was removed from a raffinate containing 4.6 mg/L U and 17160 mg/L Fe (Herrmann, 2016). Approximately 30% of the acid in the raffinate was collected in the permeate and could be recycled.

Precipitation of impurities

The loaded strip liquor or eluate produced in the SX or IX circuit is subjected to the precipitation process. However, in some plants, the concentration of impurities is still too high to generate sufficiently pure uranium concentrate. An additional purification step may be required prior to uranium precipitation (Edwards, 2000).

Lime or magnesia is typically added to the uranium solution to produce a precipitate containing iron, calcium, thorium, rare earths, titanium, some occluded uranium, and other sulfates. If arsenic is present, it will be co-precipitated as ferric arsenate (Boydell, 1980). Purification is usually carried out at a pH between 1 and 4.

Using CaO, the effect of pH on Fe removal from the eluate containing 22.1 g/L U and 184 g/L acid, contaminated with Fe, was reported by Nazarov (2011). The precipitate obtained after acid pre-neutralisation with CaO to pH 1.15, followed by U precipitation with ammonia, contained 62% U and 1.6% Fe. When pre-neutralisation was done to pH 2.05, the yellow cake contained 66% U and 0.26% Fe. The advantage of CaO as a precipitation reagent is its low cost. In addition to that, the solid particles serve as coagulation centres for ferric hydroxide, enhancing the removal of iron. It was reported that an increase in temperature improves Fe precipitation efficiency and minimises U co-precipitation (Rowson, 1987).

U precipitation

Once a satisfactory solution purity has been achieved, the uranium concentrate is precipitated. A number of different precipitants, such as ammonia, magnesium oxide, sodium hydroxide, and hydrogen peroxide, have been found to be effective (Merrit, 1971). The type of precipitating reagent chosen can affect the quality of the product (Gupta, 2004). Figure 7 shows the U precipitation set-up used at Mintek.

Figure 7: U precipitation set-up.

The precipitation of ammonium diuranate with ammonia at pH 6-7 is the most commonly used and proceeds according to the following reaction:

$$2\ UO_2(SO_4)_3^{4-} + 6\ NH_3 + 3\ H_2O \rightarrow (NH_4)_2U_2O_7 + 6\ SO_4^{2-} + 4\ NH_4^+ \qquad (7)$$

Impurities present in the solution, such as Fe^{3+}, Al, Cu, Cr, and Th will co-precipitate with U; while Ca, Mg, Mn^{2+}, Fe^{2+}, Ni, and Co will stay in the solution. The sodium diuranate is formed based on the reaction:

$$2\ UO_2(SO_4)_3^{4-} + 2\ Na^+ + 6\ OH^- = Na_2U_2O_7 + 6\ SO_4^{2-} + 3\ H_2O \qquad (8)$$

The advantage of NaOH over ammonia is a lower cost and easier transportation.

Contamination with phosphate and vanadate can be eliminated at a pH above 10. The product is not pure enough due to high Na and other impurities precipitated at the high pH, to allow the sale of the product without incurring substantial penalties. Uranium can also be precipitated by adding milk of magnesia to a final pH value of between 7.0 and 7.5 according to the following reaction (Uranium extraction technology, 1993):

$$UO_2(SO4)_3^{4-} + MgO + H_2O = UO_3{\cdot}H_2O + 3\ SO_4^{2-} + Mg^{2+} \qquad (9)$$

The challenge of using magnesia is to obtain a suitable MgO reagent that could meet the requirements of high reactivity and purity, as impurities in the reagent would likely be transferred to the uranium concentrate (Rowson, 1987). Uranium peroxide precipitation is based on the reaction

$$UO_2(SO4)_3^{4-} + H_2O_2 + 2\ H_2O = UO_4{\cdot}2H_2O + 3\ SO_4^{2-} + 2H^+ \qquad (10)$$

This method is more expensive, but allows for the production of a cleaner precipitate. Typically, precipitation is done under the following conditions: pH=2.5-3.5; T= 40-45 C; U concentration 25-240 g/L; H_2O_2 110% of stoichiometric addition. Under these conditions, ferric co-precipitates with uranium. To minimise contamination with Fe, it is recommended to conduct the precipitation at pH < 2.2 (Litz, and Coleman, 1980).

CONCLUSIONS

Iron can affect uranium processing significantly. It is a common impurity in the uranium PLS. Moreover, ferric ion plays a crucial role in uranium acid leaching by acting as a primary oxidant to convert uranium into the hexavalent state. The presence of ferric in the leach is therefore desirable; ferric salts may even be added to the leach circuit to improve uranium extraction. The ferric in the sulfuric acid PLS exists in the form of an anionic complex species, similar to uranium, and can follow uranium in different processing steps, contaminating the final product.

The ion exchange process utilises strong base anion exchangers that are selective for uranium. However, ferric present in the solution co-loads onto the resin to a certain extent, depending on PLS composition and resin used. Aa few approaches have been developed to mitigate ferric levels in the IX circuit, including selective elution and scrubbing with diluted acid or pre-neutralised eluate.

Uranium purification via solvent extraction is often based on the use of tertiary amines, such as Alamine 336. This reagent does not extract ferric, but the contamination of the organic phase happens due to physical entrainment, and at low levels. Iron can be removed from the organic by a diluted acid scrub.

Nano filtration recently found implementation in the uranium circuit, mainly for reagent recovery. In the NF process, iron follows uranium and cannot be separated.

The ferric reporting to the uranium solution co-precipitates with uranium, regardless of precipitation method is used. To minimise contamination of the final concentrate with ferric impurities, an impurity removal step can be introduced by pre-neutralising the uranium solution to pH 1-4 with lime or magnesia.

The strategies mentioned above, or their combination, allows the production of yellow cake that meets the specifications of the nuclear industry.

REFERENCES

Alfredson, P.G. (1980). Australian experience in the production of yellow cake and uranium fluorides. Production of yellow cake and uranium fluorides. *Proceedings of an Advisory Group Meeting*, Paris, 5 - 8 June 1979. IAEA, Vienna, 1980. STI/PUB/553 ISBN 92-0-041080-4.

ASTM C 967-20 Specification for Uranium Ore Concentrate.

Bibler, J.P. (1990). Ion Exchange in the Nuclear Industry. Williams, P.A., Hudson, M.J. (eds) Recent Developments in Ion Exchange. Springer, Dordrecht. https://doi.org/10.1007/978-94-009-0777-513.

Boydell, D.W. (1980). Impurities in uranium process solutions. Production of yellow cake and uranium fluorides. *Proceedings of an Advisory Group Meeting*, Paris, 5 - 8 June 1979. IAEA, Vienna, 1980. STI/PUB/553 ISBN 92-0-041080-4.

Cameron, R. Edwards, C. (2012). Membrane technology applications in mineral processing. *Proceedings of the 44th Annual Canadian Mineral Processors Operators Conference*, Ottawa, Ontario, Canada, 17–19 January 2012.

Crane, P., Virnig, M., Bender, J., Mackenzie, M., and Dudley, K. (2010). Analysis and troubleshooting in uranium solvent extraction circuits. *Proceedings of ALTA Uranium Conference 2010*, Perth, Australia, 27-28 May 2010.

Edwards, C.R. Oliver, A.J. (2000). Uranium processing: A review of current methods and technology. *JOM* 2000, 52, 12–20, https://doi.org/10.1007/s11837-000-0181-2.

Fleming, C. A. (1981). The chemistry of uranium recovery from leach solutions. Johannesburg, South African Institute of Mining and Metallurgy, Vacation School, Uranium Ore Processing, Jul. 1981.

Gupta, R., Pandey, V.M., Pranesh, S.R., Chakravarty, A.B. (2004). Study of an improved technique for precipitation of uranium from eluted solution, *Hydrometallurgy*, Volume 71, Issues 3–4, p. 429-434, ISSN 0304-386X, https://doi.org/10.1016/S0304-386X(03)00116-6.

Herrmann, J. (2016). Nano-filtration technology in optimizing uranium process efficiency. *Proceedings of ALTA 2016 Uranium-REE Conference*, Perth, ALTA Metallurgical Services, Australia (21–28 May 2016).

Himsley, A. (1980). Production of pure yellow cake by ion-exchange processes employing sulphate elution. Production of yellow cake and uranium fluorides. *Proceedings of an Advisory Group Meeting*, Paris, 5 - 8 June 1979. IAEA, Vienna, 1980. STI/PUB/553 ISBN 92-0-041080-4.

Khanramaki, F., Safdari, J., Shirani, A. S., and Torkaman, R. (2018). Investigations on the complete removal of iron(III) interference on the uranium(VI) extraction from sulfate leach liquor using Alamine 336 in kerosene. *Radiochimica Acta*, 106(8), 631–643. doi:10.1515/ract-2017-2906.

Litz, J.E., Coleman, R.B. (1980). A review of the United States yellow cake precipitation practice. Production of yellow cake and uranium fluorides. *Proceedings of an Advisory Group Meeting*, Paris, 5 - 8 June 1979. IAEA, Vienna, 1980. STI/PUB/553 ISBN 92-0-041080-4.

Lunt, D., Boshoff, P., Boylett, M. and El-Ansary, Z. (2007). Uranium extraction: the key process drivers. *The Journal of The Southern African Institute of Mining and Metallurgy*, v. 107, p. 419-426.

McGarvey, F. X. and Ungar, J. (1981). The influence of resin functional group on the ion-exchange recovery of uranium. *Journal of the South African Institute of Mining and Metallurgy*, p. 93-100.

Merritt, R. C. (1971). *The Extractive Metallurgy of Uranium*, Colorado School of Mines Research Institute. Chicago.

Nascimento, M. R. L., Fatibello-Filho, O., and Teixeira, L. A. (2004). Recovery of uranium from acid mine drainage waters by ion exchange. *Mineral Processing and Extractive Metallurgy Review*, 25(2), 129–142. doi:10.1080/08827500490433197.

Nazarov, K. M., Khakimov, N., Mirsaidov, I. U., Akhmedov, M. Z., and Mirsaidov, U. (2011). Precipitation of ammonium diuranate (p. 4 p.). *Proceedings of Seminar on '2011 International Year of Chemistry' and 'Radiation Safety of Tajikistan'*, Dushanbe (Tajikistan), 26-27 Sep 2011.

Peganov, V.A., Molchanova, T.V., Akimova, I.D., and Zharova, E.V. (2014). Technology of production of concentrates of natural uranium under requirements of ASTM C 967-08. *Atomic energy*, v., N. 6, p. 333-338.

Rowson, J., Superintendent, M., Nguyen, T., and Metallurgist, C. (1987). Case Studies of the Chemical Precipitation Processes at The Cluff Mining Uranium Mill. *Crystallization and Precipitation*, 167–181. doi:10.1016/b978-0-08-035751-5.50028-3.

Sharafutdinov, U.Z., Rajabboev, I.M. (2024). Issledovanie vliyaniya jeleza na process sorbcii urana v productivnyh rastvorah podzemnogo vyschelachivaniya [Investigation of the effect of iron on uranium sorption from in situ leaching solutions].Universum: technicheskie nauki: electronniy nauchniy jurnal – *Universum: technical sciences: electronic scientific journal*, 3(120) [In Russian]. URL: https://7universum.com/ru/tech/archive/item/17141 (10.04.2025).

Venter, R. and Boylett, M. (2009). The evaluation of various oxidants used in the acid leaching of uranium. *Proceedings of Hydrometallurgy Conference 2009*, The Southern African Institute of Mining and Metallurgy.

Uranium extraction technology. (1993). Vienna: International Atomic Energy Agency.

Yahorava, V., Udayar, T., and Bazhko, V. (2010). Further investigations around uranium recovery via ion exchange process. *Mintek internal report 40572*.

Zontov, N. (2006). Continuous counter-current ion exchange in uranium ore processing. *Proceedings of ALTA 2006 Uranium Conference*, p. 15-34.

Mpho Ramabulana

Senior scientist
Mintek

Mpho is a Senior Scientist at Mintek. She works on commercial and research projects in Hydrometallurgy. Her primary focus entails the recovery, purification, and separation of diverse commodities, including gold, uranium, copper, cobalt, nickel, and zinc.

Mpho started her journey at Mintek as an intern in 2011. She obtained her BSc, Honours, and MSc degrees in Chemistry from the University of Venda and is pursuing her PhD at Wits.

Application of RIP in alkaline uranium leaching process of carnotite ores

C. Bornheim

Wood Group, South Africa

Uranium is critical for the future of nuclear energy with the metallurgical extraction of uranium from ore playing a large role in the value chain. The process selection is strongly influenced by ore mineralogy, grade, impurities, byproducts, and reagent costs. Carnotite-bearing ores, typically associated with significant carbonates and high clay content, present unique challenges for acid leaching as well as for solid-liquid separation circuits.

Alkaline leaching is generally preferred for ores containing significant carbonate content to reduce reagent consumption as the acid will be neutralised by these carbonates. The complications created in the solid-liquid separation steps after alkaline leaching, due to the high clay content, increase capital and operating costs. This influences the viability and profitability of these projects.

This paper evaluates solid-liquid separation technologies and compares the approximate percentage of the total equipment capital cost of a project for the various solid-liquid separation technologies evaluated. Resin-in-pulp (RIP) technology, which directly contacts resin with slurry, is reconsidered. Historically, there have been concerns outside of the capital cost of RIP systems such as:

- Reagent recycling
- Effective separation of resin and ore
- Impurity control
- Attrition rate of resin
- Silica fouling of resin
- Leaching temperature.

Preliminary findings from research highlights RIP as a promising option for carnotite ores. RIP offers potential advantages in reducing capital expenditure, simplifying flowsheets, and improving uranium recovery under challenging ore conditions. Although the inclusion of RIP would still require a solid-liquid separation step to recover reagent and water, the uranium has already been extracted from the solid-liquid separation stage feed stream. Therefore, a much simpler and less intensive solid-liquid separation step can be implemented. Newer developments in ion exchange resins assist in relieving some of the historical concerns of implementing RIP systems in alkaline leach uranium projects.

INTRODUCTION

For nuclear energy generation to be successful, the full value chain is required to be economically viable. The first step of this value chain is the extraction of uranium from ore. The most efficient method for uranium extraction is dependent on the ore mineralogy, grade, impurities and byproducts. This ore characterisation is then used to evaluate the leach kinetics and reagent costs (including transportation costs) to determine the process route (Lunt, *et al.*, 2007).

The general process circuit for uranium extraction comprises of the following steps: size reduction (comminution/scrubbing and screening), leaching, solid-liquid separation (in the case of tank leaching), purification (solvent extraction (SX), ion exchange (IX) or a combination of IX and SX), precipitation, drying/calcining. Sometimes a roasting system and/or a radioactive sorting system prior to leaching is used. Generally, two methods of leaching uranium ore are used, namely, acid leaching with sulphuric acid or alkaline leaching with a mixture of sodium carbonate (Na_2CO_3) and sodium bicarbonate ($NaHCO_3$).

This paper focuses on uranium extraction from carnotite-bearing ore – which is normally associated with significant carbonates and high clay content. The significant carbonates necessitate an alkaline leaching process over a sulphuric acid leaching process, as the carbonates react with sulphuric acid, resulting in increased reagent consumption. The high clay content complicates the solid-liquid separation which contributes to the cost of the project substantially. These challenges make resin in pulp (RIP) technology, which was first employed by former Soviet Union countries in gold and uranium applications, particularly attractive, as it reduces the solid-liquid separation requirements. In RIP circuits, the resin is mixed directly with the slurry to adsorb the uranium from the leached solution. This allows a relaxation of the solid-liquid separation post the alkaline tank leaching circuit as the uranium has already been recovered and the main driver of this step becomes reagent and water recovery. Further dilution, to improve reagent mass recovery, can also be implemented without affecting the uranium tenor and impacting downstream processes.

An evaluation of the suitability of RIP in alkaline circuits for carnotite ores and its potential as a simplified and effective processing route are discussed.

REVIEW

Carnotite is a hydrated uranium, vanadium and potassium oxide mineral with the mineral formula of $K_2(UO_2)_2(VO_4)_2.3H_2O$ that typically occurs as a fine particle measured in the micron range. The carnotite is usually found as a dust that coats weathered granite and calcrete rock or as an encrustation on sand grains. Therefore, carnotite is often associated with carbonate minerals.

These carbonate minerals react with sulphuric acid, increasing the sulphuric acid requirements if an acid leach is employed. Therefore, an alkaline leach is normally used for carnotite-bearing ores.

Alkaline tank leaching consists of adding Na_2CO_3 and $NaHCO_3$ to the finely screened ore at temperatures varying between ambient up to 90°C. The exact conditions depend on the nature of the ore body and leach kinetics. Conventionally, the tank leach is followed by a solid-liquid separation process to allow the uranium-rich liquor to proceed to the purification step while the barren ore is sent to tailings. This solid-liquid separation step represents a large portion of the capital cost of the project.

The conventional solid-liquid separation technologies used after the uranium alkaline tank leach circuit are:

- Counter-current decantation (CCD) thickeners
- Filter presses.

CCD thickeners

Due to the high clay content of the weathered granite and associated ultra fine material (smaller than 10 µm), dewatering steps are challenging. The slow settling rates and low terminal densities impact the use of CCD thickeners. This increases the size and number of CCD thickeners required to achieve effective product and reagent recoveries. A final dewatering step after the CCD thickeners is required to have a stable dry tailings facility as well as to recover the water for re-use in the circuit.

For this flowsheet option, a single stage of filter presses for the final dewatering step is used.

Filter presses
The ultra fine particle size and high clay content cause poor filtration fluxes and high cake moistures. This results in poor washability and the loss of reagent and leached uranium or in an increase in capital due to an increase in the number of stages to achieve sufficient washing efficiency.

For this flowsheet option, two stages of filter presses are used. Repulping between the two stages is required to improve uranium and reagent recovery.

Considering the above challenges, alternative solid-liquid separation options and variations are evaluated. These are:

- Counter-current washing vacuum belt filter circuit (washing on the belt required)
- Pre-leach roasting in combination with single stage post-leach filter presses
- Two stage filter presses with coarse sand addition (filter aid)
- Two stage centrifuges in combination with final stage filter presses
- CCD thickeners in combination with final stage tailings dam including liquor recovery
- RIP with single stage filter presses.

A high-level block diagram of how the various options fit into a generic flow diagram is shown in Figure 1.

Counter-current washing vacuum belt filter circuit
Vacuum belt filters were initially considered in this application due to the possibility of improved displacement washing. However, the low driving force associated with vacuum systems and the particle shape of the clays result in the liquor being trapped within the layers resulting in insufficient dewatering. For this reason, this option is not considered further.

Pre-leach roasting in combination with single stage post-leach filter presses
Test work completed in the 1940s, on ore representative from the Colorado Plateau area, established the optimum roasting and carbonate leaching conditions of four types of uranium or vanadium associated ores. These four types were: carnotite ores, roscoelite ores, high-lime ore (calcareous shale) and a slime concentrate. The test work identified that roasting the ore prior to carbonate leaching improves the filterability and washability of the leached ore significantly compared to unroasted ore. As the roasting temperature was increased, the washing efficiency increased, filtration cycle time decreased and cake moisture decreased (Richardson, *et al.*, 1949). Improved filterability and washability resulted in the reduction of the required multiple stages of post-leach dewatering to a single stage. Roasting of the ore alters the physical properties of the clay minerals through dehydration and, in some cases, a breakdown along the mineral grains (Merritt, 1971).

The test work completed on Bald Eagle ore showed that a temperature of 390°F (199°C) decreased the filtration cycle time by 50% and cake moisture by 2%. Increased temperatures on Bald Eagle ore resulted in lower uranium extraction for an alkaline (soda soluble) leach. However, extending the leaching time can compensate for this effect and achieve comparable recoveries within certain temperature ranges (up to 750°F or 399°C).

Test work completed on Wild Steer ore showed that temperatures above 570°F (299°C) resulted in a reduction of uranium extraction in the leach (Richardson, *et al.*, 1949). Therefore, it is critical to identify the highest roasting temperature required to improve filtration performance while minimising the negative effect on the uranium extraction efficiency in the leach. If vanadium recovery is also targeted, then much higher roasting temperatures should be used (800 - 900°C) (Merritt, 1971).

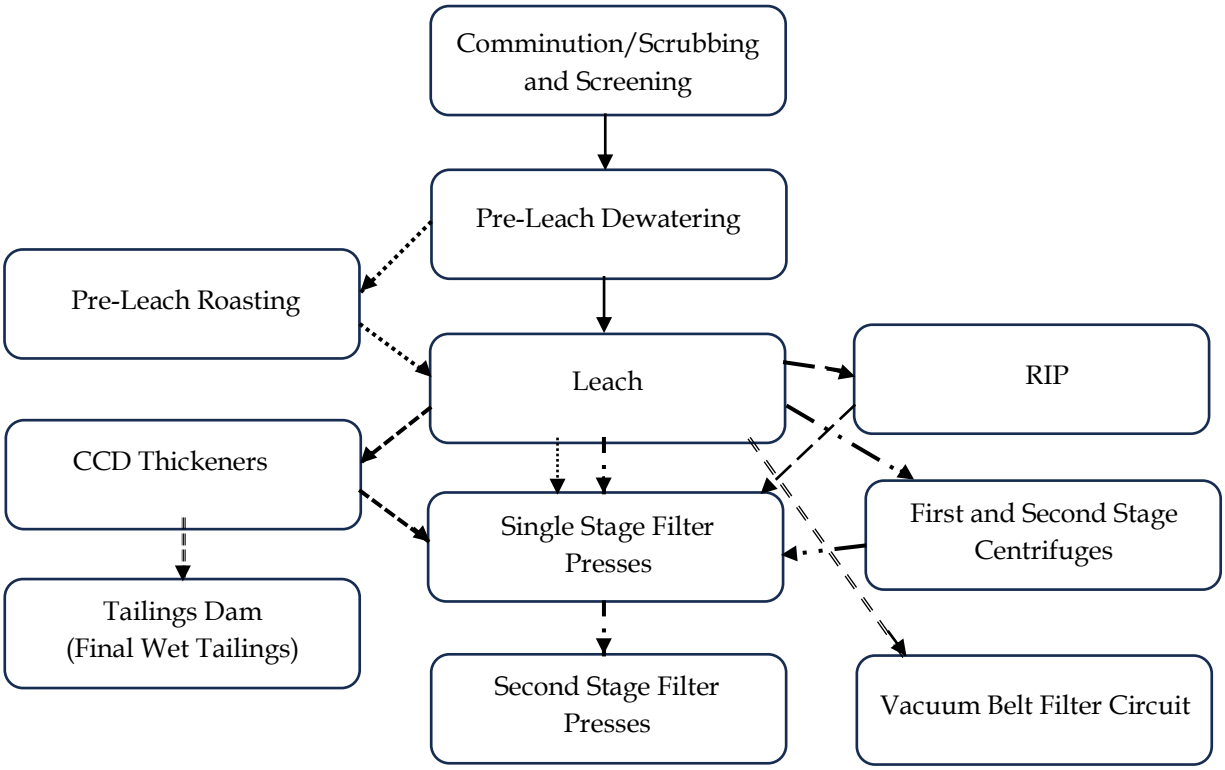

Legend			
------	CCD Thickener + Filter Press or Tailings Dam	.....	Pre-Leach Roasting + Filter Press
— · -	Two Stage Filter Press (With & Without filter aid)	— · —	Two Stage Centrifuge + Filter Press
═══	CC Vacuum Belt Filter	— — ·	RIP + Filter Press
———	Common to multiple systems		

Figure 1: High level block flow diagram of options identified.

For all options presented in this paper, it is assumed that a pre-leach dewatering stage is required to facilitate soluble impurity removal (specifically the chlorides and sulphates dissolved during the wet screening step of the process). In addition to impurity removal, a pre-leach dewatering stage increases the solids percentage that is to be treated further, thereby increasing the viability of pre-leach roasting. For pre-leach roasting to be effective, the feed to the pre-leach roaster should be as dry as possible to minimise energy consumption associated with the evaporation of free water and maximises energy absorbed by the ore. Where soluble impurity removal is not required, an additional pre-leach dewatering step is required to support the pre-leach roaster, thus increasing the cost of this option relative to the other options.

Two stage filter presses with coarse sand addition or alternative filter aid

The addition of a filter aid or coarse sand, if it is readily available, aids in the post-leach filtration process and reduces the impact of the fine clay material. This improves the filtration fluxes and final cake moisture. This results in a reduced cycle time. The drawback of adding a filter aid is that an increase in the filter press plant throughput is required and although the final cake moisture is reduced, the total mass of solution associated with the cake is hardly decreased. A second stage of filter presses is required

to treat the repulped cake from the first stage. This repulping acts as a dilution wash, thereby improving the overall uranium and reagent recovery.

Washability of the cake, after the addition of a filter aid, is improved but it could still require a large amount of wash liquor. This results in the dilution of the pregnant leach solution (filtrate). The filter aid is lost as it reports to the tailings and cannot be recycled into the process.

Two stage centrifuges with final stage filter presses
A decanter type centrifuge is considered for the centrifuge option. When compared to the filter presses, the centrifuge will produce a cleaner solution stream, but the cake will have a higher moisture content. The benefit of this system is that the feed to the second stage can be diluted to significantly lower solid concentrations, thus improving the dilution washing and therefore uranium and reagent recovery.

Since the centrifuges cannot achieve stackable tailings for this material; a final stage of filter presses is still required.

CCD thickeners with final tailings dam and liquor recovery
A tailings dam cannot be used as the first dewatering stage as the low terminal densities of high clay material will cause excessive uranium and reagent loss. If a tailings dam is used as the secondary dewatering stage, then the liquor associated with the leached solids needs to have low uranium and reagent content to minimise losses.

CCD thickeners will be used as the first stage of the dewatering process.

RIP with single stage filter presses
RIP will load the uranium onto resin after the leach circuit and therefore reduce the potential loss to the post-leach dewatering stage. By moving the purification step earlier, compared to conventional circuits, there is no risk of diluting the product stream. This also allows the first stage of post-leach dewatering to be diluted with water to reduce the reagent concentrations and therefore reduce the losses of reagent in the cake moistures. In this instance, a single stage of filter presses can achieve the uranium and reagent recovery requirements.

In this flowsheet option, leaching and IX adsorption occur under the same conditions. This reduces the ability for impurity control.

CAPITAL COST COMPARISON

An approximate percentage share of the capital cost associated with the plant process equipment for conventional and alternative solid-liquid separation technology options is completed below. The comparison is based on achieving similar uranium and reagent recovery from each option; therefore, an optimised case of each option is not necessarily considered. Operating costs and maintenance costs have not been considered.

The basis for the costing is a slurry feed to leach of:

- 100 t/h solids
- 30% mass/mass
- High clay content
- Ultra fine particle size (P_{100} < 100 µm).

From Table I, it can be seen that the two lowest capital cost options are the CCD thickeners with a final stage tailings dam and the RIP with a single stage filter press option. The cost of the tailings dam will increase as the plant continues its operation to accommodate for the cumulative tailings tonnage – only the cost of the first year of the tailings dam has been included in the costing. Therefore, the tailings dam

carries deferred costs, as expansion will be required over time to accommodate the accumulating plant tailings.

Table I. *Share of process equipment capital costs attributed to the specific process option*

Technology and description	Approximate % of plant process equipment cost
CCD thickeners with second stage filter presses	33%
Two stage filter presses	43%
Pre-leach roasting with single stage filter presses	35%
Two stage centrifuges and final stage filter presses	34%
Two stage filter press with coarse sand addition (filter aid)	45%
CCD thickeners with final stage tailings dam	24%
RIP with single stage filter presses	28%

HISTORICAL RIP CONCERNS

Historically, there are concerns of using RIP in alkaline leach circuits, such as:

- Reagent recycling
- Effective separation of resin and ore
- Impurity control
- Attrition rate of resin
- Silica fouling of resin
- Leaching temperature.

Reagent recycling

Since the uranium will be already loaded onto the resin, dilution of the post-leached slurry is possible without affecting the purification step equipment sizes. The dilution of this slurry will also reduce the reagent concentration and therefore the mass of reagent lost to the moisture associated with the tailings (dewatered barren ore). Reagents can be recycled to the leach feed or to reagent make-up to reintroduce the recovered reagents back into the circuit.

Effective separation of resin and ore

Larger resin beads have slower diffusion kinetics but allow for better separation from ore. Generally, the size of resin beads varies from 325 µm to 1180 µm, depending on the resin selection. The resin beads are significantly larger than the ore particles (specifically for carnotite ore) and separation of even the finest resin sizes from the ore can be achieved effectively.

In cases where plants aim for a coarser screened ore, with a typical top size of 500 µm, larger, more specific RIP type resins should be used. These more specific RIP type resins have a typical average diameter between 850 µm and 1000 µm (van Deventer, 2013). The increase in elution equipment size, to accommodate slower elution kinetics, is negligible compared to the dewatering equipment cost and the RIP option remains economically viable.

The viscosity of the leach slurry can also impact the effective separation of resin from the leached ore (van Tonder & Van Hege, 2007). This can be mitigated by washing during the resin/ore separation step or diluting the slurry after leach, as the solids concentration has a direct correlation to viscosity (lower solids concentration results in lower slurry viscosity).

Impurity control
The main impurities that affect the loading of uranium onto resin in an alkaline circuit are chlorides and sulphates. Since most of the chlorides and sulphates are in soluble forms for this process, there is no additional impact compared to having the leaching and IX adsorption as separate steps. pH is the main driver for leaching and IX loading impurity control.

The leach pH is managed to balance leaching performance and slurry rheology. Due to the negative impact of increased pH on fine clay viscosity, slurry viscosities can reach points where agitation is not possible, resulting in equipment damage and compromising plant production.

Carnotite contains equimolar quantities of vanadium and uranium. The vanadium can be seen as either an impurity or as a byproduct – depending on whether the owner of the plant has an appetite to sell the vanadium. If vanadium is seen as an impurity, a common way to reject the vanadium in the circuit is by leaching at higher pH. With a higher operating pH in the leaching circuit (still below viscosity limitations), vanadium tends to stay in the solid phase and not leach with the uranium. For further rejection in the IX circuit, operating at even higher pH will result in preferential loading of uranium compared to vanadium.

If vanadium is seen as a byproduct rather than an impurity, a lower leach pH will be targeted to leach the vanadium with the uranium. The vanadium will be separated from the uranium in the IX circuit with staged pH systems or after IX with a selective precipitation system.

Since the adsorption step of an RIP circuit occurs under the same conditions as the leach, some flexibility with regards to the pH of the leach and the pH of the IX adsorption is lost but it is still possible to achieve sufficient vanadium rejection or separation by employing a pH-staged elution. The leach pH cannot be increased too high due to the risk of viscosity issues.

Attrition rate of resin
With the resin being introduced into a slurry circuit, it is expected that the attrition rate of the resin would become of concern. However, from studies conducted on a pilot scale level, no sign of resin breakage was observed after multiple weeks of operation.

Resin experiences a higher attrition rate when the ore is highly siliceous (van Deventer, 2013) and when the ore particles are coarse (van Tonder & Van Hege, 2007). Since carnotite ores have a high clay content and are associated with fine particles, the attrition rate on the resin is expected to be within acceptable ranges.

Silica fouling of resin
Silica can impact the metallurgical performance of the resin by impacting the required residence time of the resin in the adsorption and elution stages. Silica fouling mainly occurs in acidic solutions as the silica takes the form of monosilicic acid ($Si(OH)_4$) at a pH of around 2. Polymerisation of monosilicic acid occurs when an aged and supersaturated form is realised. This form penetrates the resin bead and causes the fouling to occur (Zaganiaris, 1981).

This concern is lower in alkaline leach circuits as these are operated at much higher pH values and therefore the polymerisation of silica reduces and the silica solubility increases. This reduces the risk of silica fouling in alkali conditions (Meyers, n.d.).

Leaching temperature
Alkaline leaching systems can require leach temperatures up to 90°C for optimal uranium extraction. Since RIP systems have the resin at the same conditions as the leach tanks, the resin needs to be able to withstand this leaching temperature. At high temperatures, anion exchange resins can undergo degradation. Strong base anion exchange resins are commonly used for uranium extraction plants and generally have a temperature limit of 100°C. Nevertheless, the operating temperature of the leach

should be run as low as possible while still achieving the uranium extraction requirements to reduce energy costs and improve resin life.

In most cases, dropping the temperature to around 80°C will require a longer leaching time to achieve the required uranium extraction. Although the leach operates at a temperature below the resin limit, operating for extended periods above 60°C reduces the life of the resin exponentially as the temperature increases. Projects that want to make use of the RIP system need to evaluate the impact of temperature on the resin life as well as the uranium recovery. If the leaching temperature cannot be reduced due to its impact on uranium extraction, the RIP system can be implemented after the heat recovery process to improve resin longevity. This modification would result in a minor increase in capital cost and footprint – this was not considered in the capital cost comparison section.

CONCLUSION

The high clay content and significant carbonate levels associated with carnotite-bearing ores substantially complicate solid–liquid separation following alkaline leaching. This challenge is reflected in the considerable share of process equipment capital costs attributed to this step. The most expensive option involves two-stage filter presses, which account for 43% of the capital cost without filter aid addition and 45% with filter aid addition.

By contrast, the lowest capital cost alternatives are CCD thickeners with a final-stage tailings dam and RIP combined with a single-stage filter press, representing 24% and 28% of the capital cost, respectively. It should be noted, however, that the tailings dam carries deferred costs, as expansion will be required over time to accommodate accumulating plant tailings.

RIP technology emerges as a particularly promising option. By integrating leaching and IX adsorption into a single stage, RIP simplifies the flowsheet, reduces reliance on complex solid–liquid separation, and still achieves the necessary uranium and reagent recovery. This integration contributes to lower overall capital expenditure for the plant.

Although most historical concerns regarding RIP systems in alkaline leach circuits have been addressed through advances in resin technology, leach temperature remains a critical factor requiring careful consideration. However, alternative flowsheet configurations are available to mitigate these concerns and support resin longevity.

In summary, RIP demonstrates strong potential to enhance the capital economic viability of uranium projects involving carnotite ores and alkaline leaching circuits. By mitigating both technical and cost-related challenges, it offers a pathway towards more efficient and sustainable uranium extraction, reinforcing its importance in the future of nuclear energy.

REFERENCES

Lunt, D., Boshoff, P., Boylett, M. & El-Ansary, Z. (2007). Uranium Extraction: The Key Process Drivers. *The Journal of The Southern African Institute of Mining and Metallurgy,* pp. 419-426.

Merritt, R. C. (1971). *The Extractive Metallurgy of Uranium.* First ed. Colorado: Colorado School of Mines Research Institute.

Meyers, P., n.d. Behaviour of Silica in Ion Exchange Systems. *The Analyst,* 25(2), pp. 12-20.

Richardson, A. C., Stephens, F.M., Rabb, D.D., Merritt, R.C., Kesler, R.D. (1949). *The Recovery of Uranium from Carnotite Ores.* Columbus, Ohio: Battelle Memorial Institure.

van Deventer, J. (2013). *Ion Exchange Resins for Uranium Recovery: The Durability Question Explored.* Perth, Alta.

van Tonder, D. & Van Hege, B. (2007). Uranium Recovery from Acid Leach Liquors: The Optimisation of RIP/SX Based Flowsheets. *The Southern African Institute of Mining and Metallurgy,* The Fourth Southern African Conference on Base Metals, pp. 241-260.

Zaganiaris, E. J. (1981). Effect of Physical and Chemical Structure of Ion Exchange Resins on Silica Fouling in Acid Leach Liquors in Uranium Hydrometallurgy. *Hydrometallurgy 81,* pp. E4/1-E4/15.

Craig Bornheim

Senior Process Engineer
Wood PLC

Craig Bornheim graduated from the University of Pretoria with a degree in chemical engineering (B.Eng. Chemical). Over the past decade, he has built extensive experience in the chemical and mineral processing industry, contributing to projects across a wide range of commodities which include gold, copper, cobalt, diamonds, mineral sands, PGMs, chrome, vanadium and uranium. His career spans the full project lifecycle, from concept design through to commissioning and operational support.

Since joining Wood PLC in 2024, Craig has focused on uranium processing and has been involved in the design of two green-fields uranium projects. He has collaborated with leading experts in the uranium processing field during these projects while also drawing on his diverse background in other commodities to bring fresh perspectives to conventional approaches in uranium extraction. His ability to integrate cross-commodity insights with specialized uranium knowledge positions him as a valuable contributor to advancing innovative and practical solutions for the improvement of uranium processing.

Technical and economic evaluation of hydrogen peroxide as an alternative to pyrolusite in uranium oxidative leaching

W.A. Ngobeni, D. Verwey

BME Metallurgy, A Division of the Omnia Group. South Africa

Uranium ore predominantly occurs in insoluble tetravalent and soluble hexavalent oxidation states. Invariably, tetravalent uranium must be oxidised to the hexavalent state for effective extraction. Thus, maintaining a leachable oxidation state is crucial for efficient extraction. The common oxidant used for this is pyrolusite, although its commercial purity ranges from 30 to 50% MnO_2. However, using pyrolusite poses operational and safety challenges, including the generation of solid residue and manganese dust, handling challenges, and high reagent consumption. Consequently, the mine is seeking alternatives to eliminate these challenges. Hydrogen peroxide offers advantages such as no solid residue or dust generation, ease of handling and low reagent consumption. This paper investigated the techno-economic feasibility of replacing pyrolusite with hydrogen peroxide in the oxidative leaching of tetravalent uranium ore at a Namibian operation. Laboratory tests compared hydrogen peroxide and pyrolusite in terms of uranium extraction efficiency, oxidant and acid consumption, redox control, and iron speciation. Results showed that both oxidants achieved similar uranium extraction efficiencies (>89%). However, only 0.0354 kg/t of hydrogen peroxide was required, compared with 0.7118 kg/t of MnO_2, and acid consumption was slightly reduced by 0.9 kg/t. An economic evaluation based on these findings indicated total annual savings of US$ 3.5 million. The savings were primarily attributable to the lower oxidant requirement, as uranium extraction performance was similar for both oxidants, and acid consumption differed only marginally. Based on the techno-economic benefits shown above, a plant trial to validate performance under operational conditions was recommended.

Keywords: Uranium, oxidative leaching, hydrogen peroxide, pyrolusite, sulfuric acid, hydrometallurgy.

INTRODUCTION

Uranium is a vital strategic metal worldwide because of its key role in nuclear power production and its contribution to low-carbon energy systems (Li *et al.*, 2025). Although over 200 uranium-bearing minerals have been identified globally, only a few are of economic importance because most occur at low abundances, contain insufficient uranium, or are not amenable to cost-effective extraction and processing. The economically important ones include uraninite, pitchblende, coffinite, brannerite, and carnotite (Bhargava *et al.*, 2015; Pownceby & Johnson, 2014; Bowell *et al.*, 2011; Nagar *et al.*, 2021). These minerals may be broadly classified according to the oxidation state of uranium: tetravalent (U^{4+}) and hexavalent (U^{6+}).

Among the economically important uranium minerals, carnotite is regarded as a secondary ore. It mainly occurs in the U^{6+} oxidation state, whereas uraninite, pitchblende, coffinite, and brannerite are primary uranium minerals in which uranium occurs mainly as U^{4+} (Gilligan & Nikoloski, 2015; Pownceby & Johnson, 2014; Bowell *et al.*, 2011; Nagar *et al.*, 2021).

This difference is important in hydrometallurgical processing, as uranium solubility is strongly dependent on its oxidation state. Hexavalent uranium forms soluble uranyl complexes that readily dissolve in both dilute acidic and alkaline leaching media, whereas tetravalent uranium is sparingly soluble under similar conditions (Ibrahim *et al*., 2013; Bhargava *et al*., 2015; Pownceby & Johnson, 2014; Nagar *et al*., 2021). Consequently, the oxidation of U^{4+} to U^{6+} is required for effective uranium extraction from most uranium ores.

Sulfuric acid leaching is the most used process for uranium extraction worldwide, due to its relatively low cost, abundance, and high leaching efficiency (Bhargava *et al*., 2015). In sulfuric acid systems, tetravalent uranium dissolution and extraction require a suitable oxidative environment. Therefore, both chemical equilibria and redox kinetics need to be maintained to achieve economical uranium recovery. To achieve this, chemical reagents are used, including ferric (Fe^{3+}) ions and other oxidants. The uranium leaching is a multi-stage process consisting of two interdependent steps, viz., ferric ions are responsible for oxidising tetravalent uranium (UO_2) to the soluble hexavalent uranyl ion (UO_2^{2+}) in step 1, as illustrated in Equation 1. This is followed by step 2, where an oxidant is used to convert ferrous (Fe^{2+}) back to Fe^{3+} ions, Equation 2 with pyrolusite as an oxidant or Equation 3 with hydrogen peroxide as an oxidant. Therefore, considering Equation 3, using hydrogen peroxide to oxidise uranium in Equation 1 would theoretically require 50% less sulfuric acid compared to using pyrolusite in Equation 2.

$$UO_2 + 2Fe^{3+} = UO_2^{2+} + 2Fe^{2+} \quad [1]$$

$$2Fe^{2+} + MnO_2 + 4H^+ = 2Fe^{3+} + Mn^{2+}2H_2O \quad [2]$$

$$2Fe^{2+} + H_2O_2 + 2H^+ = 2Fe^{3+} + 2H_2O \quad [3]$$

The choice of oxidant significantly influences leaching kinetics, reagent consumption, operational stability, and overall process economics. There are different oxidants used commercially for this purpose, including pyrolusite (MnO_2), hydrogen peroxide (H_2O_2), Caro's acid (H_2SO_5), sodium chlorate ($NaClO_3$), oxygen (O_2), sulfur dioxide (SO_2), and air (Bowell *et al*., 2011; Bhargava *et al*., 2015; Gilligan & Nikoloski, 2015; Nagar *et al*., 2021). Pyrolusite has long been the preferred oxidant in many uranium processing operations, especially in sulfuric acid leach circuits. This could be attributed to its availability, lower cost, and proven ability to regenerate ferric ions. Despite its established role, commercially available pyrolusite is seldom pure, typically containing only 30% to 50% MnO_2, with the remainder comprising gangue minerals that contribute little to oxidation and may act as acid consumers (Nagar *et al*., 2021). The implications of these impurities include elevated reagent consumption, inconsistent oxidation potential, and increased generation of solid residue. Furthermore, the handling of pyrolusite introduces health, safety, and environmental challenges associated with manganese dust and disposal of Mn-bearing residues. These drawbacks have prompted industry interest in exploring alternative oxidants that are more efficient, cleaner, and easier to manage operationally. Moreover, variability in MnO_2 content can result in inconsistent oxidation-reduction potential (ORP) control, complicating process optimisation. The use of pyrolusite also increases solid residue generation and introduces environmental, health, and safety concerns related to manganese dust handling and the disposal of Mn-bearing residues.

The growing emphasis on cost reduction, environmental stewardship, and Environmental, Social and Governance (ESG) performance has prompted the uranium industry to re-evaluate traditional oxidants and explore alternative reagents that deliver improved operational and environmental outcomes. Hydrogen peroxide has emerged as a promising alternative oxidant due to its high oxidation potential, clean decomposition products (water and oxygen), and suitability for controlled dosing. From an environmental perspective, hydrogen peroxide offers the potential to reduce secondary waste generation and eliminate manganese-related residue management challenges (Clarens *et al*., 2005; Nagar *et al*., 2021). Operationally, its rapid reaction kinetics and ease of handling may facilitate improved redox control within leaching circuits.

However, despite these advantages, the large-scale adoption of hydrogen peroxide in uranium leaching operations has been limited (Nicol, 2020). Key concerns include its cost relative to solid oxidants, decomposition under acidic and catalytic conditions, and uncertainties regarding its interaction with iron speciation, acid consumption, and oxidation-reduction potential stability under plant-specific operating conditions. As a result, there remains a need for systematic, site-specific investigations to evaluate both the technical and economic implications of replacing pyrolusite with hydrogen peroxide in sulfuric acid uranium leaching circuits.

To address this knowledge gap, the paper investigates the feasibility of replacing pyrolusite with hydrogen peroxide as the primary oxidant for uranium leaching in Namibia. Laboratory leaching tests were conducted under controlled conditions to compare the two oxidants in terms of uranium extraction efficiency, oxidant and sulfuric acid consumption, oxidation-reduction potential, and effects on the Fe^{3+}/Fe^{2+} ion equilibria.

In addition, a cost-benefit analysis was conducted using data from this study to determine whether there was economic merit to warrant a plant trial. The 13-hour leach tests were conducted on BULK12 LOT G ore at the target pH of 1.5, temperature of 35ºC, Fe^{3+}/Fe^{2+} ratio of 3.7, and ORP of 525 mV. The only variable investigated was the choice of the oxidant, i.e., manganese dioxide or hydrogen peroxide.

METHODOLOGY AND EXPERIMENTAL

Materials

Low-grade uraninite ore from a Namibian operation was used for the leaching experiments. Sulfuric acid (1.8 g/L) was used as the leaching medium, and 50% hydrogen peroxide and pyrolusite (assaying 47 wt.% MnO_2) was suspended in water prior to addition to the leach reactor were used as the two oxidants. The leach test parameters are summarised in Table I.

*Table **I**. The summary of the leach test parameters*

	Units	Pyrolusite	Hydrogen peroxide
Ore type		Weekly composite	Weekly composite
Volume of the leach tank	L	5	5
Ore mass	kg	2.5	2.5
RDS (return dam solution)	L	1.7	1.7
% solids	% (w/w)	63.8	63.8
Leach duration	Hrs	13	13
Leach temperature	°C	35	35
Target pH		1.5	1.5
$Fe_2SO_4.7H_20$ addition	g	3	3
ORP set point	mV (Ag/AgCl)	525	525
Acid dosing solution	%	98	98
Oxidant strength	%	47.47	50
Oxidant form		Slurry	Liquid
Sampling interval	Hrs	2,5,7,8,10,12	2,5,7,8,10, 12

Experimental procedure

Before each leaching experiment, the hydrogen peroxide solution was analysed by titration to determine its concentration. The pH and ORP probes were calibrated before testing and checked periodically throughout the experiments to ensure measurement reliability. A representative composite feed sample was prepared by combining leach feed samples (BULK12 LOT G) collected during the week before the test campaign. This composite was homogenised and then split into 2.5 kg aliquots using a rotary splitter. Each aliquot was mixed with 900 g of return dam solution to prepare the leach slurry. The slurry was transferred into two separate 5-litre leach vessels, one for pyrolusite and one for hydrogen peroxide. Both vessels were placed in a temperature-controlled water bath maintained at 35°C. Agitation was

started and maintained at 350 rpm to ensure uniform suspension and increased to 450 rpm once the solids were fully mixed. Care was taken to maintain the rpm at 450 for the duration of each leach test, which ran for 13 hours. The slurry's pH was initially adjusted to ~1.5 ± 0.5 and was recorded every 15 minutes throughout the test. The ORP set point was 525 mV, and ORP was also measured every 15 minutes. Both oxidants (hydrogen peroxide and manganese dioxide) and sulphuric acid (H_2SO_4) were automatically dosed using an auto-dosing system, with all additions recorded for comparative evaluation of the two oxidants. Slurry samples of 200 g were withdrawn from each vessel at 2, 5, 7, 8, 10, and 12 hours. Each sample was centrifuged and then vacuum-filtered to separate solids from liquids. The liquids were titrated to determine the concentrations of Fe^{3+}, Fe^{2+}, and free acid. The solid residues from each sample were washed with a pH 2 solution, vacuum-filtered, dried at 110°C, pulverised, and analysed for residual uranium using ICP-OES. At the end of each 13-hour leaching run, the remaining slurry was pressure-filtered to recover the final pregnant leach solution for uranium analysis. The solid residues were washed with a pH 2 solution, oven-dried at

110°C, pulverised, and analysed for uranium content to determine final extraction efficiencies and compare oxidant performance. All the analyses were conducted independently by the internal analytical laboratory. The data presented here are averages from quadruplicate tests conducted on different days. To ensure experimental consistency and reliability, only tests with variances below 5% were included in the averages. This was also to reduce the influence of outliers and experimental anomalies, often caused by dosing equipment issues, thereby improving the validity of the results. Pyrolusite consumption values are reported on an as-received basis; the corresponding MnO_2 consumption was calculated using the measured MnO_2 content of the pyrolusite ore (47.17 wt.% MnO_2) and calculated using Equation [4].

$$MnO_2 = Pyrolusite \times \frac{MnO_2\ assay\ (\%)}{100} \quad [4]$$

RESULTS AND DISCUSSIONS

The comparative findings highlight differences between the two oxidants under similar conditions in uranium extraction, acid and oxidant consumption. Additional parameters, including pH change, variation in oxidation-reduction potential, ferric-to-ferrous ratio, and free acid, were also calculated.

Oxidants comparison on uranium extraction

Figure 1 shows the uranium extraction efficiencies achieved with hydrogen peroxide and manganese dioxide as oxidising agents. Both oxidising agents yielded similar uranium recovery under the tested conditions. The average uranium extraction was roughly 89%, indicating the effectiveness of both oxidants in aiding leaching. Uranium extraction reached a plateau after approximately 6 h of leaching, indicating that leaching was effectively complete. The tests were nevertheless continued to 13 h to assess longer-term oxidant consumption and redox control. The results support the claim made by Nagar *et al.,* (2021) that pyrolusite has long been the preferred oxidant in many uranium processing operations, especially in sulfuric acid leach circuits. This could be due to its availability, lower cost, and, most importantly, proven technical ability to regenerate ferric ions as confirmed in this pape. Hydrogen peroxide, recognised for its strong oxidative properties and relatively low environmental impact (Clarens *et al.*, 2005; Nagar *et al.,* 2021), performed on par with manganese dioxide, an existing oxidant at this Namibian operation. The similarity in uranium extraction achieved with pyrolusite and hydrogen peroxide can be attributed to both oxidants ultimately promoting the oxidation of relatively insoluble U4+ species to soluble U6+ by oxidising ferrous iron to ferric iron in the leach solution. Venter and Boylett (2009) reported that a variety of oxidants, including manganese dioxide and hydrogen peroxide, can effectively extract uranium when suitable oxidation potentials are maintained.

The comparable uranium recoveries observed in the present study therefore suggest that both oxidants provided sufficient oxidising capacity under the tested conditions, resulting in similar uranium dissolution kinetics. While these results do not indicate a metallurgical advantage of one oxidant over the other in terms of extraction efficiency, hydrogen peroxide may be a technically viable alternative to

pyrolusite, particularly where environmental, operational, or ESG considerations favour a reagent that does not introduce manganese into the process stream.

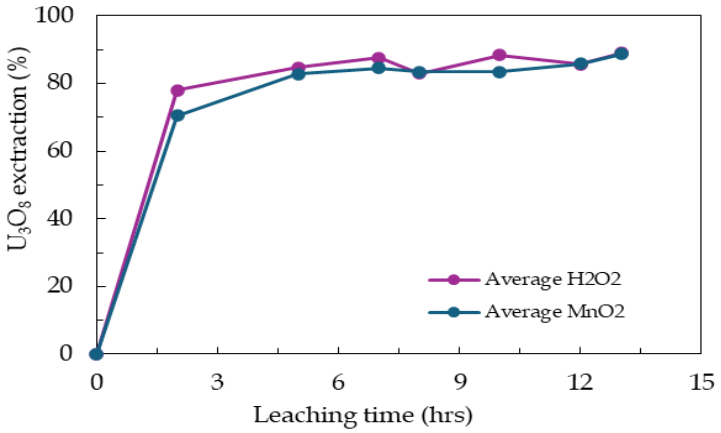

Figure 1. Average uranium extraction obtained with H_2O_2 vs MnO_2.

Oxidants comparison on acid consumption

Figure 2 presents the acid consumption results associated with uranium oxidative leaching using hydrogen peroxide and manganese dioxide as oxidising agents. The results reveal a slight difference in acid requirements between the two oxidants. The average acid consumption was measured at 29.8 kg/t for hydrogen peroxide and 30.7 kg/t for MnO_2 (~3% oxidant reduction). Although hydrogen peroxide exhibited slightly lower acid consumption than pyrolusite, the difference was small and cannot be confidently attributed to differences in leaching chemistry. It is more likely the result of variability in gangue acid consumption. Looking at Equations 2 and 3, half of the sulfuric acid would be required to oxidise uranium in Equation 1 using hydrogen peroxide compared to pyrolusite. However, the expectation of approximately 50% lower sulfuric acid consumption with hydrogen peroxide is based on ideal oxidation-reduction reactions of U^{4+} to $U^{6+}$and does not account for gangue dissolution, whereas an operating leach system is much more complex due to the presence of acid-consuming gangue. These gangue minerals consume sulfuric acid regardless of the oxidant used, thereby dominating the overall acid demand of the leaching system. For an ore containing approximately

150 ppm U and using 90% uranium extraction achieved in this study, the theoretical acid requirement for uranium dissolution is only about 0.06 kg H_2SO_4/t ore. This is negligible compared with the measured acid consumption of ~30 kg of H_2SO_4 per tonne of ore achieved with both oxidants, indicating that the acid consumption reported in Figure 2 is overwhelmingly controlled by gangue mineral dissolution rather than uranium extraction. This is because the total measured acid consumption depends not only on oxidant stoichiometry but also on ore mineralogy and solution chemistry. Although the difference is relatively small compared to theoretical expectations, it may have practical implications in large-scale operations, where even minor reductions in reagent use can lead to significant cost savings and environmental benefits.

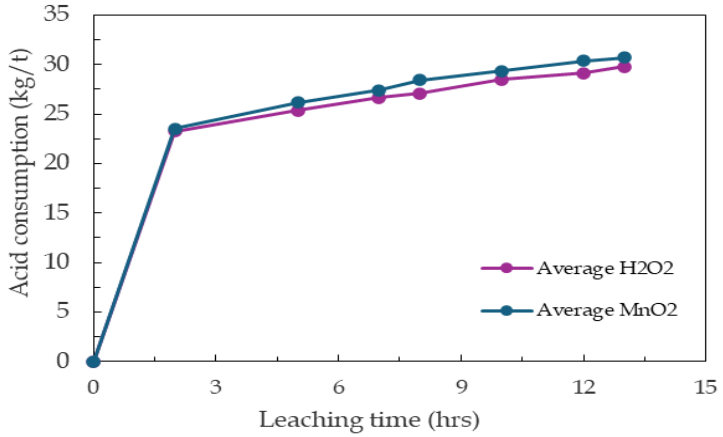

Figure 2. Average acid consumption achieved with H_2O_2 vs MnO_2.

Oxidants comparison on oxidant consumption

Figure 3 presents the results of oxidant consumption during uranium oxidative leaching with H_2O_2 and MnO_2. The results showed a significant difference in the amount of oxidant required between the two oxidants. The average oxidant consumption was 0.04 kg/t for H_2O_2, compared to 0.7 kg/t after 12 hours of leaching for MnO_2. Again, based on equations 1-3, theoretically, 2.56 times as much MnO_2 was required to oxidise uraninite in Equation. 1 as in H_2O_2. Thus, reduced oxidant consumption was expected when using H_2O_2. However, the magnitude of oxidant reduction was 20 times higher. This substantial reduction in oxidant consumption with H_2O_2 highlights its superior efficiency as an oxidising agent for uraninite oxidative leaching, as corroborated by Clarens *et al.,* (2005) and Nagar *et al.*, (2021). Lower consumption suggests a more reactive and efficient oxidation process, with potential cost savings. The much lower amount of H_2O_2 required to achieve similar uranium recovery may reduce operational costs. These findings reinforce the potential advantages of adopting H_2O_2 in uraninite leaching. The measured hydrogen peroxide consumption includes any losses due to decomposition, which may be higher in plant conditions. In contrast, MnO_2 consumption continued to increase throughout the leaching period, even after uranium extraction had effectively reached completion. Although the exact cause was not investigated in this paper, the continued demand for MnO_2 likely reflects additional oxidant consumption by species other than uranium, thereby sustaining the need to maintain the target redox potential.

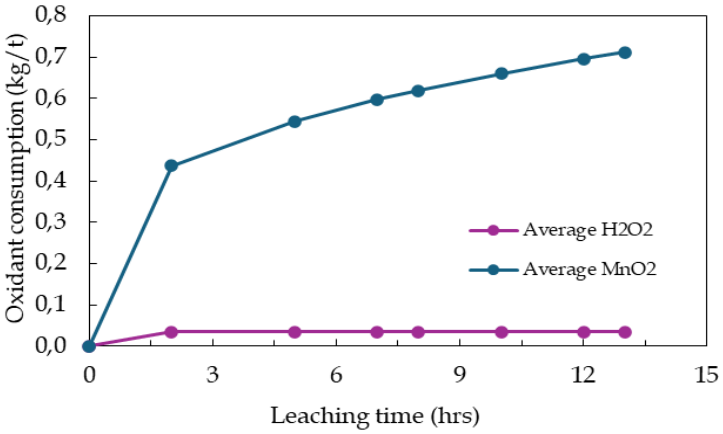

Figure 1. Average oxidant consumption achieved with H_2O_2 vs MnO_2.

Oxidants comparisons on pH change

Figure 4 illustrates the pH profiles observed during the uranium oxidative leaching using H_2O_2 and MnO_2 as oxidising agents. The results indicate that the pH followed a similar trend for both oxidants throughout the leaching process. This consistency suggests that the choice of oxidant had little influence on the overall pH behaviour under experimental conditions. Both systems maintained comparable acidity levels, which are critical for optimal uranium solubility and leaching efficiency. Given that pH was maintained at the same target value across all tests, any small deviations are likely attributable to control system performance rather than to the choice of oxidant. And the results showed that the control system was adequate.

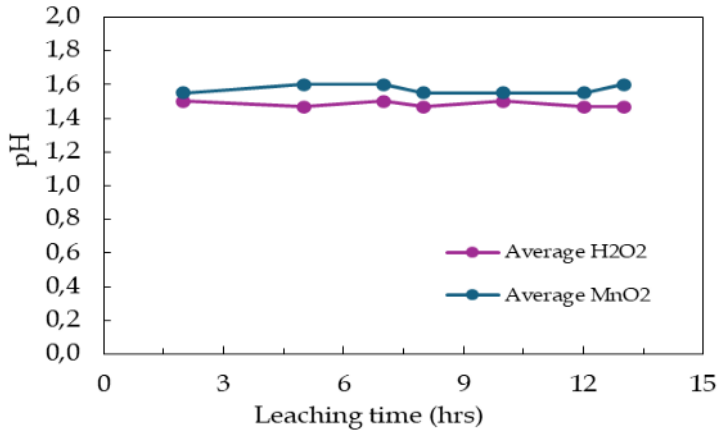

Figure 4. Average pH change achieved with H_2O_2 vs MnO_2.

Oxidants comparisons on oxidation-reduction potential

Figure 5 presents the oxidation-reduction potential profiles recorded during uranium leaching with H_2O_2 and MnO_2 as oxidants. The results show that while both oxidants followed a similar trend in ORP over time, H_2O_2 consistently yielded higher ORP values than MnO_2. The ORP values for the H_2O_2 system averaged above 630 mV for the duration of the experiment, whereas the MnO_2 system averaged around 528 mV. Although slightly higher oxidation-reduction potentials were observed in the H_2O_2 tests, both leaching systems were operated to the same target redox potential. The observed difference is therefore more likely attributable to normal variability in redox control than to an inherent characteristic of the oxidants. Furthermore, the higher redox potential did not translate into improved uranium extraction, as comparable extraction efficiencies were achieved with both oxidants. The trend similarity indicates that both oxidants consistently influence the redox environment, but the higher ORP of H_2O_2 could offer advantages in reaction kinetics and process control.

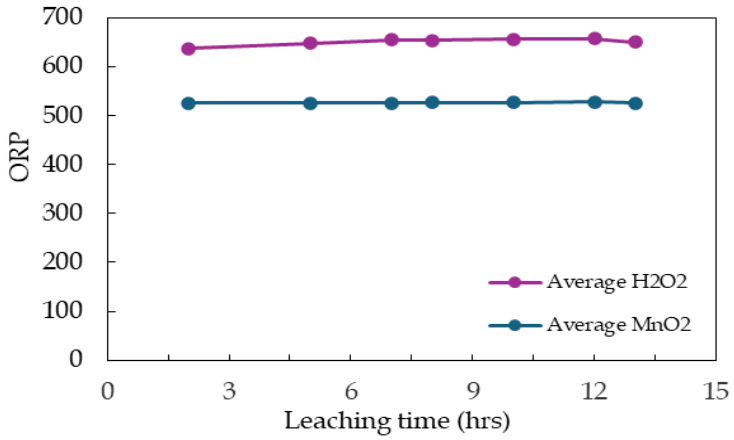

Figure 5. Average oxidation-reduction potential achieved with H_2O_2 vs MnO_2.

Oxidants comparison on the ferric to ferrous ratio

Figure 6 presents the ferric-to-ferrous (Fe^{3+}/Fe^{2+}) ratio profiles observed during uranium leaching with H_2O_2 and MnO_2 as oxidants. The results show that while both oxidants followed a similar trend over time, the Fe^{3+}/Fe^{2+} ratio achieved with H_2O_2 was consistently higher than that obtained with MnO_2. This higher Fe^{3+}/Fe^{2+} ratio in the H_2O_2 system suggests a more oxidising environment, consistent with the higher oxidation-reduction potentials observed for H_2O_2. The Fe^{3+}/Fe^{2+} corroborated the higher oxidation-reduction potential values, as these two parameters are not independent indicators but rather different expressions of the same solution redox state. A higher Fe^{3+}/Fe^{2+} ratio is generally favourable in uranium leaching, as Fe^{3+} ions are mainly responsible for oxidising uranium, as shown in Equation. 1. Therefore, the enhanced oxidative conditions provided by H_2O_2 were expected to contribute to higher effectiveness in uranium extraction, despite its lower consumption compared to MnO_2. However, the higher values did not yield improved uranium extraction, as comparable extraction efficiencies were achieved with both oxidants.

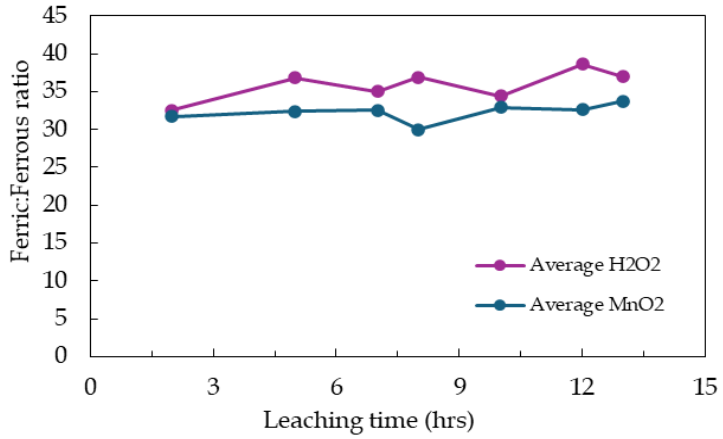

Figure 6. Average ferric-to-ferrous ratio attained with H_2O_2 vs MnO_2.

Oxidants comparison on free acid

Figure 7 shows the free acid concentration measured over time during uranium leaching with H_2O_2 and MnO_2. The results show that the free acid concentration obtained with H_2O_2 was consistently slightly higher than that observed with MnO_2 at all corresponding leaching times except at the 10-hour mark, where both oxidants yielded nearly identical free acid concentrations. H_2O_2 is a weak acid with a dissociation constant of 11.6 at 25°C (Nicol, 2020), while MnO_2 does not have acidity. Therefore, it is hypothesised that H_2O_2 may contribute to a slightly more acidic leaching environment, potentially through its decomposition products (Equation 5) or interactions with the leaching medium.

$$H_2O_2\ (aq) \leftrightarrow HO_2^- + H^+ \qquad [5]$$

Free acid concentrations remained broadly similar for both oxidants throughout the tests. Although minor differences were observed at certain sampling points, these are not considered indicative of systematic differences in leaching behaviour, particularly because pH was controlled to the same target value and uranium extraction profiles were comparable. Consequently, no substantive interpretation is drawn from the observed variations in free acid concentration.

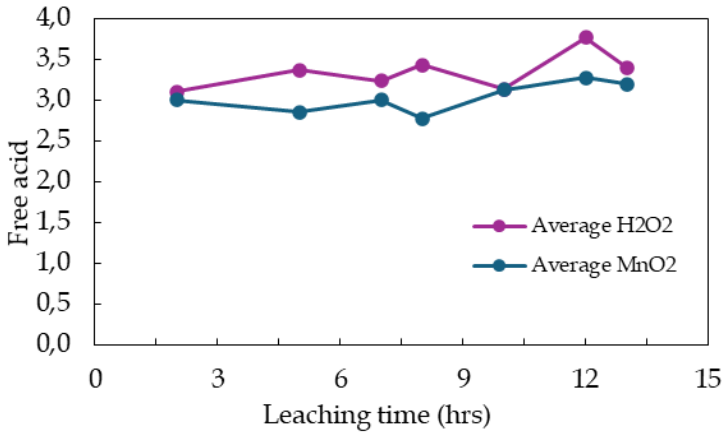

Figure 7. Average free acid achieved with H_2O_2 vs MnO_2.

Cost-benefit analysis

This section presents a cost-benefit analysis for replacing pyrolusite with hydrogen peroxide, based on the laboratory data (which still need to be validated with plant trial data). Furthermore, these calculations are based on a plant annual throughput of 10 000 000 tpa and reagent cost presented in Table II. The results presented in Table III show that the hydrogen peroxide process would achieve annual oxidant savings of ~US$3.2 million, annual acid savings of ~US$1.2 million, and total annual savings of ~US$3.5 million compared to the pyrolusite process. The economic evaluation is based exclusively on laboratory consumption data and does not account for potential changes in reagent efficiency, peroxide decomposition, storage, safety infrastructure, or dosing requirements at plant scale. Consequently, the analysis should be regarded as indicative.

Table I. Reagents, strength costs and annual tonnage used for cost benefit analysis

Product	**Strength**	**US$/mt - DDP**
MnO_2	47%	365.36
H_2O_2	70%	1120.00
H_2SO_4	98%	127.64

Table III. Cost calculations for hydrogen peroxide and manganese dioxide based on laboratory data

	10 000 000 tpa	**kg/t**	**tpa (100%)**	**US$/mt ore**	**Cost 10 M tpa**	**Total Cost**
H_2O_2 Process	H_2O_2 (50%)	0.02529	253	$0.03	$283 200	$39 096 180
	H_2SO_4	29.8	298000	$3.88	$38 812 980	
MnO_2 Process	MnO_2 (47%)	0.718	7180	$0.26	$2 623 285	$42 608 468
	H_2SO_4	30.7	307000	$4.00	$39 985 184	
Total oxidant saving - $ per annum						**$2 340 085**
Total acid saving - $ per annum						**$1 172 204**
H_2O_2 process cost saving - $ per annum						**$3 512 289**

Sensitivity analysis

To assess the robustness of the projected cost savings and account for uncertainties associated with scale-up and market variability, a sensitivity analysis was conducted.

Three primary variables were examined, as these are expected to have the greatest influence on overall operating cost: oxidant unit cost, sulfuric acid unit cost and hydrogen peroxide consumption efficiency at the plant scale. Each parameter was varied independently by ±20% from the base-case values used in the cost-benefit analysis (Table III), while all other variables were held constant. A ±20% range was selected to represent short- to medium-term price volatility and potential deviations between laboratory and plant reagent consumption.

Effect of oxidant price variation
Hydrogen peroxide pricing can be influenced by supplier location, transportation costs, and market demand. A ±20% variation in hydrogen peroxide unit cost resulted in annual cost savings of approximately US$2.9-4.1 million compared with the pyrolusite-based process. Even at the upper end of the peroxide price range, the hydrogen peroxide option remained economically favourable due to its substantially lower consumption rate.

Similarly, a ±20% variation in pyrolusite price had a proportionally smaller impact on the overall cost differential, as oxidant consumption in the manganese dioxide process is significantly higher. This result indicates that the economic advantage of hydrogen peroxide is more sensitive to consumption efficiency than to fluctuations in unit price.

Effect of sulfuric acid price variation
Sulfuric acid typically represents a major operating cost in uranium leaching circuits. A ±20% change in sulfuric acid price resulted in a variation of approximately ±US$0.23 million per annum in the total projected savings. Although hydrogen peroxide exhibited slightly lower acid consumption than pyrolusite under laboratory conditions, the sensitivity analysis confirms that acid price variability does not materially change the relative economic ranking of the two oxidants.

Effect of hydrogen peroxide consumption efficiency
To account for potential losses due to peroxide decomposition, incomplete utilisation, or less efficient dosing under plant conditions, hydrogen peroxide consumption was increased by up to 20% relative to the laboratory-measured value. Under this conservative assumption, the hydrogen peroxide consumption increased from 0.0354 kg/t to approximately 0.0425 kg/t.

Even under this worst-case consumption scenario, the hydrogen peroxide process continued to demonstrate annual savings exceeding US$2.6 million, confirming that the economic benefit is resilient to reasonable inefficiencies during scale-up.

CONCLUSION AND RECOMMENDATIONS

The paper showed that hydrogen peroxide demonstrated clear potential as an alternative oxidant to pyrolusite, achieving comparable uranium extraction while consuming significantly less oxidant. This indicates a promising opportunity to enhance process economics, ESG compliance, environmental stewardship, and eliminate secondary waste and manganese dust while improving metallurgical performance. The cost-benefit analysis further supports this transition, revealing a potential total annual saving of approximately US$3.5 million. This includes US$2.3 million in oxidant cost savings and US$1.2 million in acid cost savings.

The sensitivity analysis demonstrates that the economic advantage of hydrogen peroxide over pyrolusite is robust across a realistic range of reagent prices and consumption efficiencies. The dominant driver of cost savings remains the significantly lower oxidant consumption associated with hydrogen

peroxide. Variations in unit reagent prices or modest increases in peroxide consumption at the plant scale do not negate the overall economic benefit. These findings support the conclusion that hydrogen peroxide represents a lower-risk economic alternative to pyrolusite, provided that appropriate dosing control and storage practices are implemented during plant-scale operation.

Based on the techno-economic benefits shown above, a plant trial to validate performance under operational conditions was recommended. This trial would serve to validate the laboratory results under real-world operating conditions and assess the scalability of the process improvements.

ACKNOWLEDGMENTS

The authors gratefully acknowledge the support of BME Metallurgy management, who granted permission to publish this work. Mrs Jacqualine Aresesis for invaluable assistance with leaching tests, and Mr Herman Kalimbo are also acknowledged for coordinating and overseeing the whole test programme.

REFERENCES

Bhargava, S.K., Ram, R., Pownceby, M.I., Grocott, S., Ring, B., Tardio, J., & Jones, L. (2015). A review of acid leaching of uraninite. *Hydrometallurgy*, vol. 151, pp. 10–24. https://doi.org/10.1016/j.hydromet.2014.10.015

Bowell, R.J., Grogan, J., Hutton-Ashkenny, M., Brough, C., Penman, K., & Sapsford, D.J. (2011). Geometallurgy of uranium deposits. *Minerals Engineering*, vol. 24, no. 12, pp. 1305–1313. https://doi.org/10.1016/j.mineng.2011.05.005

Clarens, F., de Pablo, J., Casas, I., Giménez, J., Rovira, M., Merino, J., Cera, E., Bruno, J., Quiñones, J. & Martínez-Esparza, A. (2005). The oxidative dissolution of unirradiated UO_2 by hydrogen peroxide as a function of pH. *Journal of Nuclear Materials*, 345(2–3), pp. 225–231. https://doi.org/10.1016/j.jnucmat.2005.06.002

Gilligan, R. & Nikoloski, A.N. (2015). The extraction of uranium from brannerite – A literature review. *Minerals Engineering*, vol. 71, pp. 34–48. https://doi.org/10.1016/j.mineng.2014.10.007

Ibrahim, M.E., Lasheen, T.A., Hassib, H.B., & Helal, A.S. (2013). Oxidative leaching kinetics of a U(IV) deposit under acidic, oxidising conditions. *Journal of Environmental Chemical Engineering*, vol. 1, no. 4, pp. 1194–1198. https://doi.org/10.1016/j.jece.2013.09.007

Li, S., Xu, H, Cao, Y., Deng, J., Sun, X., Kang, Y., Ma, L. & Xie, M. (2025). Uranium in coal by-product and unconventional resources: occurrence characteristics and extraction methods. Separation and Purification Technology, 379, 135163. https://doi.org/10.1016/j.seppur.2025.135163

Nagar, M.S., Morsy, W.M., Bayoumi, M.B., & Shalan, A.S. (2021). Potentiality of Caro's acid in the leaching of uranium from Abu-Rusheid mylonitic gneiss rocks, South Eastern Desert, Egypt. *Results in Materials*, vol. 11, article 100214. https://doi.org/10.1016/j.rinma.2021.100214

Nicol, M.J. (2020). The role and use of hydrogen peroxide as an oxidant in the leaching of minerals. II. alkaline solutions. *Hydrometallurgy*, Vol. 194, 105365 https://doi.org/10.1016/j.hydromet.2020.105365

Pownceby, M.I. & Johnson, C. (2014). Geometallurgy of Australian uranium deposits. *Ore Geology Reviews*, vol. 56, pp. 25–44. https://doi.org/10.1016/j.oregeorev.2013.07.001

Venter, R. & Boylett, M. (2009). The evaluation of various oxidants used in acid leaching of uranium. *Hydrometallurgy Conference 2009, The Southern African Institute of Mining and Metallurgy.*

Dr Walter Amos Ngobeni

Technical Manager – Mining and Metallurgy
BME Metallurgy, A Division of the Omnia Group

Dr Walter Amos Ngobeni is a metallurgical engineer and extractive metallurgy expert with over 16 years of experience spanning mineral processing, hydrometallurgy, product development, research and development. He holds a PhD in Metallurgical Engineering from the University of Johannesburg, where he was also honoured with the prestigious Golden Key Award for academic excellence.

Dr Ngobeni currently serves as Technical Manager – Mining & Metallurgy at BME Metallurgy, a division of the Omnia Group. His technical expertise covers a broad spectrum of commodities, including Aluminium, Coal, Cobalt, Copper, Gold, Iron, Lead, Lithium, Mineral Sands, Nickel, Platinum Group Metals, Phosphate, Rare Earth Elements, Uranium, and Zinc.

Dr Walter Amos Ngobeni is committed to advancing academic excellence and promoting professional development within the field of mineral science. He is a regular contributor to both local and international conferences. His work is published in peer-reviewed journals. Beyond his technical contributions, he serves on the Advisory Board of the Vaal University of Technology, where he actively shapes curriculum standards, promotes industry-academic collaboration, and mentors emerging talent in metallurgical engineering. Additionally, he serves as a peer reviewer for the Minerals Engineering journal, lending his technical expertise to uphold the integrity and quality of scholarly research in mineral processing and extractive metallurgy.

Purification of the nanofiltration product using magnesium oxide to remove iron and other impurities from uranium

W.A. Ngobeni, D. Verwey

BME Metallurgy, A Division of the Omnia Group. South Africa

Solvent extraction is a process that uses solvents to remove impurities and purify uranium before the final product is precipitated. These solvents are hazardous, flammable and costly. Despite its effectiveness, the process is associated with high operating costs, emulsion formation, and environmental and health hazards. To address these challenges, reduce costs, eliminate safety hazards, and improve the Environmental, Social and Governance score, a Namibian operation investigated the feasibility of replacing solvent extraction with nanofiltration. The investigation showed that nanofiltration successfully upgraded uranium, reduced product stream volume by 75%, and produced clean, recyclable acid. However, nanofiltration was less selective than solvent extraction and yielded a product with higher impurities, requiring further purification to meet the target product specification. The objective of this study was to precipitate nanofiltration product impurities without co-precipitating uranium. Precipitation was performed using high and low-purity magnesium oxide (MgO). Furthermore, to assess the effect of iron oxidation state, precipitation was conducted on the sample with and without a ferric–ferrous redox buffer wire. The results with wire showed that ferric precipitation above 90% was achievable, but ferrous precipitation was low under all conditions tested. Tests without wire showed improved performance, including partial ferrous precipitation (70%). Low-purity MgO achieved higher iron precipitation but also increased uranium co-precipitation. Based on these results, it was concluded that selective precipitation with MgO is technically feasible, provided ferrous is oxidised to ferric before precipitation. Further optimisation of MgO dosing and redox control is recommended to minimise uranium co-precipitation and achieve the target product specification.

Keywords: Uranium, precipitation, hydrogen peroxide, magnesium oxide, Pourbaix diagram, hydrometallurgy, solvent extraction

INTRODUCTION

Uranium operations involve two major activities, namely mining uranium-bearing rock and processing it into uranium oxide. The alaskite, a granitic uranium rock, is mined in an open-pit mine. The mined rock undergoes primary crushing, followed by fine crushing and hydrometallurgical processing to produce triuranium octaoxide (U_3O_8), commonly known as yellowcake. These hydrometallurgical processes include solid-liquid separation, counter-current ion exchange (CIX) and solvent extraction (SX) (Kiegiel *et al.*, 2016). Since most uranium ores contain other metals that coexist with uranium, post-leaching liquors usually contain a mixture of metal ions that must be separated from UO_2^{2+} using a series of hydrometallurgical processes (Kiegiel *et al.*, 2016). Solvent extraction is the final step before uranium oxide is precipitated. It is an important method that uses organic solvents and extractants to remove impurities and purify uranium oxide, ensuring that the yellowcake meets the specification. This refined product is securely packaged and shipped to customers worldwide.

The organic solvents and extractants used in solvent extraction are hazardous, volatile, flammable and costly. Despite its effectiveness, the SX process is associated with high operating costs, emulsion and crud formation, and environmental and health hazards. All these factors affect the overall productivity, operational profitability, and environmental and occupational safety of the uranium processing plant. These advantages have prompted industry interest in exploring alternative hydrometallurgical processes that are more efficient, cleaner, and easier to manage operationally.

Nanofiltration (NF) membrane technology offers advantages, including the elimination of hazardous solvents and extractants, thereby improving the Environmental, Social and Governance (ESG) score; improved process control and efficiency; reduced downtime due to crud emulsion and crud formation; reduced reagent costs associated with procuring solvents and extractants and production of clean recyclable acid, which would further reduce operational cost due to reduction in fresh acid requirement.

One of Namibia's uranium operations is investigating the technical feasibility of replacing the SX processing step with NF membrane technology in uranium hydrometallurgy. The investigation showed that, compared to SX, nanofiltration yielded 23 times better uranium upgrade, reduced the product stream volume by 70%, and produced clean, recyclable acid. However, NF membrane technology was less selective than SX and yielded a product with higher impurities, requiring further purification to meet the target yellow cake specification.

Precipitation is a method that can be used to further purify the NF product and meet the required yellow cake specification. However, post-nanofiltration impurity removal remains under-reported in the literature. Dutrizac (1985) proposed five criteria that must be satisfied for precipitation to be considered a viable purification technique: the precipitate must (i) be easy to wash and filter, (ii) not co-precipitate valuable metals, (iii) be cost-effective and compatible with the downstream processes, (iv) keep the other impurities under control and (v) yield a precipitate that is easy to handle, reusable or preferably saleable. If the precipitated iron in this study meets the five criteria proposed by Dutrizac (1985), it may be recycled as an oxidant for uranium leaching, offering further potential reductions in overall operating costs.

Precipitation is a chemical method used to recover metal components by exploiting the specific solubility characteristics of different dissolved metal ions, which form insoluble compounds (Seo *et al.*, 2016; Nguegang & Ambushe, 2024; Gangadari *et al.*,2025). In precipitation, the precipitant gradually increases the pH and selectively targets specific ions based on their oxidation state, leaving unwanted ions in solution. Three stages must be met for a specific ion to precipitate successfully: nucleation, particle growth, and Ostwald ripening (Nguegang & Ambushe, 2024). The process was chosen because it is fast, easy to operate, has a low footprint, is cost-effective, and requires low dosages (Yang *et al.*, 2025; Nguegang & Ambushe, 2024). There are different precipitants used commercially for this purpose, including sodium hydroxide (NaOH), calcium hydroxide ($(Ca(OH)_2$), sodium carbonate (Na_2CO_3) (Seo *et al.*, 2016), hydrogen peroxide (H_2O_2) (Yamine & Waters, 1980), magnesium oxide (MgO)(Nguegang & Ambushe, 2024), oxygen (O_2), sulfur dioxide (SO_2) (Yang *et al.*, 2025) and ammonia (NH3)(Yamine & Waters, 1980). Among all commercially available precipitants, MgO has emerged as a promising precipitant because it is soluble in acidic solutions and has a high alkalinity-generating potential (AGP). The high AGP indicates that a small amount can be used to treat a large volume of solutions, thereby reducing sludge generation (Nguegang & Ambushe, 2024).

The objective of this study was to precipitate nanofiltration product impurities without co-precipitating uranium. This was performed using high (HP) and low-purity (LP) MgO. Furthermore, to assess the effect of iron oxidation state, precipitation was conducted on the sample with and without a ferric–ferrous redox buffer wire. The precipitation tests were conducted at the Fe:MgO ratio of 1:1, selected to ensure sufficient alkalinity generation while limiting excess MgO addition, and a precipitation duration of two hours. These were based on optimisation tests, which fall outside the scope of this paper. Filtrate and solids were analysed for uranium, total iron, ferric iron, and ferrous iron. The performance of the two MgO (low- and high-purity) samples was evaluated based on iron species precipitation and selectivity between uranium and iron species. The precipitation tests were performed on the CIX eluate, with (W/W) and without a wire (N/W), after concentration in the NF pilot plant.

METHODOLOGY AND EXPERIMENTAL

Materials

Feed composition

The NF products were characterised prior to precipitation testing with respect to key dissolved constituents relevant to the study, including uranium, iron, manganese, magnesium, and other associated elements. The NF product compositions used in the precipitation tests, with and without wire addition, are summarised in Table I.

Table I. NF products with and without wire addition elemental composition in ml/L

	Na	Ca	Mn	Mg	V	Al	Cr	U	Fe	Fe^{2+}	Fe^{3+}
W/wire	302.73	40.00	132.92	142.88	0.96	91.68	6.45	3162	2254.90	17.00	26.93
N/wire	305.28	42.80	168.68	146.32	1.050	93.93	7.12	3346	2540.19	12.50	46.50

Reagents

Proprietary high- and low-purity MgO samples supplied by BME Metallurgy (Pty) Ltd., Wadeville, South Africa, were used as precipitants in this study. The MgO samples were received as white powders. A high level of active MgO content and low impurities characterised the high-purity MgO sample. In contrast, the low-purity MgO sample contained higher impurities and lower active content. Both reagents were used as received, without further purification or pre-treatment, to ensure that the test conditions reflected practical industrial application. The use of proprietary materials is acknowledged, and detailed compositional data are therefore not disclosed; however, the comparative evaluation of high- and low-purity MgO allowed assessment of reagent quality on precipitation efficiency and selectivity under controlled laboratory conditions.

Experimental parameters

A summary of the key parameters applied during the precipitation test work is provided in Table II. These parameters include the relevant operating and experimental conditions under which the tests were conducted, such as NF product with (W/W) or without the wire (N/W), MgO purity, MgO/Fe ratio, solution volume, initial pH, precipitation duration, and pH monitoring intervals.

Table II. The summary of the precipitation test parameters with and without the wire

	Units	High purity MgO	Low purity MgO
NF product sample		W/W or N/W	W/W or N/W
Sample volume	ml	400	400
Precipitation duration	Hrs	2	2
Precipitant/Fe ratio	-	1.1	1.1
Initial pH	-	0.48	0.48
pH interval	Min	0, 15, 30, 45, 60, 75,90,105,120	0, 15, 30, 45, 60,75,90,105,120

The composition of the SX product targeted by the precipitation test work is presented in Table III. This composition represents the desired downstream solution quality following successful precipitation and serves as a benchmark against which the experimental results were evaluated. The SX product composition was defined based on typical process requirements, including acceptable uranium and selected impurity concentrations (e.g., iron, manganese, and magnesium), to ensure compatibility with subsequent uranium final product precipitation (yellow cake).

Table III: Solvent extraction product composition

Parameter	Value	Units
Sodium as Na	131	mg/l
Magnesium as Mg	6.4	mg/l
Calcium as Ca	14	mg/l
Manganese as Mn	1.6	mg/l
Iron as Fe	<0.01	mg/l
Chromium as Cr	5.7	mg/l
Aluminium as Al	<0.01	mg/l
Vanadium as V	<0.01	mg/l

Experimental procedure

Laboratory precipitation test work was conducted on site on the nanofiltration product with and without a wire in accordance with the standard BME Metallurgy operating procedure. A 400 mL aliquot of the NF product solution was measured, transferred to a 600 mL beaker, and agitated on a magnetic stirrer with the hot plate switched off, ensuring all tests were stirred at a consistent speed. Precipitants corresponding to the required MgO/Fe ratio were weighed accurately to the nearest 0.001 g and added to the agitated solutions, at which point timing was initiated. Tests were staggered at one-minute intervals to allow sufficient time for pH measurement and filtration. Beakers were alternated between magnetic stirrer positions every 30 minutes to minimise positional effects. The pH and temperature of each solution were recorded at 0, 15, 30, 45, 60, 75, 90, 105 and 120 minutes. After a precipitation duration of two hours, the solutions were filtered, and the filtrates were retained for analysis of uranium, total iron, calcium, sodium, manganese, and magnesium using Inductively Coupled Plasma Optical Emission Spectroscopy (ICP-OES) (PerkinElmer, South Africa), while ferric iron and ferrous iron were determined by titration. The collected solids were oven-dried and weighed, after which the residues were analysed for total iron, sodium, calcium, manganese, magnesium, and uranium using ICP-OES (PerkinElmer, South Africa). Precipitation efficiency and selectivity were subsequently calculated based on the solution and solid analyses. For quality control and assurance, each precipitation condition was evaluated in duplicate, and the reported results represent average values. To ensure experimental consistency and reliability, all tests with a variance above 5% were repeated, and only those with a variance below 5% between duplicate tests were included in the averaged results.

RESULTS AND DISCUSSIONS

This section presents a comparative analysis of experimental results obtained with low-purity and high-purity MgO for precipitating the NF product, with and without a ferric–ferrous redox buffer wire. The data presented here are averages from duplicate tests conducted on different days. To ensure experimental consistency and reliability, only tests with variances below 5% were included in the averages. The primary response variable investigated in this study and presented in this section was the percentage precipitation of total iron, ferrous iron, ferric iron species and uranium. These variables were selected to evaluate the effectiveness and selectivity of the precipitation process under varying MgO purity and iron redox-reduction conditions. The objective of this paper was to achieve a balance between maximising iron species precipitation while minimising co-precipitation of uranium. This balance is critical for optimising downstream process performance, as preferential iron removal reduces impurity loading while retaining uranium in solution for subsequent recovery. The precipitation efficiencies of the individual iron species and uranium were therefore quantified and compared to assess selectivity and to identify conditions that favour selective iron removal with minimal uranium losses.

Precipitation rate was calculated using Equation 1, which relates the concentration of a given species in solution before and after precipitation to quantify the extent of removal. This calculation provides a normalised measure of precipitation performance, expressed as a percentage, and enables direct comparison between different test conditions (Nguegang & Ambushe, 2024).

$$Precipitation = \left(\frac{C_i - C_f}{C_f}\right) \times 100 \quad [1]$$

where C_i refers to the initial concentration of the species of interest in the precipitation feed, and C_f is its final concentration at the end of the experiment, after the prescribed precipitation time and subsequent filtration. The difference between these concentrations reflects the degree to which the species has been removed from solution by precipitation.

Comparison of LP and HP MgO on the NF product with the wire

The comparative precipitation results obtained using low-and high-purity MgO on the NF product with the wire are presented in Figure 1. High-purity MgO yielded higher iron species precipitation than low-purity MgO. The precipitation values were 94%, 60% and 6% for ferric iron, total iron and ferrous iron, respectively. On the contrary, the precipitation values achieved with low-purity MgO were 5%, 29% and 5%, respectively. Uranium co-precipitation was also substantially lower when using high-purity MgO (5%) compared with low-purity MgO (25%).

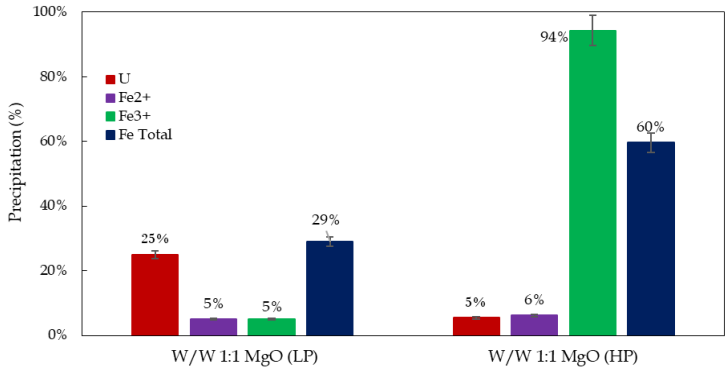

Figure 1. Comparison of LP and HP MgO on the NF product sample with the wire.

From a theoretical perspective, the effectiveness of MgO as a precipitant is governed primarily by its hydration rate to magnesium hydroxide ($Mg(OH)_2$), as shown in Equation 2.

$$Mg^{2+} + 2H_2O \rightarrow Mg(OH)_2 \quad [2]$$

The release of hydroxide ions in Equation 2 increases solution pH, thereby promoting precipitation (Nguegang & Ambushe, 2024). In general, high-purity MgO would be more reactive, leading to a more rapid and higher degree of MgO content, which would result in sustained alkalinity generation. This promotes favourable conditions for the hydrolysis and precipitation of ferric iron as amorphous iron hydroxides, which precipitate efficiently from pH 3.5 (Seo *et al*., 2017). The high precipitation of ferric iron observed with high-purity MgO is therefore consistent with classical iron hydrolysis theory, in which Fe^{3+} readily forms insoluble hydroxides once sufficient alkalinity is achieved.

By contrast, ferrous iron precipitation is kinetically and thermodynamically less favourable under the same conditions, as Fe^{2+} requires either oxidation to Fe^{3+} or pH values above 6 to precipitate directly as ferrous hydroxide (Seo *et al*., 2017; Gangadari *et al*.,2025). The iron Pourbaix diagram in Figure 2 further illustrates this.

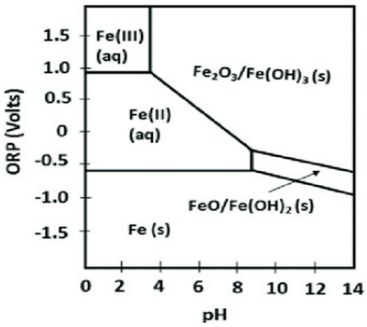

Figure 2. Illustration of an iron Pourbaix diagram adapted from Beverskog & Puigvomenech (1996), pp. 2130 .

The low ferrous iron precipitation (≤6%) observed for both MgO grades suggests that limited oxidation occurred during the test work and that the pH achieved was low. In contrast, sufficient ferric iron precipitation remained inadequate for effective ferrous iron precipitation (Gangadari *et al.*, 2025). Consequently, total iron precipitation was largely governed by the fraction of iron present in the ferric state.

The lower precipitation observed with low-purity MgO can be attributed to impurities that may have reduced its alkalinity-generating potential. Additionally, slower hydration kinetics associated with lower MgO purity can result in insufficient hydroxide availability during the reaction time, thereby limiting iron hydrolysis and precipitation. These factors also explain the higher uranium co-precipitation observed with low-purity MgO. In alkaline systems, uranium precipitation often occurs via adsorption or co-precipitation onto freshly formed iron hydroxides; less selective, poorly crystalline precipitates formed under sub-optimal alkalinity can enhance unintended uranium removal.

Although the use of high-purity MgO improved iron selectivity and reduced uranium losses, the overall performance remained inadequate relative to downstream process requirements. At the conclusion of the tests, more than 95% of ferrous iron and approximately 40% of total iron remained in solution. This indicates that, despite improved ferric iron removal, the precipitation system was constrained by insufficient ferrous iron conversion and inadequate pH elevation. From a process design perspective, these results highlight the need for an upstream oxidation step to convert Fe^{2+} to Fe^{3+}.

Comparison of LP and HP MgO on the NF product sample without the wire

The results comparing precipitation achieved with low-purity and high-purity MgO on the NF product without the wire are presented in Figure 3. Contrary to the trends observed for the NF product with the wire, the results showed that low-purity MgO yielded higher precipitation of iron species than high-purity MgO. The precipitation values were 97%, 92% and 78% for ferric iron, total iron and ferrous iron, respectively. On the contrary, the precipitation values achieved with high-purity MgO were 68%, 69% and 73%, respectively. Furthermore, the high-purity MgO yielded a lower uranium co-precipitation (20%) than low-purity MgO (31%), as observed in the previous section with the wire.

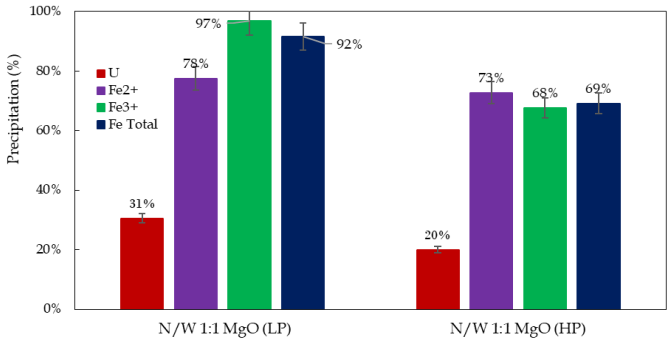

Figure 3. Comparison of LP and HP MgO on the NF product sample without the wire.

These results corroborated the hypothesis presented in the previous section that the upstream oxidation step is needed to convert Fe^{2+} to Fe^{3+}, as Fe^{3+} accounted for 79% in the sample without the wire, compared with 56% in the sample with the wire (Table I). There is a noticeable difference in the precipitation, especially with the low-purity sample. This speciation difference provides a mechanistic explanation for the markedly improved iron precipitation observed in these experiments.

Under these conditions, the presence of ferric iron was the driving force for precipitation, masking the effect of MgO reactivity. Hence, low-purity MgO, despite containing lower active MgO content, was able to generate sufficient alkalinity to promote precipitation.

The lower iron precipitation observed with high-purity MgO in this instance may be attributed to its higher hydration rate and the faster release of hydroxide ions. A faster localised pH increase can lead to the formation of fine particles due to insufficient time for growth and Ostwald ripening, thereby reducing precipitation efficiency (Nguegang & Ambushe, 2024).

Ferrous iron precipitation remained lower than ferric iron precipitation across both MgO grades, consistent with theoretical expectations. Although some ferrous iron precipitation was observed, it could not have been due to ferrous oxide or ferrous hydroxides, as the pH was too low for them to be thermodynamically stable. However, there is a critical pH above which ferric hydrolysis leads to the hydrolytic precipitation of other species (Yang *et al.*, 2025). This is because the ferric hydroxide precipitate has a high surface area and unsaturated Fe^{3+} and OH^- bonds that can attach to different impurity elements via chemical bonding or surface adsorption (Dutrizac, 1985). This is a more plausible explanation for the observed increase in ferrous precipitation.

Uranium behaviour followed trends consistent with co-precipitation theory. Uranium in alkaline systems is commonly removed through adsorption onto freshly formed iron hydroxide precipitates rather than direct precipitation. The higher uranium losses associated with low-purity MgO correlate with the substantially higher iron precipitation and the formation of larger quantities of iron hydroxide solids. Conversely, high-purity MgO, while less effective for iron removal in this instance, maintained improved selectivity by limiting excessive iron precipitation and, therefore, reducing uranium adsorption sites.

Performance of LP MgO on NF product with and without the wire

The results comparing precipitation with low-purity MgO on the NF product, with and without the wire, are presented in Figure 4. The results showed that precipitation of iron species was higher in the absence of the wire than in its presence. The precipitation values were 97%, 92% and 78% for ferric iron, total iron and ferrous iron, respectively. On the contrary, the precipitation values obtained with the wire were 5%, 29%, and 5%, respectively. However, the results with the wire showed a lower uranium co-precipitation rate (25%) than those without the wire (31%).

These results corroborated the hypothesis presented in the previous section that the upstream oxidation step is needed to convert Fe^{2+} to Fe^{3+}, as Fe^{3+} accounted for 79% in the sample without the wire, compared with 56% in the sample with the wire (Table I). There is a noticeable difference in the precipitation, especially with the low-purity sample.

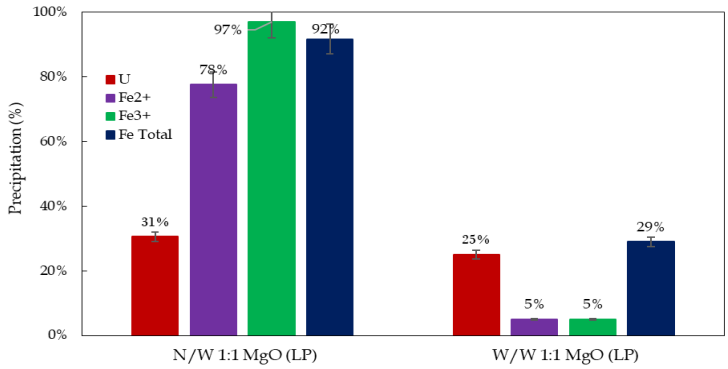

Figure 4. Performance of LP MgO on NF product with and without the wire.

The precipitation performance observed for the NF product treated with low-purity MgO aligns with established theory on iron redox and hydrolysis discussed in earlier sections. Ferric iron hydrolyses and precipitates readily at pH 3.5 (Seo *et al*., 2017), whereas ferrous iron remains relatively soluble unless the pH rises above 6 (Seo *et al.,* 2017; Gangadari *et al.,* 2025). Consequently, effective iron precipitation using MgO is primarily driven by the iron oxidation state.

The comparatively low precipitation observed in the wire-containing system is therefore attributed to insufficient availability of ferric iron rather than to the effect of MgO. This effect was particularly evident with low-purity MgO, whose slower dissolution kinetics require favourable iron speciation to achieve effective precipitation. Under these conditions, incomplete oxidation resulted in minimal precipitation of ferrous iron.

Uranium co-precipitation was lower in the presence of the wire (25%) than in its absence (31%). This trend is consistent with uranium surface adsorption onto freshly precipitated ferric hydroxides; reduced ferric hydroxide precipitation correspondingly limited uranium co-precipitation.

Performance of HP MgO on NF product with and without the wire

The results comparing precipitation with high-purity MgO on the NF product, with and without the wire, are presented in Figure 5. The results showed that higher total iron, ferrous iron, and uranium were achieved with wire than without. The precipitation values were 73%, 69% and 20% for ferrous iron, total iron and uranium co-precipitation, respectively. On the contrary, the precipitation values obtained with the wire were 6%, 60%, and 20%, respectively. However, the results with the wire showed a lower ferrous precipitation (94%) than those without the wire (68%).

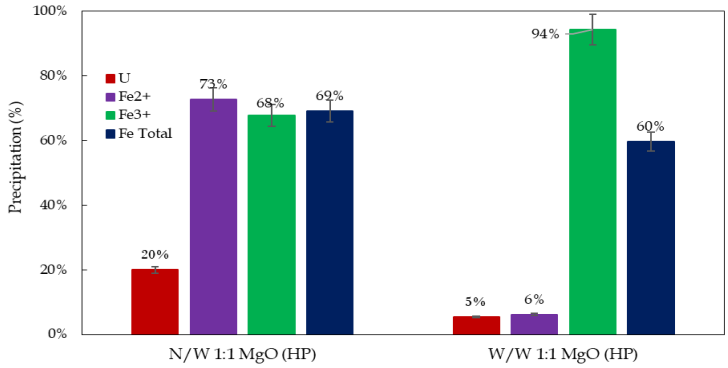

Figure 5. Performance of HP MgO on NF product with and without the wire.

The precipitation behaviour observed with high-purity MgO differs from that obtained with low-purity MgO, reflecting the higher reactivity and faster dissolution kinetics of the reagent. High-purity MgO provides faster pH change, enabling effective iron precipitation even under less favourable oxidation conditions.

The high-purity MgO showed reduced dependency on iron speciation, achieving moderate total iron precipitation even when the oxidation-reduction environment changed. This behaviour is attributed to the faster dissolution of high-purity MgO, which promotes precipitation at higher pH values. However, the observed difference in ferrous iron precipitation confirms that oxidation was still one of the factors controlling the efficiency of iron precipitation.

Uranium co-precipitation was low and similar under both conditions, indicating limited sensitivity to oxidation state and supporting adsorption-based mechanisms onto ferric precipitates once sufficient iron solids are present.

CONCLUSION AND RECOMMENDATIONS

This paper evaluated the feasibility of selectively removing iron impurities from a nanofiltration product using magnesium oxide, with particular emphasis on the effects of MgO purity and iron oxidation state. The results demonstrate that iron precipitation efficiency depended mainly on iron speciation rather than MgO purity.

As theoretically and thermodynamically expected, ferric iron precipitated sufficiently once sufficient alkalinity was created across all test conditions. Ferrous iron precipitation was lower because pH did not increase sufficiently to promote its precipitation. Tests conducted without the wire consistently achieved higher total and ferrous iron precipitation for both MgO grades. This supported the hypothesis that oxidation of Fe^{2+} to Fe^{3+} was required to achieve effective iron precipitation at these low pH values. Low-purity MgO achieved higher overall iron precipitation under favourable oxidation conditions but also led to increased uranium co-precipitation. In contrast, high-purity MgO provided improved selectivity and lower uranium losses, particularly when oxidation-reduction environment effects were less pronounced, owing to its higher reactivity and faster alkalinity generation potential. However, high-purity MgO alone was insufficient to cater for poor ferrous oxidation.

Uranium behaviour was consistent with co-precipitation and adsorption theory, with uranium losses increasing in proportion to ferric hydroxide formation. Selective iron precipitation, therefore, requires careful control of both oxidation and precipitation conditions to limit the formation of excessive iron hydroxide surfaces. The study showed that selective impurity precipitation of NF products using MgO was technically feasible, but fine-tuning and optimisation would be required to meet the final product specification. Furthermore, the results showed that both MgO purity and oxidation-reduction conditions contribute in complementary ways to precipitation. Therefore, a multi-lever approach would be required to achieve the objectives sufficiently. Therefore, pre-oxidation of ferrous iron to ferric iron using hydrogen peroxide before MgO precipitation is recommended. Hydrogen peroxide is preferred because it provides a faster, more controlled, and residue-free oxidation environment for converting Fe^{2+} to Fe^{3+} without introducing additional dissolved solids.

ACKNOWLEDGMENTS

The authors gratefully acknowledge the support of BME Metallurgy management, who granted permission to publish this work. Mr Reinhold Katti is acknowledged for their invaluable assistance with precipitation tests, and Mr Lawrence Tjatindi is also acknowledged for coordinating and overseeing the whole test programme.

REFERENCES

Beverskog, B. & I. Puigdomenech, I. (1996). Revised Pourbaix diagrams for iron at 25 – 300 ºC.

Dutrizac, J.E. (1985). An Overview of Iron Precipitation in Hydrometallurgy. Canmet, pp. 259 – 283.

Gangadari, T., Mohammad Rezaee, M., & Pisupati, S.V. (2025). A critical review on selective separation of scandium and iron from aqueous solutions. *Hydrometallurgy*, vol. 236, pp. 106514. https://doi.org/10.1016/j.hydromet.2025.106514

Kiegiel, K., Abramowska, A., Biełuszka, P., Zakrzewska-Kołtuniewicz, G., Wołkowicz, S. (2016). Solvent extraction of uranium from leach solutions obtained in processing of Polish low-grade ores. *J Radioanal Nucl Chem*, vol. 311, pp. 589–598. https://doi.org/10.1007/s10967-016-5029-5

Nguegang, B., & Ambushe, A.A. (2024). Insight into the chemical and biochemical mechanisms governing inorganic contaminants removal by selective precipitation and neutralization in acid mine drainage treatment using MgO: A comparative study. Journal of Water Process Engineering, vol. 59, pp. 104924. https://doi.org/10.1016/j.jwpe.2024.104924.

Seo, E.Y., Cheong, Y.W., Yim, G.J., Min, K.W., & Geroni, J.N. (2017). Recovery of Fe, Al and Mn in acid coal mine drainage by sequential selective precipitation with control of pH. *Catena*, vol. 148, pp. 11–16. http://dx.doi.org/10.1016/j.catena.2016.07.022

Yamine, M., & Waters, D.J. (1980). An improved precipitation technique for recovery of uranium from its liquors. *Chemeca*, 80, pp. 127–133.

Yang, Z., Shi, Y., Xu, J., Yiquan Yang, Y., Wang, Z., Ba, H., Zhang, Y., Yang, B., Cai, Y., Wang, J., Jianyu Zhu, J., Qiu, G., & Min Gan, M. (2025). Advances in iron and manganese removal technologies for sustainable copper-cobalt hydrometallurgy. *Minerals Engineering*, vol. 234, pp. 109771. https://doi.org/10.1016/j.mineng.2025.109771

Dr Walter Amos Ngobeni

Technical Manager – Mining and Metallurgy
BME Metallurgy, A Division of the Omnia Group

Dr Walter Amos Ngobeni is a metallurgical engineer and extractive metallurgy expert with over 16 years of experience spanning mineral processing, hydrometallurgy, product development, research and development. He holds a PhD in Metallurgical Engineering from the University of Johannesburg, where he was also honoured with the prestigious Golden Key Award for academic excellence.

Dr Ngobeni currently serves as Technical Manager – Mining & Metallurgy at BME Metallurgy, a division of the Omnia Group. His technical expertise covers a broad spectrum of commodities, including Aluminium, Coal, Cobalt, Copper, Gold, Iron, Lead, Lithium, Mineral Sands, Nickel, Platinum Group Metals, Phosphate, Rare Earth Elements, Uranium, and Zinc.

Dr Walter Amos Ngobeni is committed to advancing academic excellence and promoting professional development within the field of mineral science. He is a regular contributor to both local and international conferences. His work is published in peer-reviewed journals. Beyond his technical contributions, he serves on the Advisory Board of the Vaal University of Technology, where he actively shapes curriculum standards, promotes industry-academic collaboration, and mentors emerging talent in metallurgical engineering. Additionally, he serves as a peer reviewer for the Minerals Engineering journal, lending his technical expertise to uphold the integrity and quality of scholarly research in mineral processing and extractive metallurgy.

Transforming uranium hydrometallurgy: Reagent recovery and operational expenditure optimization through nanofiltration

L. Bartel[1], T. Coetzee[1], W. Ngobeni[2], D. Verwey[2]

[1]Memcon, South Africa
[2]BME Metallurgy, A Division of the Omnia Group, South Africa

Acid and alkaline leaching are the two traditional hydrometallurgical routes for uranium processing. These traditional routes are associated with high reagent consumption, large waste generation, increased operating costs and environmental impacts. This has prompted the uranium industry to look for alternative separation technologies that enable reagent recycling and process simplification. This study presents pilot-scale results from two case studies that integrated membrane technology into uranium hydrometallurgy: one based on an alkaline route and the other on an acidic route. In both cases, ultrafiltration (UF) was used to remove suspended solids, followed by nanofiltration (NF) for selective uranium concentration and reagent recovery. The NF stage used multiple 4040 spiral-wound modules to evaluate commercially available membranes under representative process conditions. The acidic pilot campaign was conducted at a uranium processing plant in Namibia, while the alkaline trials were completed at a research facility in France. Results showed that UF achieved effective removal of solids and colloids. NF selectively concentrated uranium while allowing reagents to permeate, enabling recycling of sulphuric acid in the acidic circuit and sodium bicarbonate and sodium carbonate in the alkaline circuit. Uranium concentrations increased from 375 mg/L in the feed to 2,470 mg/L in the NF concentrate. Reagent recoveries of up to 97% sulphuric acid and 89–94% carbonate were achieved. Overall mass balances demonstrated good accountability. The pilot results confirm that integrated UF–NF circuits offer a technically viable option for reducing reagent consumption, simplifying flowsheets, and lowering environmental impact in commercial uranium hydrometallurgical operations.

Keywords: Uranium; nanofiltration; ultrafiltration; reagent recycle; sulphuric acid; hydrometallurgy; sodium carbonate; sodium bicarbonate.

INTRODUCTION

Acid (sulphuric acid) or alkaline (sodium carbonate/sodium bicarbonate) leaching are the two main hydrometallurgical routes for uranium processing. The choice of hydrometallurgical route depends on the mineralogy of the ore, the type of gangue minerals present in the ore, and the downstream processing requirements. Acid or alkaline leaching routes are well established and technically reliable. However, they are generally associated with high reagent consumption, high liquid circulation volumes, and large volumes of solid waste, all of which contribute significantly to operational expenditure (OPEX) and negative environmental impact (Venter & Boylett, 2009; Giusti et al., 2024).

In traditional uranium flowsheets, recovered uranium is further concentrated and purified using a combination of counter-current ion exchange (CIX) and solvent extraction (SX), followed by precipitation to produce a yellowcake product (Kiegiel et al., 2016). Although these processes have been used successfully for decades, they are not foolproof, as they rely heavily on hazardous, volatile, and flammable chemical reagents that pose safety and environmental risks and operational constraints. For instance, solvent extraction, the use of organic solvents, is characterised by operational risks such as fire hazard due to the use of flammable and volatile solvents, solvent losses, phase disengagement time (PDT) challenges, and emulsion and crud formation (Giusti et al., 2024). The increasing pressure to reduce reagent consumption, lower operational costs, improve resource efficiency, minimise the environmental footprint, and boost Environmental, Social and Governance (ESG) scores has therefore prompted the uranium industry to explore alternative or complementary concentration and purification technologies.

Integrating membrane separation technologies, especially ultrafiltration (UF) and nanofiltration (NF), as alternatives or complements to traditional hydrometallurgical circuits has shown promising results. Originally developed for water and wastewater treatment, membrane technology is increasingly being adopted in hydrometallurgy for metal concentration and reagent recycle due to their low energy demand, low footprint, and ability to selectively separate monovalent from divalent and multivalent species by pore size-exclusion (Peng et al., 2024; Wen et al., 2024), Donnan exclusion, and electrostatic charge repulsion (Botelho Junior et al., 2025; Yazzie et al., 2024). Separation in membrane technology is achieved by membranes' ability to allow monovalent ions, such as hydrogen, bicarbonate, and carbonate species, to permeate while retaining divalent and multivalent species (Yazzie et al., 2024). Pore-size rejection performance in membrane technology is ranked in the following order: RO > NF > UF.

Recent studies have demonstrated the potential of NF membranes for uranium-bearing solutions, including groundwater remediation, seawater extraction, and treatment of alkaline leach solutions. These studies have shown that uranium rejection is strongly influenced by solution chemistry, membrane surface charge, pH, and ionic strength, highlighting the importance of membrane selection and process configuration (Wanjiya et al., 2024; Yazzie et al., 2024; Saeed et al., 2005). However, most published work remains limited to laboratory-scale investigations, with no pilot-scale studies. Therefore, this study aimed to address this research gap by presenting pilot-scale results from two uranium-processing case studies, one from an acid leach operation and the other from an alkaline operation, in which an integrated UF–NF membrane system was evaluated. In this integrated system, UF was used to remove solids and organic foulants, while NF was used to concentrate uranium and recover reagents. The nanofiltration stage used multiple 4040 spiral-wound membrane modules, primarily for comparative screening of commercially available NF membrane types. The work focused on the comparative performance of commercially available UF and NF membranes under representative process conditions, assessing uranium retention, reagent permeation (sulphuric acid, sodium carbonate and sodium bicarbonate), membrane stability, fouling behaviour and flux. The pilot programme ran for approximately nine weeks of cumulative operation, enabling assessment of process stability, membrane performance and fouling behaviour during extended operation. By demonstrating sustained performance over the extended pilot operation, the study aimed to establish membrane-integrated circuits as a technically and economically viable option for reagent recovery and OPEX reduction in commercial uranium hydrometallurgical operations.

From a process optimisation perspective, integrating membrane technology offers opportunities not only for uranium concentration but also for reagent recovery and recycling. For instance, acidic circuits may benefit from the recovery and recycling of sulphuric acid, while alkaline circuits may benefit from sodium bicarbonate and sodium carbonate. This would reduce the need for fresh reagents and reduce the downstream volume requirement. Thereby, ensuring a closed-loop reagent management and improved ESG compliance.

Experimental

Acidic pilot work
Test work was performed at a Uranium mine in Namibia. The primary focus of the tests was to recover unreacted sulphuric acid that was used in excess during elution of the IX process step. Table 1 below indicates a grab sample for the main components of interest for the CIX Eluate produced on site.

Table 1. CIX Eluate solution composition

		CIX eluate solution
Species	Units	Value
Uranium	g/L	3.4
Fe^{2+}	ppm	6.7
H_2SO_4	g/L	98.6

Alkali pilot work
Test work was performed at a Uranium mine in Namibia and at a different uranium source at a research facility in France. The primary focus of the tests was to recover unreacted sodium carbonate and sodium bicarbonate that were used in excess during elution or in an SX strip step. Table 2 below indicates a grab sample for the main components of interest for the SX strip produced on-site.

Table 2. Alkali solution composition

		Eluate (Namibia)	SX Strip (France)
Species	Units	Value	Value
Uranium	g/L	0.37	10
Na_2CO_3	mol/L	0.38	0.09
$NaHCO_3$	mol/L	0.87	0.56

Membranes
Flat-sheet ultrafiltration and nanofiltration membranes were used in this study. Commercially available membranes were used in this study, namely a Hollow fibre type UF membrane and 4040 size NF membranes. The NF membrane used was an acid-stable membrane (for the acid leach) and an alkaline-stable NF membrane (for the alkali leach). The process flow diagram for cross-flow filtration is shown in Figure 1.

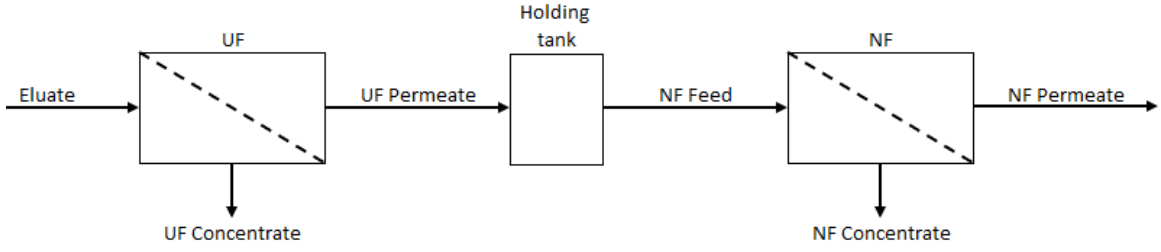

Figure 1: The illustration of the process flow diagram for the cross-flow filtration setup.

Experimental conditions and procedures
The UF and NF mobile pilot plants were transported to two sites (Namibia and France) to process uranium-bearing streams. The acid-leaching study was conducted in Namibia, on an active uranium

mine. The test work was conducted on the CIX eluate stream. A UF pilot plant was set up using a hollow fibre type membrane to pre-condition the fluid for NF separation. The UF plant removes solids from the CIX eluate, which can damage and foul the NF membranes.

A fixed volume of 600 L of feed solution, consisting of CIX eluate, was charged to the UF pilot plant holding tank. The feed stream was circulated through the UF membrane module under controlled pressure conditions to facilitate filtration. Permeate generated during operation was continuously measured and directed to a separate permeate holding tank, while the concentrate stream was recirculated to the feed holding tank. As a result, solute species rejected by the membrane accumulated progressively in the recirculating feed reservoir.

The transmembrane pressure was carefully regulated to maintain the target permeate flux, while ensuring that the maximum allowable operating pressure of the membrane module was not exceeded. The system was operated in batch concentration mode, with the trial continuing until the minimum feed tank level (36 L) was reached (max concentration). Throughout the experiment, key hydraulic parameters, including flow rates and operating pressures, were continuously monitored and recorded. Permeate generated from the UF pilot plant and collected in the holding tank was used as the feed stream for the NF trials. 180 L of this solution was introduced to the NF membrane module under controlled pressure conditions to enable separation. The NF permeate stream flow was continuously measured and collected in designated containers (155 L), while the concentrate stream was recirculated to the holding tank. Consequently, solute species rejected by the NF membrane accumulated within the recirculating feed reservoir over the duration of the trial.

The feed pressure to the NF membrane module was carefully regulated to maintain a target permeate flux, while ensuring that the maximum allowable operating pressure of the membrane was not exceeded. The system was operated in batch concentration mode, with each trial continuing until the minimum holding volume of the feed (holding) tank was achieved (25 L). Samples of both NF permeate and concentrate were collected at defined intervals for subsequent chemical analysis. In parallel, key hydraulic parameters, including flow rates and operating pressures, were continuously monitored and recorded throughout the trial. An acid-stable NF membrane was used in this trial due to its operability at low pH ranges.

The Alkali leaching application was conducted in Namibia on an active uranium mine and in France at a nuclear research facility. The test work was conducted on both the CIX eluate stream (73 L feed) and on the SX strip stream (60 L). The above mentioned experimental setup was followed exactly, except that the NF membrane type changed from an acid stable NF to a alkaline-stable NF and the feed volumes varied slightly.

RESULTS AND DISCUSSION

Ultra filtration pretreatment

The mining process studied typically contains suspended solids, colloids and organic matter that can damage the NF membrane by fouling or abrasion. The UF is commonly used as a pretreatment step to remove the impurities that can cause such damage.

In this study, the eluate was taken and sometimes did not contain significant foulants, meaning the UF was not required to protect the NF membrane. However, to keep the NF feed consistent the UF pretreatment was done and testing was conducted to evaluate the performance and generate data for scale-up, where pretreatment will be necessary for real world mining streams.

The UF system performed as expected, achieving roughly 99% hydraulic recovery and maintaining a stable permeate flux, without signs of fouling or a decrease in permeate flux.

While these results indicate strong UF performance, a lower flux and increased fouling are expected under real process conditions. Therefore, UF remains a vital pretreatment for the plant-scale application.

Acidic pilot work
The NF membrane tested for sulphuric acid recovery achieved a volumetric recovery of 86% v/v. The separation of sulphuric acid from uranium is shown in Figure 2. In the test, 91% of the uranium was recovered in the NF concentrate, and 86% of the sulphuric acid was in the NF permeate.

The separation of uranium from sulphuric acid was as expected. This was because a high volumetric recovery was achieved by the NF membrane system, and the split of uranium and sulphuric acid over the NF membrane was definitive.

The NF permeate can be recycled and reused in the leaching upstream. The reuse of the sulphuric acid will reduce the cost of fresh acid required for leaching and downstream pH neutralization reactions will require less basic reagent volume.

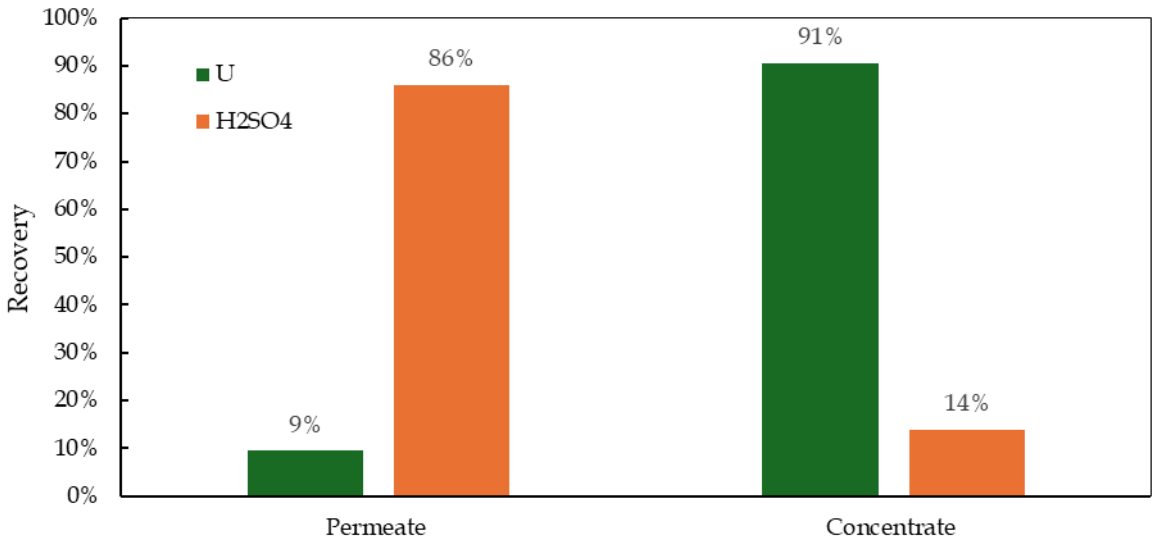

Figure 2: Percentage recoveries of the NF membrane for the acidic pilot trial.

Figure 3 below shows the samples taken during trial work. The samples were analysed by the mine's onsite laboratory. The visual results show a clear separation between the darker concentrate samples and the lighter permeate samples.

Figure 3: Acidic pilot trial samples; feed, concentrates and permeates.

Alkali pilot work

The alkali pilot trial in Namibia reached a volumetric recovery of 92% v/v. The uranium recovery in the NF concentrate was 94%, sodium carbonate recovered in the permeate was 94% and the sodium bicarbonate in the permeate was 89%.

The values are shown in Figure 4 and shows the effective separation of uranium from the mining reagents, sodium carbonate and sodium bicarbonate. The separation was as expected because of the high volumetric recovery. The reason for the difference in sodium carbonate and sodium bicarbonate recovery was not clearly defined and requires further investigation.

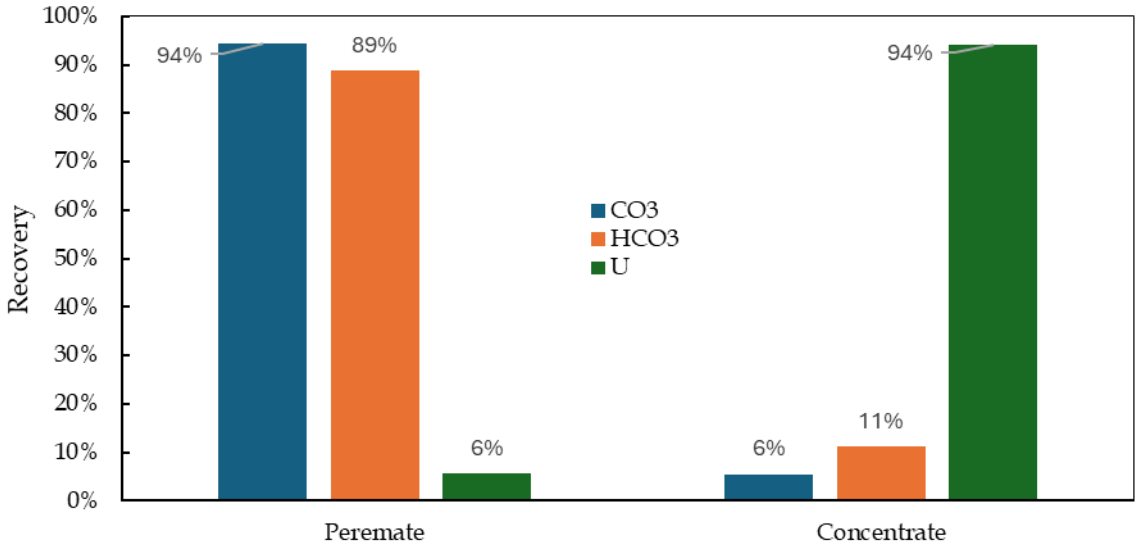

Figure 1: Percentage recoveries of the NF membrane for the alkali pilot trial in Namibia.

Figure 5 shows the samples that were taken during the trial to determine the extent of uranium and reagent separation. The separation between the darker concentrate and the lighter permeate was evident.

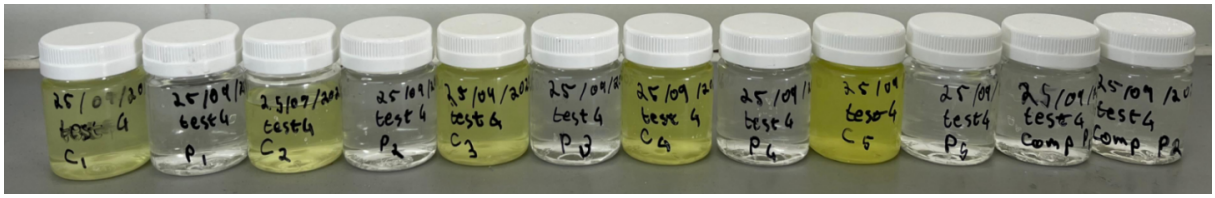

Figure 5: Namibian alkali pilot trial samples, concentrates, and permeates at various concentrations.

The alkali pilot trial in France reached a volumetric recovery of 80% v/v. The uranium concentration in the NF concentrate was 99%, while the carbonate concentration in the permeate was 67% concentration in the NF concentrate was 99%, while the sodium carbonate concentration in the permeate was 67%, and the sodium bicarbonate concentration was 69%. The efficient separation is shown in Figure 6.

The recovery of uranium in the concentrate was as expected. However, the lower recovery of sodium carbonate and sodium bicarbonate in the permeate was not expected. The two alkali trials must be investigated further to determine the cause of the difference in sodium carbonate and sodium bicarbonate recoveries but it is theorised this is due to charge density differences between the two species. The observed difference in permeation of sodium carbonate and sodium bicarbonate is likely attributable to differences in ionic valence and effective charge density. Carbonate ions (CO_3^{2-}), being

divalent, experience stronger electrostatic repulsion from the negatively charged nanofiltration membrane surface compared to monovalent bicarbonate ions (HCO_3^-), consistent with Donnan exclusion effects. As a result, carbonate exhibits higher rejection relative to bicarbonate.

The separation of uranium, sodium carbonate and sodium bicarbonate was significant, and the recoveries are suitable to be implemented in a scale-up plant in order to save on reagent cost. The savings will be due to the sodium carbonate and sodium bicarbonate removed from the concentrate before pH neutralization.

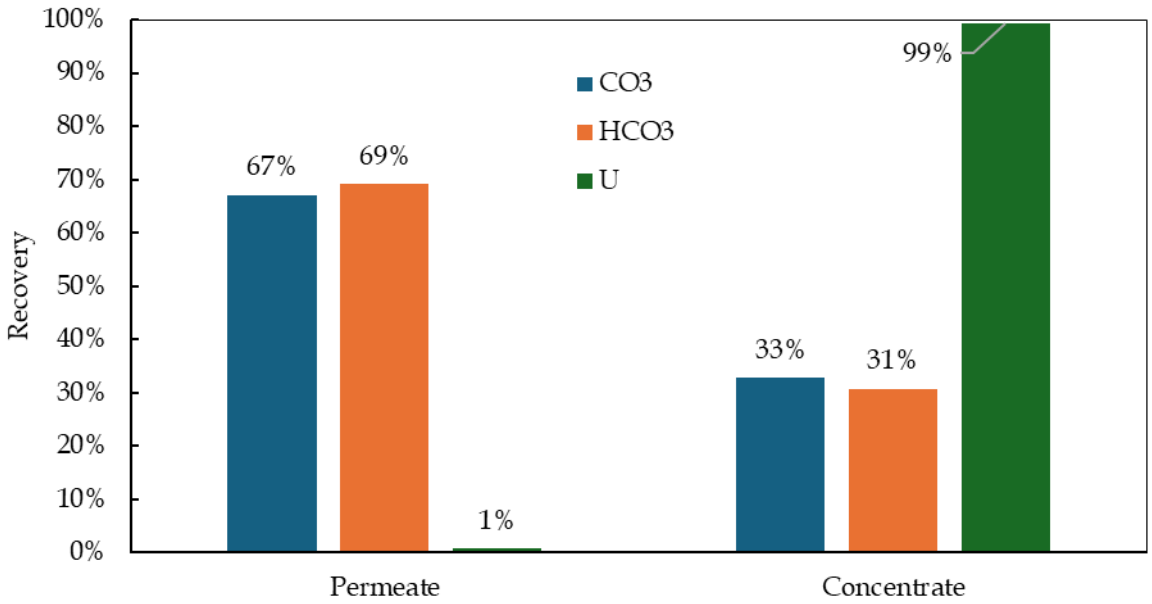

Figure 6: Percentage recoveries of the NF membrane for the alkali pilot trial in France.

Figure 7 shows the battery of samples that were taken to determine the trial results. The samples were analysed by the laboratory at the research centre. The separation between dark concentrate and light permeate is definitive.

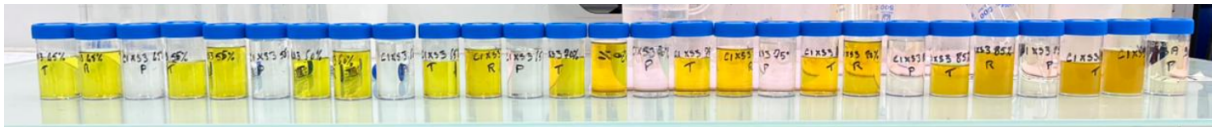

Figure 7: French alkali pilot trial samples; feeds, concentrates and permeates at various concentrations.

The alkali test results for the Namibian and French cases reiterate advantageous recycling of sodium carbonate and sodium bicarbonate to the upstream processes. Uranium losses will not be significant because it is also being re-incorporated into the process.

CONCLUSION

Pilot-scale evaluation of integrated UF–NF circuits in Namibia and France has confirmed the technical viability of membrane technology in both acidic and alkaline uranium processing routes. UF provided effective removal of suspended solids, enabling stable downstream NF operation, while NF achieved significant uranium concentration and high levels of reagent recovery, with up to 97% sulphuric acid

and 89–94% carbonate recovered. The high degree of reagent recovery translates directly into reduced reagent make-up requirements, representing a significant operational cost saving, particularly in remote mining operations where reagent supply and transport contribute substantially to overall costs. In addition, reduced reagent losses lower the load on downstream treatment systems, further decreasing operating and environmental management costs.

Overall, the integration of UF–NF circuits offers a practical and scalable solution to reduce reagent consumption, simplify process flowsheets, improve economic performance, and lower environmental impact in uranium hydrometallurgical operations.

ACKNOWLEDGMENTS

The authors gratefully acknowledge the support of BME Metallurgy management, who granted permission to publish this work.

REFERENCES

Botelho Junior, A.B., Peng, H., & Kim, J. (2025). Membrane application in hydrometallurgical processing. JOM, 77, 8227–8229. https://doi.org/10.1007/s11837-025-07213-5

Giusti, F., Guerinoni, E., Lemire, D., Thimotée, M., Arrachart, G., Dourdain, S., & Pellet-Rostaing, S. (2024). Solvent extraction of uranium from an acidic medium for the front-end of the nuclear fuel cycle. *Comptes Rendus Chimie*, vol. 27(S4), pp.1–31. https://cea.hal.science/cea-04528746v1

Kiegiel, K., Abramowska, A., Bieluszka, P., & Zakrzewska-Kołtuniewicz, G. (2016). Solvent extraction of uranium from acidic and alkaline leach solutions. *Journal of Radioanalytical and Nuclear Chemistry*, vol. 311, pp. 589–598. https://doi:10.1007/s10967-016-5029-5

Peng, H.Y., Lau, S.K., Yong, W.F. (2024). Recent advances of thin film composite nanofiltration membranes for Mg2+/Li+ separation. Advanced Membranes. 4, 100093. https://doi.org/10.1016/j.advmem.2024.100093.

Saeed, G., Alam, A., Vinodh, R., Dasha Kumar, D.K.M., Gopi, C., Kim, K.H., Tadesse, B. (2025). Two-dimensional (2D) material nanofiltration membranes for effective recovery of lithium. Journal of Industrial and Engineering Chemistry. 150, 116–133. https://doi.org/10.1016/j.jiec.2025.03.004.

Venter, R., & Boylett, M. (2009). The evaluation of various oxidants used in the acid leaching of uranium. *Hydrometallurgy Conference*, SAIMM.

Wanjiya, M., Zhang, J.-C., Wu, B., Yin, M.-J., An, Q.-F. (2024). Nanofiltration membranes for sustainable removal of heavy metal ions from polluted water: A review and future perspective. Desalination. 578, 117441. https://doi.org/10.1016/j.desal.2024.117441.

Wen, H., Liu, Z., Xu, J., Chen, J.P., 2024. Nanofiltration membrane for enhancement in lithium recovery from salt-lake brine: A review. Desalination. 591, 117967. https://doi.org/10.1016/j.desal.2024.117967.

Yazzie, C.B., Elias, C., & Karanikola, V. (2024). Uranium rejection with nanofiltration membranes and the influence of mono- and divalent cations. Environmental Science: *Water Research & Technology*, vol. 10, pp. 2075–2086. https://doi.org/10.1039/D4EW00324A

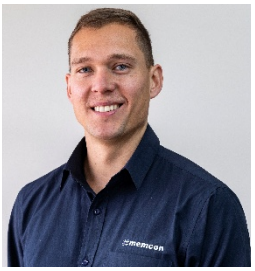

Leon Bartel

Process Engineer
Memcon (Pty) Ltd

Leon has worked in industry for 3 years. Starting his professional career with Memcon and has been focused on membrane technology. He has done pilot plant test work in South Africa, Namibia and France to apply membrane technology to the mining industry. Leon is currently a Process Engineer at Memcon based in JHB, South Africa. He aims to build solutions in the mining and hydrometallurgy industry on the massive benefits that membrane technology offers to these industries.

Trade-offs between settling rate and turbidity in uranium processing: A case for circuit-specific flocculant design

N.J. Shackleton[1], D. Prinsloo[1], M. Borotho[1], G. Van Der Merwe[2], S. Siguqa[1], S. Engelbrecht[1]

[1]AECI Mining Chemicals, South Africa
[2]AECI Mining Chemicals, Namibia

Flocculant selection in uranium processing circuits is governed by competing performance requirements, particularly in operations employing both pre-leach thickening and Counter Current Decantation (CCD) systems. While pre-leach performance is primarily driven by settling rate and underflow density, CCD circuits impose an additional and critical constraint in the form of overflow turbidity, which directly impacts downstream ion exchange (IX) efficiency.

This paper investigates the trade-off between settling performance and overflow clarity through a structured evaluation of a baseline (standard) flocculant and a series of developmental polymer formulations (DevProd variants) derived from a common base polymer platform. Testing was conducted on slurry samples from a Namibian uranium processing operation under conditions representative of both pre-leach and CCD circuits. Performance was assessed in terms of settling rate, underflow density, and overflow turbidity.

The results show that multiple developmental formulations significantly outperform the baseline (standard) product in the pre-leach circuit, confirming that throughput-related performance is readily achievable. In contrast, CCD performance is strongly constrained by turbidity, with most high-settling formulations producing elevated overflow turbidity due to the formation of open, permeable floc structures. A subset of formulations demonstrated improved turbidity performance at moderate settling rates, indicating that fines capture and floc structure can be influenced through targeted modification of polymer characteristics.

The results define a bounded performance envelope, as demonstrated by the absence of achievable conditions combining high settling rate and low turbidity. No single formulation was found to simultaneously optimise both parameters. These findings demonstrate that the concept of a universal flocculant is not supported for systems with fundamentally different separation requirements.

The paper therefore establishes a case for circuit-specific flocculant design, where formulations are tailored to the dominant performance constraints of each unit operation. This approach provides a more robust framework for optimising solid–liquid separation in uranium processing and supports the development of next-generation flocculants designed to operate within defined performance windows rather than attempting to maximise individual parameters.

Keywords: Flocculants, Pre-Leach, CCD, Uranium

INTRODUCTION

Solid–liquid separation is a critical component of uranium processing operations, directly influencing plant throughput, recovery efficiency, and downstream process performance. Thickening circuits, particularly pre-leach thickeners and Counter Current Decantation (CCD) systems, are central to this function, enabling solids handling and recovery of dissolved uranium values (Wills & Finch, 2016). The effectiveness of these circuits is strongly dependent on flocculant selection, which governs particle aggregation, settling behaviour, and overflow clarity (Gregory, 2006).

The performance requirements of pre-leach and CCD circuits differ fundamentally. Pre-leach thickening is primarily throughput-driven, where rapid settling and adequate underflow density are required. In contrast, CCD circuits impose an additional constraint in the form of overflow turbidity, which directly impacts downstream ion exchange (IX) performance through resin fouling and reduced mass transfer efficiency (Bolto & Gregory, 2007; Habashi, 1999). As a result, turbidity becomes the dominant performance parameter in CCD operation.

Flocculation in mineral processing systems is achieved through the addition of high molecular weight polymers, which promote particle aggregation primarily via bridging mechanisms. These interactions produce flocs whose structure governs separation performance. Systems dominated by strong bridging interactions typically form large, open, and permeable flocs that settle rapidly but allow fine and colloidal particles to remain suspended. Conversely, systems that promote fines capture tend to form smaller, denser, and more compact flocs, improving overflow clarity but often at reduced settling rates (Gregory & Barany, 2011; Zhang *et al.,* 2013).

This behaviour gives rise to a fundamental trade-off between settling rate and turbidity. Enhancing floc size and settling kinetics generally increases floc permeability and reduces fines capture, while improving clarity requires structural changes that constrain settling performance. The relationship between these parameters defines a bounded performance envelope, within which achievable operating conditions are limited.

Despite this, flocculant development strategies often aim to produce a single formulation capable of performing across multiple circuits. This implicitly assumes that polymer chemistry can simultaneously optimise competing performance requirements. However, both theoretical understanding and operational experience suggest that this expectation may not be realistic in systems where different separation mechanisms dominate.

This paper investigates this challenge through an evaluation of a baseline (standard) flocculant currently used in the plant, and a series of developmental polymer formulations (DevProd variants) derived from a common baseline polymer platform. Testing was conducted on slurry samples from a uranium processing operation in Namibia under conditions representative of both pre-leach and CCD circuits. Performance was assessed in terms of settling rate, underflow density, and overflow turbidity.

The objective of the paper is to evaluate whether a single flocculant can satisfy the combined requirements of both circuits, and to determine whether a shift toward application-specific flocculant design represents a more effective strategy for optimising solid–liquid separation performance.

EXPERIMENTAL METHODS

Materials

Slurry samples used in this study were obtained from a uranium processing facility in Namibia, representing both pre-leach thickener feed and Counter Current Decantation (CCD) feed streams. Process water and barren solution samples were also collected and used in slurry preparation to replicate plant conditions as closely as possible.

The flocculants evaluated comprised:

- A baseline (standard) product currently used in the plant
- A baseline polymer platform
- A series of developmental formulations (DevProd variants) derived from the baseline polymer platform

The DevProd variants were designed to systematically explore the impact of polymer properties such as molecular weight distribution, charge density, and ionic modification on floc structure and performance. These included both analytical-grade and industrial-grade formulations to assess the influence of raw material selection and manufacturability.

Experimental Design Approach
The experimental programme was structured to evaluate flocculant performance across two fundamentally different operating environments: pre-leach thickening and CCD clarification.

Rather than treating the study as a simple product screening exercise, the test work was designed to:

- Compare performance relative to the baseline (standard) product
- Identify performance trends across formulation variants – baseline polymer platform and variants thereof (DevProd 1–8)
- Evaluate the relationship between settling rate and turbidity
- Assess whether a single formulation could satisfy both circuit requirements.

Testing was conducted in two phases:

- Phase 1 (Initial Screening): Comparative evaluation across a broad set of DevProd variants to establish performance envelopes and identify key trends
- Phase 2 (Refined Testing): Focused evaluation of selected high-performing candidates under improved and more representative slurry preparation conditions

This staged approach enabled both broad comparison and increased confidence in final performance interpretation.

Sample Preparation
Test slurries were prepared using plant-derived slurry and process water to achieve representative operating conditions. The target slurry specific gravity (SG) was maintained within a narrow range (approximately 1.11–1.13), corresponding to typical plant solids concentrations.

Two preparation methodologies were employed:

- *Initial testing:* Slurry preparation prioritised consistency across samples, but did not explicitly preserve the original particle size distribution (PSD)
- *Refined testing:* Improved preparation techniques were implemented to better maintain the original slurry PSD, resulting in conditions more representative of plant operation

Flocculant stock solutions were prepared at a concentration of 0.25% (m/v) and subsequently diluted to a 0.05% (v/v) working solution. Fresh working solutions were prepared daily to ensure consistency and reproducibility.

Settling Test Procedure
Settling performance was evaluated using standard laboratory cylinder tests.

For each test:

- A fixed volume of prepared slurry was transferred into a graduated cylinder
- Flocculant solution was added at a predetermined dosage, typically applied as a split dose to simulate plant addition conditions
- The slurry was mixed through controlled inversion to ensure uniform flocculant distribution
- The position of the mudline interface was monitored over time.

Settling rate (m/hr) was calculated based on the time required for the interface to traverse a defined distance within the cylinder.

Performance Measurements
Flocculant performance was assessed using three key metrics:

- *Settling rate (m/hr):* Determined from mudline displacement over time and used as the primary indicator of separation kinetics
- *Underflow density (SG):* Estimated from settled solids volume after a fixed time period
- *Overflow turbidity (NTU):* Measured using a turbidity meter for CCD samples and used as the primary indicator of clarification performance

For pre-leach tests, overflow clarity was also assessed using a visual clarity scale; however, turbidity was the primary differentiating parameter for CCD performance.

Test Programme
The experimental programme included:

- Evaluation of the baseline (standard) product, the baseline polymer platform, and DevProd formulations across a range of dosages representative of plant conditions
- Testing under both pre-leach and CCD slurry conditions
- Comparative assessment between analytical-grade and industrial-grade variants
- Evaluation of raw material variants to assess manufacturability impacts.

Following initial screening, a subset of high-performing DevProd formulations was selected for further testing under refined conditions. This enabled targeted evaluation of performance trade-offs and improved reliability of the final dataset.

Data Analysis Approach
Results were analysed by comparing flocculant performance across settling rate, underflow density, and turbidity, with particular emphasis on identifying relationships between settling behaviour and overflow clarity. Overflow quality was assessed using different methods in the two circuits. In the pre-leach circuit, overflow clarity was evaluated using a wedge method against an operational target range, whereas in the CCD circuit, turbidity was measured instrumentally in NTU due to the higher sensitivity of this circuit to fines carry-over. Because these methods are not directly equivalent, overflow quality was interpreted within each circuit independently rather than compared numerically across circuits.

Comparative analysis focused on:

- Performance relative to the baseline product
- Differences between DevProd variants
- The influence of formulation variables on floc structure and separation performance
- Identification of a performance envelope defining the trade-off between settling rate and turbidity.

This approach allowed the experimental results to be interpreted within the theoretical framework of floc structure and mechanism, rather than as isolated performance outcomes.

Methodological Considerations
It is recognised that laboratory settling tests do not fully replicate plant-scale hydrodynamics; particularly with respect to shear conditions, feedwell design, and mixing energy. However, the methodology employed provides a consistent and controlled basis for comparative evaluation of flocculant performance.

The use of refined slurry preparation techniques in Phase 2 testing improved the representativeness of the results and increased confidence in the observed performance trends.

The importance of hydrodynamic conditions and scale effects in thickening performance has been well documented, and laboratory-scale tests should therefore be interpreted as comparative rather than absolute predictors of plant behaviour (Gladman *et al.*, 2010).

RESULTS AND DISCUSSION

Although clarity is reported using different measurement methods in the two circuits, both datasets demonstrate the same underlying trade-off between settling performance and overflow quality.

Pre-Leach Circuit Performance
Figure 1 demonstrates that overflow clarity in the pre-leach circuit is consistently high and does not limit performance. The broader spread in settling rate confirms that settling performance, rather than clarity, is the primary differentiating parameter in this circuit. Consequently, Figure 2 focuses on the effect of flocculant dosage on settling rate for selected formulations, highlighting the parameters relevant to operational optimisation. Underflow densities remained comparable across all formulations and did not provide meaningful differentiation between products. This contrasts directly with CCD behaviour (Section 4.2), where clarity becomes the primary limiting parameter.

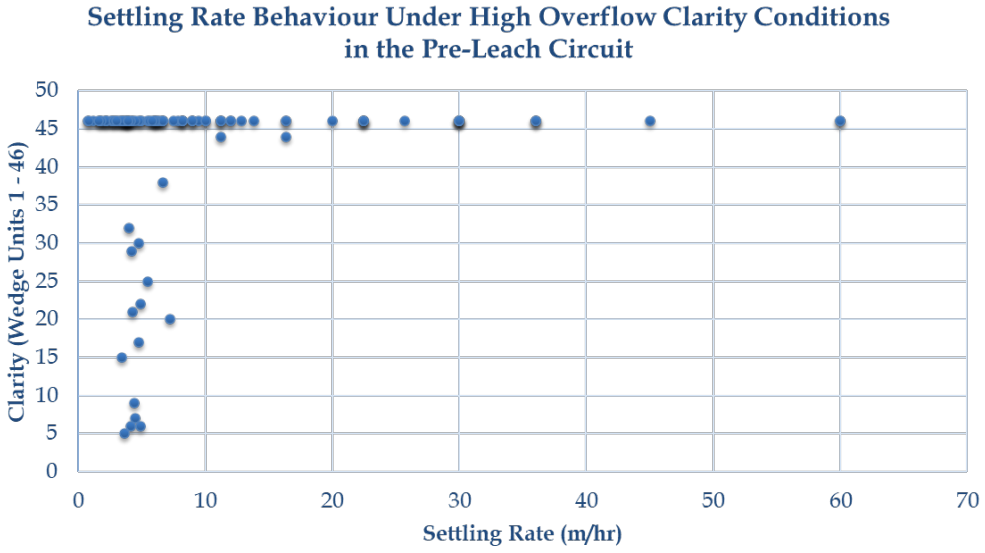

Figure 1. Relationship between settling rate and overflow clarity in the pre-leach circuit.

The results obtained under pre-leach conditions demonstrate that settling performance is not a limiting factor in the system. Multiple DevProd formulations significantly outperformed the baseline product in terms of settling rate, with several achieving substantially higher separation kinetics across the tested dosage range. Figure 2 shows that all plotted points achieved overflow clarity of approximately 46 wedge units, exceeding the pre-leach requirement of 25–30 wedge units, indicating that settling performance is the primary differentiating parameter.

In particular, DevProd variants derived from the baseline polymer platform consistently exhibited strong settling behaviour, with both analytical-grade and industrial-grade formulations demonstrating the ability to exceed baseline performance. Underflow densities across these formulations were comparable, indicating that improvements in settling rate did not adversely impact solids compaction.

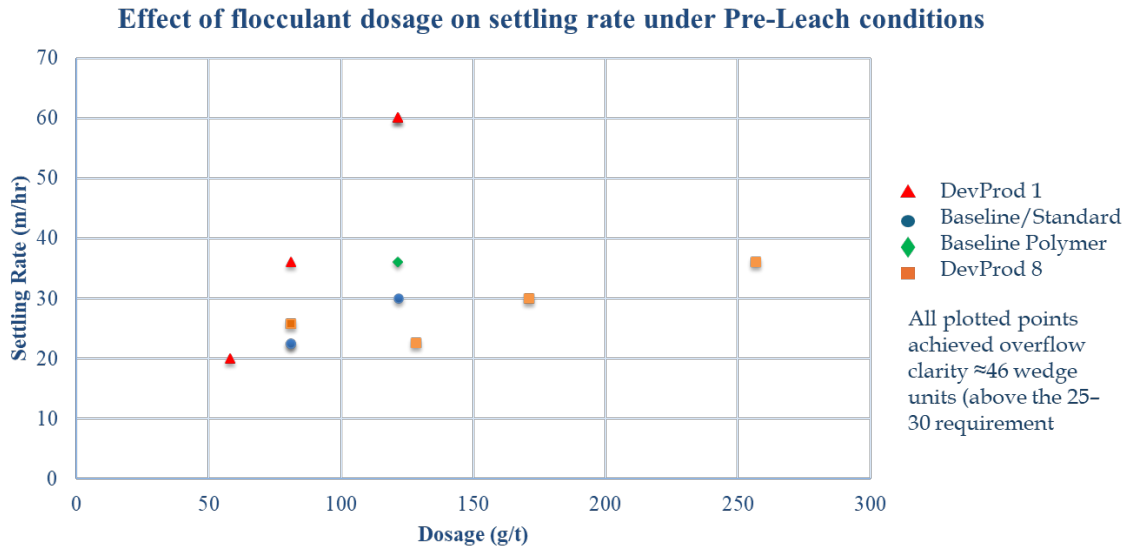

Figure 2. Effect of flocculant dosage on settling rate under pre-leach conditions for selected formulations. Each point represents a plant-representative operating condition, with dosage adjusted according to throughput at the time of sampling.

These findings are consistent with established understanding that high molecular weight polymer systems readily achieve effective particle aggregation and rapid settling in relatively unconstrained thickening environments (Gregory, 2006; Wills & Finch, 2016).

Key observation: Pre-leach performance is readily achievable and does not represent a constraint in flocculant selection.

CCD Circuit Performance

In contrast to the pre-leach results, performance under CCD conditions is characterised by a strong dependency on overflow turbidity. The data in Figure 3 show a wide distribution of turbidity values across the range of settling rates, indicating that overflow quality is highly variable under CCD conditions. Unlike the pre-leach circuit, turbidity becomes the primary controlling parameter, and improvements in settling performance do not necessarily correspond to improved overflow clarity.

CCD performance was assessed relative to the baseline product, as no fixed turbidity specification was defined. Lower turbidity values relative to the baseline were considered operationally favourable, reflecting current plant performance requirements. While several DevProd formulations achieved improved settling rates, the majority produced elevated turbidity levels, indicating that enhanced aggregation does not inherently result in improved clarification.

The baseline product consistently established a low-turbidity benchmark, demonstrating stable clarification performance across the tested conditions. In contrast, many of the higher-settling DevProd formulations produced more permeable floc structures, allowing fine and colloidal particles to remain suspended and resulting in increased turbidity.

This behaviour is consistent with established flocculation theory, where bridging-dominated systems

promote rapid aggregation but often produce open floc structures that limit fines capture (Bolto & Gregory, 2007; Zhang *et al.,* 2013).

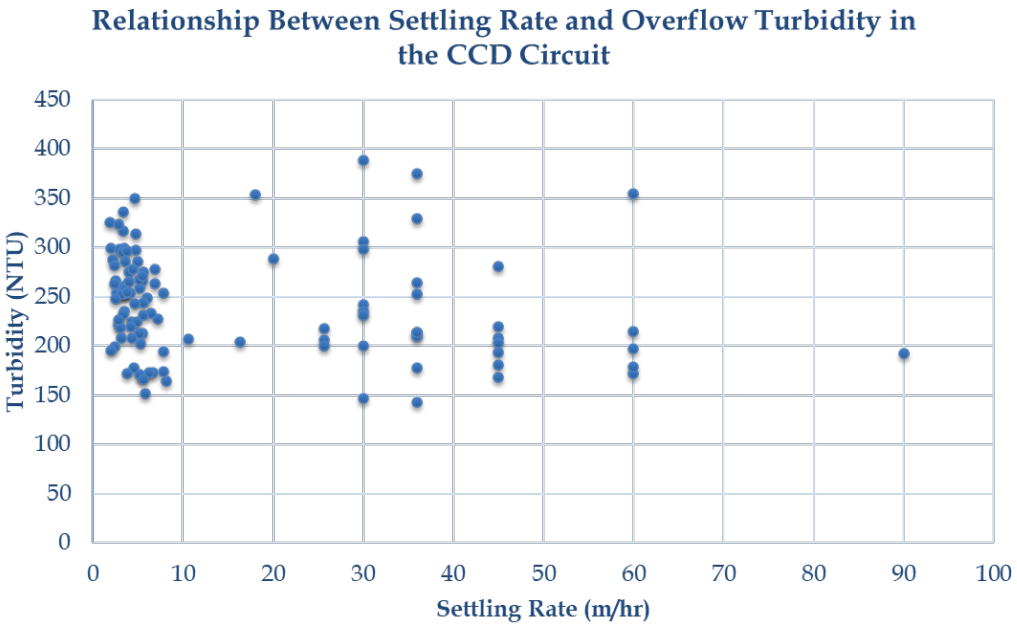

Figure 3. Relationship between settling rate and overflow turbidity in the CCD circuit.

While Figure 3 presents the full dataset, the underlying trade-off between settling rate and turbidity is more clearly illustrated in Figure 5, where the data are interpreted in terms of a bounded performance envelope.

A subset of DevProd formulations demonstrated improved turbidity performance relative to the baseline while maintaining acceptable settling rates, as shown in Figure 4. These formulations are associated with enhanced fines capture and the formation of more compact floc structures, indicating that turbidity can be influenced through targeted modification of polymer properties. However, even within this subset, improvements in clarity are generally accompanied by a reduction in maximum settling performance.

This behaviour is consistent with flocculation theory, where polymer systems that favour rapid aggregation through bridging mechanisms tend to produce open floc structures that allow fine and colloidal particles to remain suspended (Bolto & Gregory, 2007; Gregory & Barany, 2011).

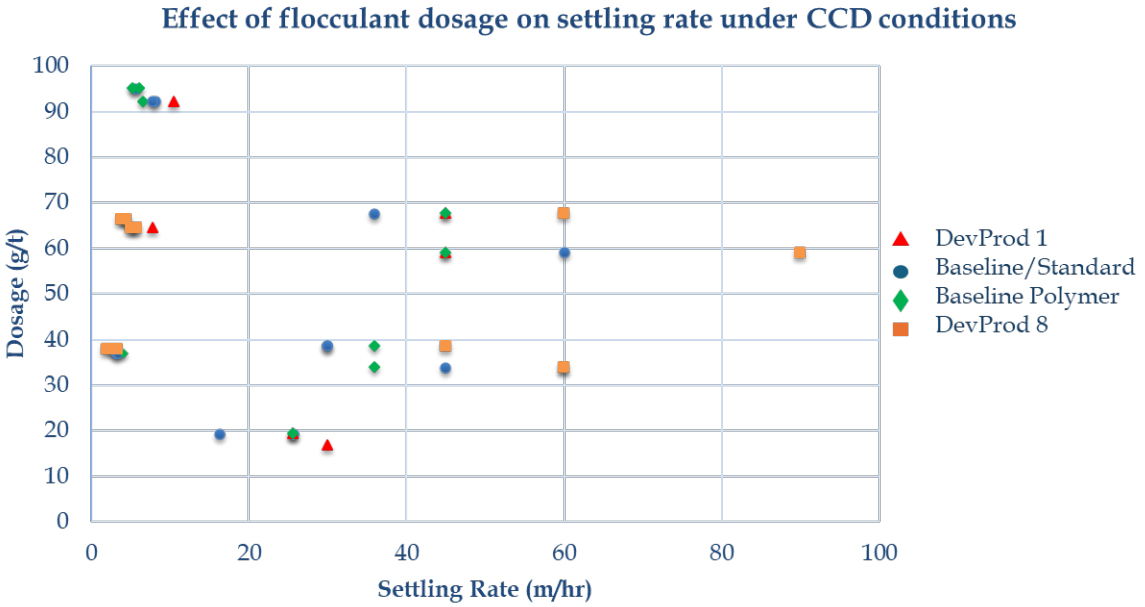

Figure 4. Effect of flocculant dosage on settling rate under CCD conditions for selected formulations. Each point represents a plant-representative operating condition, with dosage adjusted according to throughput at the time of sampling.

Key observation: CCD performance is constrained by turbidity, which becomes the primary limiting parameter in flocculant selection.

Relationship Between Settling Rate and Turbidity

A direct comparison of settling rate and turbidity across all tested formulations reveals a clear inverse relationship between these two performance parameters, as shown in Figure 5. While overflow quality was quantified differently in the pre-leach and CCD circuits, the results consistently demonstrate that product selection is circuit dependent. In pre-leach, clarity is generally acceptable and settling performance dominates, whereas in CCD, turbidity provides the primary basis for differentiation between formulations.

Formulations that achieve high settling rates, particularly those dominated by strong polymer bridging mechanisms, consistently produce higher turbidity due to the formation of open and permeable floc structures. Conversely, formulations that enhance fines capture and produce more compact flocs achieve lower turbidity, typically at moderate settling rates. This behaviour reflects the fundamental role of floc structure in governing both aggregation kinetics and particle capture efficiency (Bolto & Gregory 2007; Gregory & Barany, 2011; Zhang *et al*., 2013).

Importantly, no formulation was observed to simultaneously achieve both high settling rate and low turbidity within the range of formulations and conditions evaluated in this paper. Instead, all data points fall within a bounded performance envelope, as illustrated in Figure 5. The absence of data in the high-settling, low-turbidity region defines an unattainable operating space, confirming that improvements in one parameter inherently constrain the other.

This relationship demonstrates that the settling–turbidity trade-off is not a formulation limitation but a system-level constraint arising from the interaction between polymer properties, floc structure, and separation mechanisms. As a result, optimisation of flocculant performance must be approached within this constrained operating envelope rather than through attempts to maximise individual performance parameters.

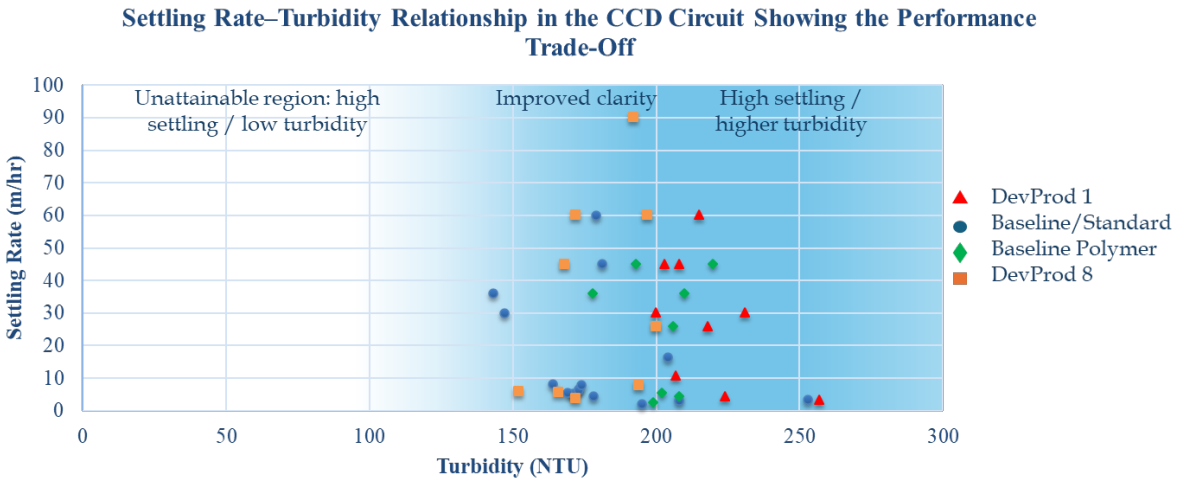

Figure 5. Settling rate–turbidity relationship for selected formulations in the CCD circuit, illustrating the performance trade-off between settling and overflow clarity. Each point represents a plant-representative operating condition.

Key observation: The settling–turbidity trade-off defines a constrained performance envelope within which all formulations operate.

Effect of Formulation Variables

Comparison between DevProd variants indicates that formulation variables such as raw material selection and polymer modification influence performance, but do not eliminate the underlying trade-off.

Industrial-grade variants generally exhibited slightly lower peak performance than analytical-grade formulations, reflecting practical manufacturing constraints. However, the relative trends between settling rate and turbidity remained consistent across both material types.

Similarly, modifications aimed at improving settling performance did not result in meaningful reductions in turbidity, indicating that changes in bulk polymer characteristics alone are insufficient to address clarity limitations. In contrast, formulations that demonstrated improved turbidity performance are likely influenced by mechanisms that enhance fines capture, such as controlled polymer conformation and ionic effects.

This observation aligns with previous studies showing that while polymer molecular weight and conformation influence aggregation kinetics, turbidity control is more strongly linked to fines capture mechanisms and floc structure rather than bulk settling behaviour alone (Bolto & Gregory, 2007).

Implications for Flocculant Selection

The results presented above demonstrate that flocculant performance is governed by fundamentally different constraints in the pre-leach and CCD circuits. This has direct implications for flocculant selection and product development strategies. Pre-leach performance is optimised by maximising settling rate, favouring bridging-dominated polymer systems. In contrast, CCD performance is constrained by turbidity, requiring enhanced fines capture and the formation of more compact floc structures.

No single formulation was able to simultaneously optimise both performance criteria. Formulations that performed optimally in pre-leach consistently failed to meet turbidity requirements in CCD, while clarity-optimised systems did not achieve maximum settling performance.

This outcome confirms that the assumption of a single flocculant capable of satisfying both circuit requirements is not supported by experimental evidence and is inconsistent with established understanding of polymer flocculation behaviour (Gregory & Barany, 2011).

Application-Specific Performance Segregation
The results define two distinct functional performance groups, reflecting the differing requirements of the two circuits. The terms DevProd PL and DevProd CCD are used here to describe these groupings rather than specific product designations:

- *Throughput-optimised formulations (DevProd PL):* High settling rate, robust aggregation, suitable for pre-leach applications
- *Clarity-optimised formulations (DevProd CCD):* Improved turbidity performance, enhanced fines capture, suitable for CCD applications.

This segregation reflects the differing process requirements of the two circuits and is consistent with the need to tailor polymer properties to specific separation objectives (Gregory, 2006).

Figures 2 and 4 demonstrate that settling performance can be improved across multiple formulations, while clarity performance is restricted to a smaller subset. Together with Figure 5, this defines the constrained performance envelope governing flocculant selection.

Overall, the results confirm that the observed trade-off between settling rate and turbidity is not a formulation-specific limitation, but a system-level constraint arising from floc structure and separation mechanisms. This provides a consistent framework for interpreting flocculant performance across both circuits.

This approach is consistent with modern perspectives on polymer-based solid–liquid separation, which emphasise optimisation within defined performance windows rather than maximisation of individual parameters (Gregory, 2006; Bolto & Gregory, 2007; Lee *et al.,* 2014).

CONCLUSIONS AND RECOMMENDATIONS

Conclusions
This study evaluated the performance of a baseline flocculant, a baseline polymer platform, and multiple development formulations under plant-representative conditions in both pre-leach and CCD circuits at the Husab Uranium Mine. The results demonstrate that flocculant performance is inherently constrained by competing mechanisms governing settling behaviour and overflow clarity.

The key findings are as follows:

Pre-leach performance is dominated by settling behaviour
Under pre-leach conditions all tested formulations achieved acceptable overflow clarity, with wedge measurements consistently exceeding operational requirements. As a result, settling rate becomes the primary differentiating parameter, driven predominantly by polymer bridging mechanisms.

CCD performance is constrained by turbidity
In contrast, CCD performance is strongly influenced by overflow turbidity, which varies significantly between formulations. Improvements in settling performance do not necessarily correspond to improved clarity, highlighting the importance of fines capture and floc structure in this circuit.

A fundamental trade-off exists between settling rate and turbidity
The results define a bounded performance envelope (Figure 5) within the range of formulations and conditions evaluated in this study; no system simultaneously achieves both high settling rates and low turbidity.

Single-product optimisation is not supported
The data indicate that no single formulation consistently outperforms across both circuits. Attempts to optimise for one performance parameter result in compromises in the other, confirming that a universal flocculant solution is not achievable under the tested conditions.

A fit-for-purpose product strategy is required
These findings support the adoption of circuit-specific flocculant formulations, where pre-leach and CCD performance objectives are addressed independently. This approach enables targeted optimisation within the constraints imposed by the performance envelope.

Recommendations
Based on these conclusions, the following recommendations are proposed to guide flocculant selection and future product development:

Adopt a fit-for-purpose flocculant strategy
Rather than pursuing a single universal product, a dual-product approach is recommended:

- *DevProd PL (pre-leach product):* A throughput-optimised formulation designed to maximise settling rate and solids handling capacity through strong bridging mechanisms
- *DevProd CCD (CCD product):* A clarity-optimised formulation designed to minimise turbidity through enhanced fines capture and the formation of compact floc structures.

This approach aligns flocculant design with circuit-specific requirements and enables optimisation within the achievable performance envelope.

Retain the baseline (standard) product as a turbidity reference standard
The baseline product flocculant should be maintained as a benchmark for CCD clarity performance during ongoing development, providing a consistent reference for evaluating improvements and ensuring that new formulations meet minimum clarification requirements.

Focus development on controlled manipulation of floc structure
Future formulation work should prioritise polymer properties that influence floc architecture, including:

- Molecular weight distribution (bridging efficiency)
- Charge density (particle interaction and adsorption)
- Polymer conformation and ionic effects (fines capture and floc compactness).

The objective should be to position formulations within defined performance windows rather than maximising individual parameters.

Investigate coagulation-assisted and hybrid systems
The integration of controlled coagulation mechanisms, through formulation design or process conditions, should be explored to enhance fines and colloidal particle capture in CCD circuits, potentially improving turbidity without excessive loss of settling efficiency.

Conduct pilot-scale and plant validation trials
Laboratory results should be validated under plant conditions to account for variability in ore composition, slurry chemistry, hydrodynamics, and interaction with existing infrastructure.

Define turbidity thresholds linked to downstream performance
Further work should establish quantitative relationships between CCD overflow turbidity and downstream ion exchange performance, enabling the definition of practical turbidity targets for flocculant design and process optimisation.

Final Statement

These findings demonstrate that flocculant selection in uranium processing cannot be treated as a single-product optimisation problem. Instead, performance is governed by a constrained balance between competing mechanisms that differ across processing stages. A shift toward application-specific, fit-for-purpose flocculant design is therefore required to achieve optimal performance in complex solid–liquid separation systems.

ACKNOWLEDGEMENTS

The authors would like to thank AECI Mining Chemicals management for support during the study and for permission to publish this paper.

REFERENCES

Bolto, B. and Gregory, J. 2007. Organic polyelectrolytes in water treatment. *Water Research*, 41(11), pp. 2301–2324. https://doi.org/10.1016/j.watres.2007.03.012

Gladman, B.R., Rudman, M. and Scales, P.J. 2010. Experimental validation of a 1-D continuous thickener model using mineral tailings. *Chemical Engineering Science*, 65(15), pp. 4293–4302. https://doi.org/10.1016/j.ces.2010.04.014

Gregory, J. 2006. *Particles in Water: Properties and Processes*. Boca Raton: CRC Press.

Gregory, J. and Barany, S. 2011. Adsorption and flocculation by polymers and polymer mixtures. *Advances in Colloid and Interface Science*, 169(1), pp. 1–12. https://doi.org/10.1016/j.cis.2011.06.004

Habashi, F. 1999. *Handbook of Extractive Metallurgy*. Weinheim: Wiley-VCH.

Lee, C.S., Robinson, J. and Chong, M.F. 2014. A review on application of flocculants in wastewater treatment. *Process Safety and Environmental Protection*, 92(6), pp. 489–508. https://doi.org/10.1016/j.psep.2014.04.010

Wills, B.A. and Finch, J. 2016. *Wills' Mineral Processing Technology: An Introduction to the Practical Aspects of Ore Treatment and Mineral Recovery*. 8th ed. Oxford: Butterworth-Heinemann.

Zhang, J., Li, C. and Tao, D. 2013. Role of polymer flocculants in the solid–liquid separation of mineral processing systems. *International Journal of Mineral Processing*, 124, pp. 15–23. https://doi.org/10.1016/j.minpro.2013.05.005

Dr Natalie J. Shackleton

R&D Manager: Mining Metallurgy
AECI Mining Chemicals

Natalie Shackleton is the R&D Manager: Mining Metallurgy at AECI Mining Chemicals, with over 40 years of experience in analytical chemistry, hydrometallurgy, mineral processing, and mineralogy. Her expertise lies in flotation, particularly surface chemistry, speciation, and reagent development for both flotation and metal refining. She has held numerous technical and leadership roles, combining strong scientific insight with practical application. Known for her structured problem-solving approach, she drives projects to successful completion while mentoring and developing technical teams. Natalie holds both an MSc and a PhD in Chemical Engineering from the University of Cape Town (UCT).

From single-parameter to multivariable sorting: full-spectrum XRF for uranium pre-concentration and mineralogical control

N. Odiar, A. Fouchee

Rados International Technologies (Pty) Ltd, South Africa

Uranium deposits in Namibia exhibit significant lithological variability at the particle scale, including granite, calcrete, feldspar-rich units, carbonate, and Fe-bearing waste lithologies. While uranium occurs in discrete mineral phases such as carnotite and uraninite, deleterious minerals contribute to dilution and increased reagent consumption during downstream processing. Effective beneficiation therefore requires discrimination based not only on uranium grade but also on mineralogical characteristics that influence processing performance. This paper evaluates the application of full-spectrum X-ray fluorescence (XRF) ore sorting across three Namibian uranium ore types: a granite-hosted alaskite system, an intrusive alaskite-related system, and a calcrete-hosted system. Full-spectrum analysis enables simultaneous measurement of uranium together with associated elements such as Rb, Ca, Fe, and Sr, allowing classification based on both grade and mineralogical proxies linked to processing behaviour.

Calibration against laboratory assays shows that uranium response can be strongly correlated to grade in systems where uranium is well expressed, with R^2 values of approximately 0.95 and mean absolute errors in the order of 30–65 ppm U. In lower-grade granite-hosted material, uranium response is not sufficiently distinct for direct sorting, and separation is instead achieved through lithological proxies across the datasets, multivariable XRF sorting improves selectivity relative to single-parameter approaches. The results demonstrate that sorting performance in Namibian uranium ores is system-dependent, ranging from lithology-driven rejection to uranium-driven separation, with intermediate cases requiring combined multivariable control.

Keywords: uranium ore sorting, sensor-based sorting, multivariable sorting, mineralogical control, pre-concentration, acid consumption

INTRODUCTION

Global applicability of multivariable XRF sorting

Uranium deposits exhibit significant variability in mineralogy, which directly influences processing performance and cost. While single-parameter sorting approaches based on radiometric response or density contrast can be effective for grade discrimination, they do not account for deleterious mineral phases such as carbonate, feldspar, and iron-bearing material that impact downstream processing (International Atomic Energy Agency, 2020).

Multivariable X-ray fluorescence (XRF) sorting enables simultaneous evaluation of uranium and associated elements, allowing classification based on both grade and mineralogical characteristics. The applicability of multivariable XRF sorting across major global uranium deposit types is summarised in Table I.

Table I. Ore sorting application across global uranium deposit types in key regions

Deposit Type (Key Regions)	Typical Characteristics	Single-Parameter Sorting	Multivariable XRF Sorting
Granite/Alaskite-Hosted (Namibia, Australia)	Disseminated U, feldspar-rich, variable carbonate, strong heterogeneity	XRF U: limited at low grades XRT: Minimal density contrast radiometric: Spectral interference from feldspar	**High Impact** U upgrade and rejection of feldspar and carbonate
Calcrete-hosted (Namibia)	Near-surface, carnotite, high carbonate variability	XRF U: Effective for grade only XRT: Minimal density contrast radiometric: Spectral interference from feldspar	**Very High Impact** U upgrade and direct rejection of carbonate
Sandstone-hosted (Kazakhstan, USA, Niger)	Stratiform, redox-controlled, variable cementation and clay content	XRF U: Effective for grade only XRT: Minimal density contrast radiometric: Effective for grade only	**Targeted Impact** U upgrade and rejection of carbonate, clay and iron-bearing minerals
Unconformity-related (Canada)	Very high grade, complex alteration halos	XRF U-only: Effective for grade only XRT: Minimal density contrast radiometric: Effective for grade only	**Incremental Impact** U upgrade and control and management of alteration-related gangue

This is particularly relevant in systems where downstream processing performance and costs are driven by gangue mineralogy rather than uranium grade alone.

Downstream Processing Impact

The primary value of multivariable XRF sorting lies in its impact on downstream processing rather than grade improvement alone. Uranium processing costs are strongly influenced by reagent consumption, throughput, and feed variability, all of which are controlled by mineralogical composition (International Atomic Energy Agency, 2020; Habashi, 1999). Uranium leaching is typically conducted using either sulfuric acid or alkaline systems, with the selection governed largely by carbonate content (World Nuclear Association, 2025; Merritt, 1971). The role of multivariable XRF sorting in acid and alkaline leach regimes are summarised in Table II.

Table II. Impact of multivariable XRF sorting on acid leach and alkaline leach processes

Parameter	Acid Leach (Low Carbonate Ore)	Acid Leach (High Carbonate Ore)
Primary constraint	Throughput, energy consumption	Carbonate-driven chemistry, slow kinetics
Role of XRF sorting	Upgrade feed and remove dilution	Reduce carbonate load and stabilise chemistry
Mass rejection impact	Reduce throughput or increase effective plant capacity	Reduce throughput or mitigate reaction kinetics limitations
Reagent impact	Reduce acid consumption	Control reagent demand
Feed consistency	Improved grade control	Stabilised solution chemistry
Operational benefit	Increased efficiency and reduced energy intensity	Improved process stability and leach performance

In acid leach systems, multivariable XRF sorting improves efficiency primarily through reduction in mass flow to downstream circuits. The removal of low-grade and diluting material reduces throughput requirements, increasing effective plant capacity and lowering energy intensity. Additional benefits include incremental reductions in acid consumption through the selective removal of residual carbonate-bearing material (Lottering, 2007).

In alkaline leach systems, the role of sorting shifts toward control of mineralogical drivers of process performance. The rejection of carbonate-rich particles reduces the carbonate load entering the circuit,

improving reagent efficiency and stabilising solution chemistry. Reduced throughput also mitigates the impact of slower leaching kinetics by effectively increasing residence time (Merritt, 1971).

Methodology

The principal deposit types considered in this work are calcrete hosted systems (Paladin Energy, 2023), granite hosted alaskite systems (Rössing Uranium Limited, 2015), and intrusive alaskite-related systems (Forsys Metals Corp, 2023), although other deposit styles such as metamorphic hosted, pegmatite hosted, structurally controlled, and phosphate associated uranium systems are also present in Namibia (IAEA, 2018).

This paper evaluates the application of full-spectrum XRF sorting across these deposit types. The approach combines uranium response with associated elemental behaviour, using ULα, ULβ, Fe, Ca, Rb and, where relevant, Sr to define a multivariable classification space.

Sample Selection

The work reported in this paper combines three uranium sorting datasets from Namibia to evaluate the application of full-spectrum XRF across different geological settings:

- Ore A: Calcrete-hosted uranium system (60 rocks from 6 lithologies)
- Ore B: Granite-hosted alaskite uranium system (196 rocks from 7 lithologies)
- Ore C: Intrusive alaskite-related uranium system (48 rocks from 4 lithologies).

The test work datasets comprise particle-by-particle based XRF measurements using proprietary Rados XRF hardware. The system operates by exposing individual particles to an X-ray source and measuring the resulting characteristic fluorescence emissions to determine elemental response. Each particle is analysed individually, with elemental intensities recorded for uranium and associated elements such as iron, calcium and rubidium.

Figure I presents a compositional summary XRF spectrum from uranium ore, illustrating the characteristic elemental responses used in particle sorting. The spectrum shows intensity as a function of energy (keV), where discrete peaks correspond to characteristic X-ray emissions of elements within the sample. Distinct peaks are observed for Ca, Fe, Rb, and Sr, as well as the uranium L series peaks (ULα and ULβ), which form the basis for defining sorting algorithms that utilise multiple variables simultaneously.

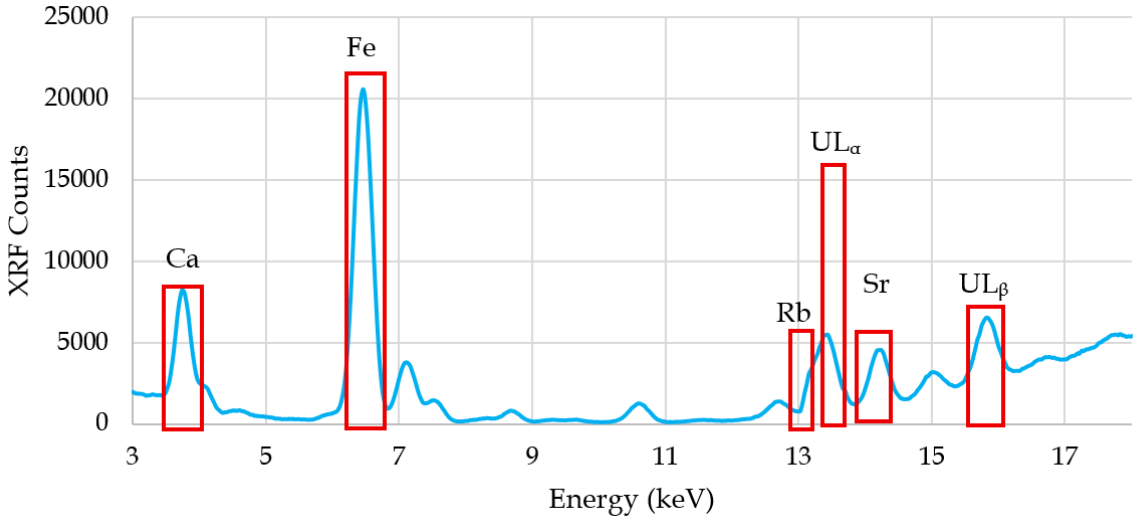

Figure 1. Composite XRF Spectrum of Uranium-Bearing Ore.

These responses are used to define sorting criteria based on threshold values or multivariable relationships. This testing procedure replicates the measurement principle during full scale operation of XRF ore sorters, allowing particle-by-particle evaluation of sorting performance under controlled conditions

Following analysis, all samples were crushed, pulverised and assayed to establish the relationship between XRF response and uranium grade. These paired measurements were used to assess sorting potential through direct comparison of threshold responses. This dataset represents particle-based sorting conditions, where each XRF sensor measurement and assay corresponds directly to an individual sortable unit.

Data interpretation and calibration

For all datasets, XRF responses were compared to laboratory assay data to establish empirical relationships for sorting, using single parameter and multi-parameter sorting algorithms. Associated elements including Fe, Ca, Rb and Sr were analysed to identify consistent relationships with lithology and to support multivariable classification. Error matrices were evaluated to determine the suitability of classification performance for sorting, with results varying depending on the ore type. For a uranium cut-off, a true positive is ore above a cut-off that is correctly classified to concentrate, while a true negative is waste below the cut-off that is correctly rejected. A false positive is waste below the cut-off incorrectly sent to concentrate and a false negative is ore above the cut-off incorrectly rejected.

Sorting performance estimation

Sorting performance was evaluated by applying threshold criteria to the particle-based datasets. For each algorithm and threshold condition, the proportion of the particles in the dataset reporting to the product stream was used to estimate the mass pull. Uranium grades for each stream were calculated using average grade from the assay data for particles that satisfy the algorithm and threshold requirements. Recovery and upgrade ratios were then derived from these values.

RESULTS AND DISCUSSION

Ore A: Calcrete-hosted system

The relative elemental XRF photon counts derived from spectra for individual lithologies in the calcrete-hosted system are illustrated in Figure 2. Calcrete material is characterised by elevated U and Ca counts, feldspar and granite exhibit higher Rb responses, and schist is distinguished by elevated Fe levels.

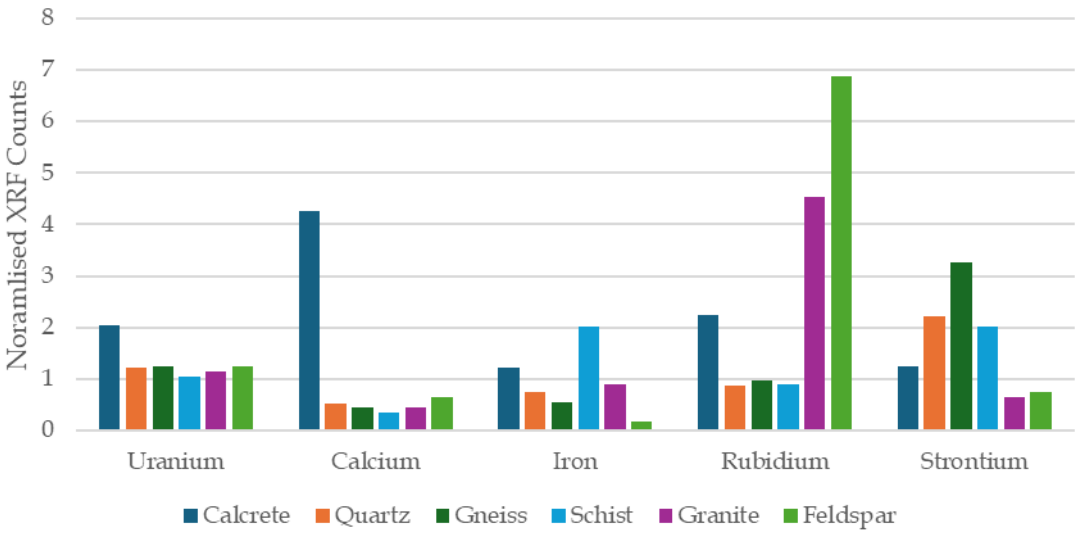

Figure 2. Normalised XRF counts by rock type for the calcrete hosted system.

Calibration of XRF response to uranium grade shows a strong linear relationship across the analysed range. The correlation coefficient of approximately 0.95 and a mean error of ~30ppm indicate that uranium can be reliably quantified from the XRF response for this material – providing a direct basis for sorting.

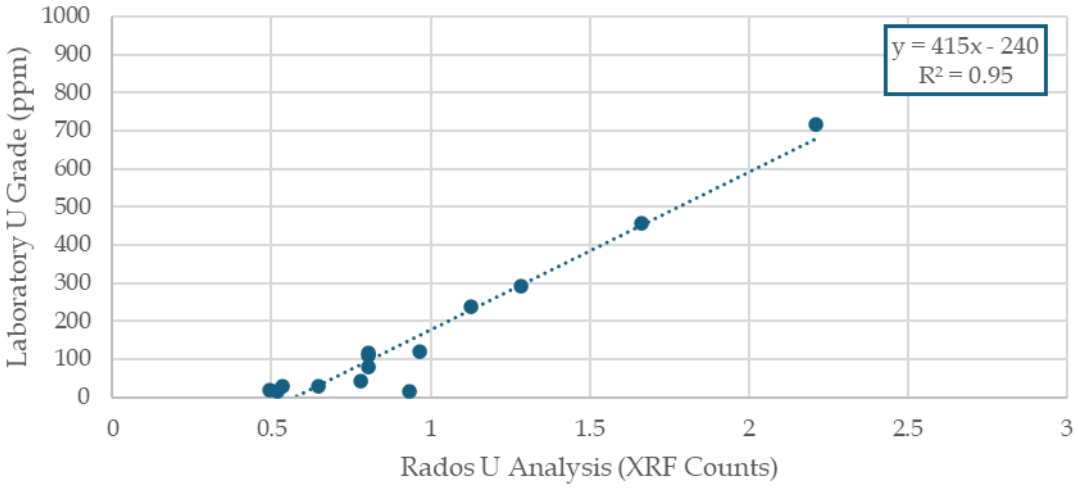

Figure 3. U calibration curve (Rados XRF Counts vs Assay.)

An error matrix developed for the classification based on Rados XRF Counts of U only is demonstrated in Table III. The model correctly classifies 82% of positives and 95% of negatives, indicating strong performance for both detection and rejection.

Table III. Error matrix for cut of 100ppm U

	Single Parameter Model	
Actual Positive	False Negative 18%	True Positive 82%
Actual Negative	True Negative 95%	False Positive 5%

Simulated sorting results demonstrate that uranium can be upgraded while maintaining high recovery. For the coarser material, an operating point achieving approximately 90% uranium recovery corresponds to a mass reduction of around 30% and an upgrade of approximately 1.3 times. Similar behaviour is observed in the finer fraction, although with a higher mass pull required to achieve comparable recovery.

Table IV. Simulated sorting results for calcrete hosted sample

Single-variable Thresholds (Rados XRF Counts of U)	Mass Pull (% Particles)	Concentrate Grade (U ppm)	Upgrade Ratio (U)	Recovery (U)	Discard Grade (U ppm)
0.45	100%	318	1.00	100%	0
0.76	94%	332	1.04	99%	52
0.82	89%	346	1.09	98%	70
0.86	84%	360	1.13	96%	83
0.89	79%	374	1.18	94%	94
0.92	74%	390	1.23	92%	102
0.95	69%	408	1.28	90%	109
0.98	64%	426	1.34	87%	118
1.01	59%	448	1.41	85%	124
1.04	54%	472	1.49	82%	131
1.07	49%	498	1.57	79%	137
1.1	44%	530	1.67	75%	143
1.14	39%	568	1.80	72%	150

These results show that, in the calcrete-hosted system, sorting is driven primarily by direct uranium detection.

Ore B: Granite-hosted alaskite system

The relative elemental photon counts for different lithologies from the granite-hosted alaskite system shows that the response is dominated by high Ca counts for the marble units, whereas the amphibolite and schist lithologies are distinguished by elevated Fe concentrations. Moderate photon responses associated with U were observed within the alaskite and gneiss lithologies.

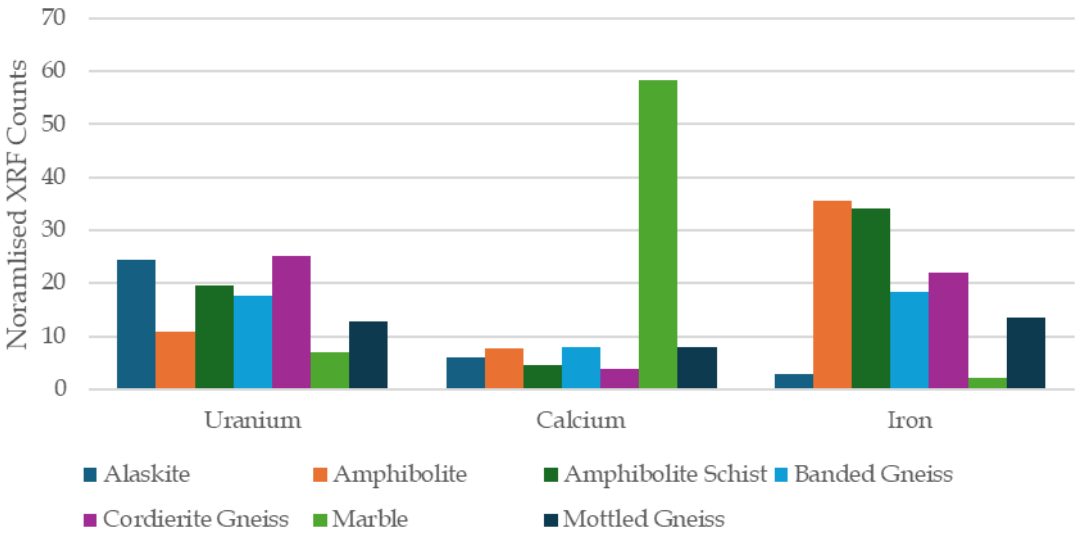

Figure 4. Normalised XRF counts by rock type for the granite-hosted alaskite system.

For the granite hosted alaskite system, marble is distinguished by elevated Ca response and Fe provides further discrimination, separating alaskite and marble from the more iron-rich amphibolite, schist and

gneiss units. This enables a simultaneous two-tier lithological separation, first removing calcareous material and then refining the remaining population based on Fe response.

An error matrix for classification based on Rados XRF counts of U and on a multivariable model is shown in Table V. At a cut-off of 23 ppm U, the multi-variable model reduces false negatives from 28% to 9% and false positives from 41% to 17%, improving positive classification from 72% to 91% and negative classification from 59% to 83% compared with the single parameter model.

Table V. Error matrix for cut of 23 ppm U

	Single Parameter Model		Multi Parameter Model	
Actual Positive	False Negative 28%	True Positive 72%	False Negative 9%	True Positive 91%
Actual Negative	True Negative 59%	False Positive 41%	True Negative 83%	False Positive 17%

Sorting simulations shows that sorting performance is dominated by the Fe threshold, with Ca providing minor refinement. Reducing Fe from 30 to 10 decreases mass pull from 35% to 13% while increasing concentrate grade from 56–60 ppm to 119–126 ppm and upgrade ratio from 2.4–2.5 to 5.1–5.4, at the cost of reduced recovery (~89.5% to ~69.9%). In contrast, changing Ca from 16 to 8 at a fixed Fe level has minimal impact on recovery and only slight increases in grade.

Table VI. Grade–recovery or mass pull vs upgrade curve for combined Ca–Fe sorting

Multivariable Thresholds (Rados XRF Counts)	Mass Pull to Concentrate (% Particles)	Concentrate Grade (U ppm)	Upgrade Ratio (U)	Recovery (U)	Discard Grade (U ppm)
Ca < 999 AND Fe < 999	100.0%	24	1.0	100.0%	
Ca < 16 AND Fe < 30	37.5%	56	2.4	89.7%	3.9
Ca < 12 AND Fe < 30	36.7%	58	2.4	89.6%	3.9
Ca < 8 AND Fe < 30	35.3%	60	2.5	89.5%	3.8
Ca < 16 AND Fe < 20	23.6%	84	3.6	84.3%	4.8
Ca < 12 AND Fe < 20	23.0%	87	3.7	84.2%	4.8
Ca < 8 AND Fe < 20	22.4%	88	3.7	84.2%	4.8
Ca < 16 AND Fe < 10	13.8%	119	5.1	69.9%	8.2
Ca < 12 AND Fe < 10	13.4%	123	5.2	69.9%	8.2
Ca < 8 AND Fe < 10	13.0%	126	5.4	69.9%	8.2

Ore C: Intrusive alaskite-related system

The XRF spectra for individual lithologies in the intrusive alaskite system confirm that uranium is detectable but also show the presence of overlapping elemental responses. The proximity of ULα and Rb peaks introduces uncertainty in uranium detection. The use of additional elements, including ULβ, Fe and Ca, provides context for interpreting these responses and identifying lithological domains.

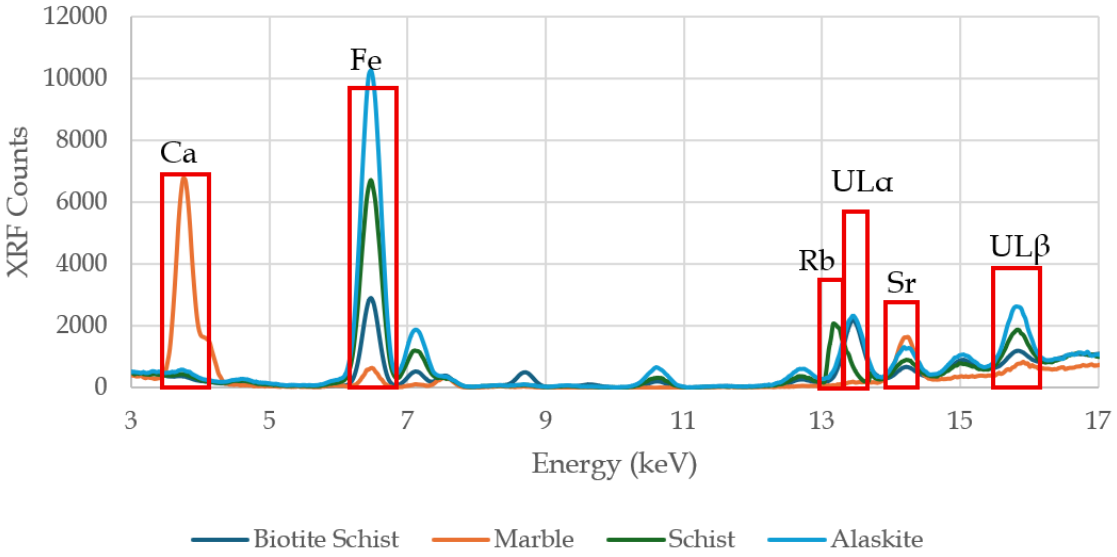

Figure 5. Representative spectra showing U peaks.

The relative elemental photon counts for lithologies in the intrusive alaskite system are shown below. Marble is defined by a strong Ca signature, while elevated Fe responses are observed in both alaskite and schist. The alaskite also exhibits a higher U response compared to the biotite schist, schist, and marble, enabling improved discrimination for sorting.

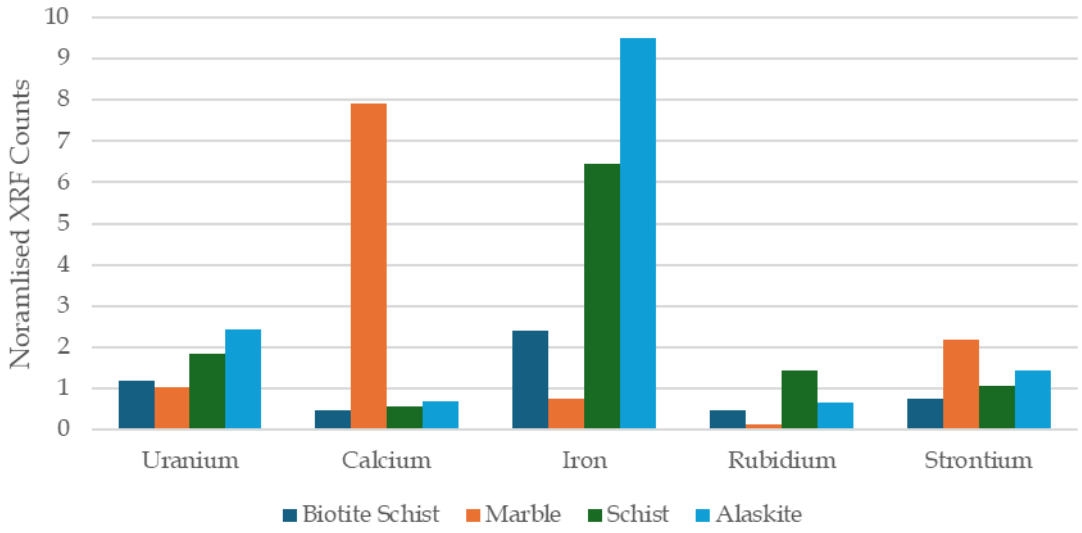

Figure 6. Normalised XRF counts by rock type for the intrusive alaskite system.

Classification in the form of an error matrix show the limitation of uranium-only sorting at 75 ppm U it misclassifies both ore and waste, whereas multivariable classification (U, Fe, Ca, Rb) achieves 100% ore identification and 90% waste rejection, eliminating false negatives and improving positives from 79% to 100% with no loss in negative performance.

Table VII. Error matrix for cut of 75 ppm U

	Single Parameter Model		Multi Parameter Model	
Actual Positive	False Negative 21%	True Positive 79%	False Negative 0%	True Positive 100%
Actual Negative	True Negative 91%	False Positive 9%	True Negative 91%	False Positive 9%

Sorting simulations confirm that this combined behaviour translates into improved performance. Uranium can be upgraded by a factor of 2.5–3.0 while maintaining recoveries in the range of 70–75%, depending on the selected cut-off. These results demonstrate a balance between direct uranium detection and lithology-based discrimination, rather than reliance on a single parameter.

Table VIII. Simulated Sorter Mass Balance using Multiparameter Ore-Sorting Thresholds

Multivariable Thresholds (Rados XRF Counts)	Mass Pull (%)	Concentrate Grade (ppm U)	UGR (U)	Recovery (% U)	Discard Grade (ppm U)
U_{LB} > 0 AND Ca < 999 AND Rb < 999	100%	146	1.00	100%	0
U_{LB} > 0.4 AND Ca < 12 AND Rb < 20	97%	150	1.03	100%	7
U_{LB} > 0.6 AND Ca < 10 AND Rb < 18	86%	167	1.14	98%	19
U_{LB} > 0.8 AND Ca < 8 AND Rb < 16	85%	168	1.15	98%	21
U_{LB} > 1 AND Ca < 6 AND Rb < 14	52%	248	1.70	88%	37
U_{LB} > 1.2 AND Ca < 4 AND Rb < 12	45%	276	1.89	85%	40
U_{LB} > 1.4 AND Ca < 2 AND Rb < 10	26%	421	2.89	74%	51

Illustrative Economic Impact

The economic impact of multivariable XRF sorting is driven primarily by reduced throughput and reagent consumption. Based on the sorting performance demonstrated in this study (~30% mass rejection at ~90% recovery), a simplified cost model was developed using representative assumptions of 500 ppm U feed grade, $15/t processing cost, $150/t sulfuric acid, and 50 kg/t acid consumption (International Atomic Energy Agency, 2020; Lottering, 2007). Sorting reduces processing cost from approximately $22.50/t to $15.75/t of run-of-mine feed, corresponding to a saving of $6.75/t. This equates to a reduction from approximately $19.23/lb to $13.46/lb U_3O_8, or ~$5.8/lb.

CONCLUSIONS

The results presented across the calcrete-hosted, granite-hosted alaskite, and intrusive alaskite-related uranium systems demonstrate that XRF ore sorting algorithms based on uranium alone cannot be applied consistently across Namibian ores. In the calcrete-hosted system, uranium response provides a direct and reliable basis for sorting. Separation in granite-hosted alaskite is achieved through lithological discrimination using iron and calcium. The intrusive alaskite-related system represents an intermediate case where uranium response is sufficiently strong to support upgrading, but classification based on uranium alone results in reduced accuracy. Incorporation of iron and rubidium improves classification by accounting for lithological variability.

These findings indicate that the application of XRF ore sorting in Namibian uranium deposits requires a system-specific approach, in which sorting criteria are defined according to specific lithologies which can be exploited by multivariate ore sorting algorithms.

REFERENCES

Chen, S., Wei, X., Lui, J., Sun, Z., Chen, G., Yang, M., Lui, Y., Wang, D., Ma, C. and Kong, D. (2022). 'Weak acid leaching of uranium ore from a high carbonate deposit', *Journal of Radioanalytical and Nuclear Chemistry*, 331, pp. 123–135.

Forsys Metals Corp (2023), *Annual Information Form for the fiscal year ended December 31, 2022*, Toronto. https://www.forsysmetals.com/wpcontent/uploads/2025/04/forsysAIF03262025JW.pdf [accessed: April 2026].

Habashi, F. (1999) *Textbook of Hydrometallurgy*. 2nd edn. Métallurgie Extractive Québec, Quebec City. International Atomic Energy Agency (2020) *World Uranium Geology, Exploration, Resources and Production*, International Atomic Energy Agency, Vienna.

Lottering, M.J. (2007). Characterisation of the uranium leaching behaviour of low-grade Vaal River ores. *M.Sc. Thesis*, Stellenbosch University, South Africa.

Merritt, R.C. (1971). *The Extractive Metallurgy of Uranium*, Colorado School of Mines Research Institute, Colorado.

Paladin Energy (2023*), Langer Heinrich Mine: corporate technical overview*, Perth. https://www.paladinenergy.com.au/our asset/langer-heinrich-mine [accessed April 2026].

Rössing Uranium Limited (2015), *2014 Stakeholder Report (Annual Environmental Report)*, rossing.com/files/reports-research/Annual Environmental Report Rossing 2014.pdf [accessed April 2026]

World Nuclear Association (2025) Uranium Mining Overview. https://world-nuclear.org/information-library/nuclear-fuel-cycle/mining-of-uranium/uranium-mining-overview [accessed April 2026]

Nashlen Odiar

Group Technical Director
Rados International Technologies

Nashlen Odiar is the Group Technical Director at Rados International Technologies, with over 15 years of experience in ore sorting, sensor-based algorithm development and minerals processing. He has led international commissioning, training and project delivery across multiple commodities in more than nine countries.

He previously served as a Process Engineer at Rados International Services, specialising in sorter calibration, commissioning, and R&D integration and as Project Chief Investigator at Mintek, where he led mineral processing testwork programmes involving advanced sensor sorting technologies.

Nashlen holds a BSc in Chemical Engineering from the University of KwaZulu-Natal and a Certificate in Data Analysis from the University of Cape Town. His experience spans base metals, precious metals and platinum group metals.

Annelize Fouchee

Business Development Director
Rados International Technologies

Annelize Fouchee is the Business Development Director at Rados International Technologies, with nearly two decades of experience in mineral processing and equipment design. She has extensive expertise in mineralogical and metallurgical characterisation, test work programmes for flowsheet development and the integration and optimisation of beneficiation and bulk materials handling systems.

Her technical experience includes equipment selection, commissioning and performance optimisation across flotation, gravity separation, dense media, magnetic separation, automated sampling systems, solid–liquid separation and sensor-based ore sorting technologies. She has led metallurgical audits, production optimisation initiatives and total cost of ownership studies across multiple operations.

Annelize has worked across a wide range of commodities including lithium, iron ore, platinum group metals, diamonds, manganese, chromite, gold, copper, silver, tin, coal, rare earths, phosphates, tantalum, zinc, potash, vanadium, mineral sands, industrial minerals and uranium.

Rethinking flocculant preparation in high-throughput mining applications: A techno-economic comparison of conventional batch vs continuous systems

S.B. Burelli, C.M. Klopper, T. Marcus

ProProcess Engineering (Pty) Ltd, South Africa

Continuous processing is generally preferred in high-throughput industrial applications due to improved process stability, reduced equipment sizing, and lower operational variability. Despite this, flocculant preparation systems within the mining and minerals processing industry remain predominantly batch-based, even as plant throughputs continue to increase.

Flocculant preparation is more complex than simple dissolution, requiring controlled wetting and hydration to achieve optimal polymer activation. Poor preparation can result in polymer agglomeration, inconsistent solution quality, and reduced downstream flocculation performance. While continuous polymer preparation technologies are widely adopted in industries with high and sustained polymer consumption, such as the energy sector, mining operations continue to rely largely on conventional batch systems.

This paper presents a techno-economic comparison between conventional batch flocculant preparation and continuous modular make-up systems for high-capacity mining applications. The assessment evaluates equipment sizing, installed power, footprint, operational stability, and modularisation potential using a representative minerals processing case study.

The analysis demonstrates that continuous systems fundamentally scale more efficiently than batch systems because equipment sizing is governed by steady-state process demand rather than intermittent peak demand associated with batch operation. The results show significant reductions in tankage, installed power, and operational complexity for continuous systems, while also improving process consistency and reducing operator dependency.

The advantages of continuous modular flocculant preparation are particularly relevant to modern hydrometallurgical operations, including uranium and critical minerals projects, where high throughput, water recovery, modular deployment, and operational reliability are increasingly important.

Keywords: Flocculant Preparation, Batch vs Continuous, Modular

INTRODUCTION

Flocculants are critical to modern minerals processing operations, particularly in thickening, clarification, and tailings management applications. As plant throughputs continue to increase across the mining industry, so does the demand for larger and more reliable reagent preparation systems.

Continuous processing is generally preferred in high-throughput industrial applications due to improved process stability, reduced equipment sizing, and lower transient variability (Perry and Green, 2008; Towler and Sinnott, 2022). Despite this, flocculant preparation systems within the mining and minerals processing industry remain predominantly batch-based, even for large-scale operations.

The mining industry has historically favoured batch preparation systems due to operational familiarity, lower complexity at smaller scale, and the intermittent nature of earlier lower-throughput operations. However, this approach presents increasing challenges as system capacity requirements grow. Batch systems are inherently transient in nature, requiring intermittent filling, metering, hydration, and transfer operations. As throughput increases, equipment must be sized around peak intermittent demand rather than average process demand, resulting in disproportionately large tankage, increased utility requirements, larger installation footprints, and greater operational complexity.

In contrast, continuous preparation systems operate under steady-state conditions in which powder metering, wetting, hydration, and transfer occur continuously at the average process demand rate. Continuous systems are well established in industries with high and sustained polymer consumption, particularly within the energy sector, where process consistency and reliability are critical.

The increasing adoption of modular process plant execution strategies within the mining industry further highlights the limitations of conventional batch systems. Large batch tanks are poorly suited to modularisation due to transport limitations and site fabrication requirements, whereas continuous systems typically utilise smaller process vessels that can be more readily integrated into modular skid-based designs.

This paper presents a techno-economic comparison between conventional batch flocculant preparation systems and continuous modular make-up systems for high-capacity mining applications. A representative minerals processing case study is used to compare equipment sizing, installed power, operational philosophy, and modularisation suitability. The paper further examines the relevance of continuous preparation systems to modern hydrometallurgical operations, including uranium and critical minerals processing applications.

FUNDAMENTAL PRINCIPLES OF FLOCCULANT PREPARATION

Flocculants used in minerals processing are typically high molecular weight polyacrylamides supplied in dry powder form. Effective flocculation performance depends heavily on achieving proper wetting and hydration of the polymer prior to dosing into the process stream (Castillo *et al*., 2023; Bonnier *et al.*, 2025).

Wetting

Wetting is the initial and most critical stage of flocculant preparation. It refers to the process of bringing individual dry polymer particles into contact with water in such a way that each particle is uniformly dispersed and hydrated without the formation of agglomerates. Dry flocculant powders are inherently hydrophilic, but hydrate relatively slowly and exhibit a strong tendency to form gel-like structures upon initial contact with water. If dispersion does not occur rapidly and uniformly, partially hydrated agglomerates, commonly referred to as ‘fish-eyes’ can form, where a hydrated outer layer encapsulates dry powder within (Castillo *et al.,* 2023). These agglomerates significantly reduce the effective active polymer concentration in solution and negatively impact downstream flocculation performance.

Figure 1. Poor wetting results in the formation of polymer fish-eyes (red arrow) which prevent further water penetration, compromising hydration.

Wetting equipment

Due to the inherent difficulty of achieving effective polymer wetting, a wide range of technologies has been developed to optimise this critical step in flocculant preparation. These technologies can broadly be categorised into two groups: static wetting devices and dynamic wetting devices.

Static wetting devices contain no moving parts, with wetting typically achieved by introducing dispersed polymer powder into a high-velocity water stream through spray nozzles, venturis, or similar hydraulic arrangements. These systems are relatively simple, robust, and cost-effective, and can be applied in both batch and continuous make-up systems. Effective operation, however, depends on maintaining a carefully controlled water-to-powder ratio to prevent agglomeration and ensure adequate particle dispersion. This limitation restricts the maximum achievable solution concentration and, in batch systems, often governs the polymer addition time, which is typically the longest step in the overall batch preparation cycle.

Dynamic wetting devices incorporate rotating mechanical components, commonly arranged in a rotor–stator configuration. In these systems, the polymer powder is rapidly dispersed and emulsified into the water under intense local shear conditions, promoting rapid and consistent wetting of individual particles before significant hydration occurs. The higher shear energy generated by dynamic systems enables substantially greater powder loading for a given water flowrate, allowing higher-capacity operation and the production of more concentrated polymer solutions than is generally achievable with static wetting devices. The increased mechanical complexity of dynamic wetting systems results in higher capital and maintenance costs compared with static devices. Consequently, they are mostly applied in continuous make-up systems where high throughput, elevated solution concentrations, and consistent solution quality justify the additional investment.

Hydration

Following wetting, hydration occurs as the polymer chains absorb water and gradually uncoil into their active state (Bonnier *et al.*, 2025). This process requires controlled residence time and low shear conditions to avoid polymer degradation. Previous studies have shown that flocculant activity is highly sensitive to preparation conditions, including wetting quality, hydration time, mixing conditions, and shear exposure (Castillo *et al.*, 2023; Beshr *et al.*, 2022). Inadequate preparation can reduce settling performance, increase reagent consumption, and negatively affect overflow clarity and solution recovery. As a result, flocculant preparation system design plays a significant role in overall plant

performance, particularly in high-throughput thickening and tailings applications.

PROCESS ENGINEERING PERSPECTIVE

Batch scaling limitations

As throughput increases, batch systems are typically forced towards either larger individual batches or increased batch frequency. Large low-frequency batches reduce the number of process transitions and operator interventions but require substantial tankage and high instantaneous utility demand. Conversely, increasing the number of smaller batches reduces individual batch volume, but increases the number of cycles required each day. At sufficiently high batch frequency, the operating philosophy begins to approach quasi-continuous operation. However, the system still retains the transient behaviour and sequencing complexity associated with batch preparation. This increases process control complexity, equipment cycling frequency, and the opportunity for operational variability.

The comparison presented in this paper represents three operating scenarios:

- batch preparation: low-frequency large-volume and medium-frequency medium-volume, and
- true steady-state continuous preparation.

Conventional batch operation

Conventional batch systems operate cyclically through a sequence of filling, powder addition, hydration, and transfer stages. Because these operations occur intermittently, equipment must be sized to accommodate peak instantaneous demand within the available batch cycle time. As throughput increases, this operating philosophy results in disproportionately larger tanks, pumps, mixers, and utility systems (Towler and Sinnott, 2022). The scaling behaviour of batch systems therefore becomes increasingly inefficient at high throughput, particularly where long polymer hydration times are required. In addition to larger equipment sizing, batch systems introduce repeated transient operating conditions with each preparation cycle. Variations in filling, powder addition, hydration, and transfer can introduce inconsistencies in solution quality and increase operator dependency.

Steady-state continuous operation

Continuous systems operate fundamentally differently. Powder metering, wetting, hydration, and transfer occur continuously under steady-state conditions at the average process demand rate (Perry and Green, 2008). Because preparation equipment sizing is governed directly by the required process throughput rather than intermittent peak demand, significantly smaller tanks and lower installed power are required. The storage tanks are sized based on peak dosing loads with suitable design factors applied to the preparation system to allow for catch-up. Continuous operation also enables more stable residence time control, more consistent hydration conditions, and tighter process control. Modern automation systems further enhance continuous operation by maintaining stable concentration, flowrate, and dosing conditions throughout operation.

Operational stability and process control

Continuous systems inherently reduce operational variability compared with batch operation (Seborg *et al*., 2017). Since the system remains in steady-state operation, fluctuations associated with repeated batch cycles are eliminated. Continuous systems also reduce the impact of process upsets. In a continuous plant, deviations in quality can typically be isolated rapidly with limited material loss. In contrast, an entire batch may become off-specification before a deviation is identified. The reduction in repeated start-stop operation also lowers mechanical stress on pumps, mixers, valves, and drive components, potentially reducing maintenance and improving long-term equipment reliability.

CASE STUDY

Case study design criteria

A representative minerals processing thickener application was selected for the techno-economic

comparison. The thickener requires 20 m^3/hr of flocculant solution at a concentration of 0.5% w/v, corresponding to a dry flocculant consumption of 100 kg/hr. A hydration time of 90 minutes was specified based on the selected high molecular weight flocculant. The design criteria for the flocculant preparation system are summarised in Table I.

Three preparation philosophies were evaluated:

- Conventional batch preparation – two and four batches per day
- Continuous modular preparation

Table I. Case study process design criteria

Design criterion	Unit	Value
Flocculant powder delivery format	-	750 kg bulk bag
Flocculant solution make-up concentration	%w/v	0.5
Flocculant solution consumption	m^3/hr	20
Dry flocculant powder consumption	kg/hr	100
Hydration time	min	90

Process description: conventional batch system

For the conventional batch make-up system, equipment sizing is governed by the batch cycle rather than by steady-state process demand. The system must prepare sufficient flocculant solution in discrete batches to sustain continuous thickener operation between preparation cycles. Tank volumes, powder feed rates, water flowrates, and transfer rates are therefore determined by the available batch cycle time. In this paper, the batch systems were designed around two and four preparation cycles per day. Each batch is therefore required to supply twelve or six hours of continuous flocculant demand. The twelve-hour or six-hour operating window establishes the maximum allowable batch cycle time, while the selected process rates determine the actual batch preparation time, as all preparation steps, including filling, powder addition, wetting, hydration, and transfer to storage, must be completed within the allowable period. The assumptions for the batch operating systems are summarised in Table II.

Table II. Batch process assumptions

Design criterion	Unit	Value (2-Batch System)	Value (4-Batch System)
Plant operating period	hr	24	24
No. of batches per day	batches/day	2	4
Batch cycle time	hr/batch	12	8
Make-up tank volume	m^3	240	120
Dry powder requirement per batch	kg/batch	1200	600
Storage tank sizing factor		1.5	1.5
Storage volume	m^3	360	180

A process flow diagram (PFD) of a typical batch make-up system is presented as Figure 2.

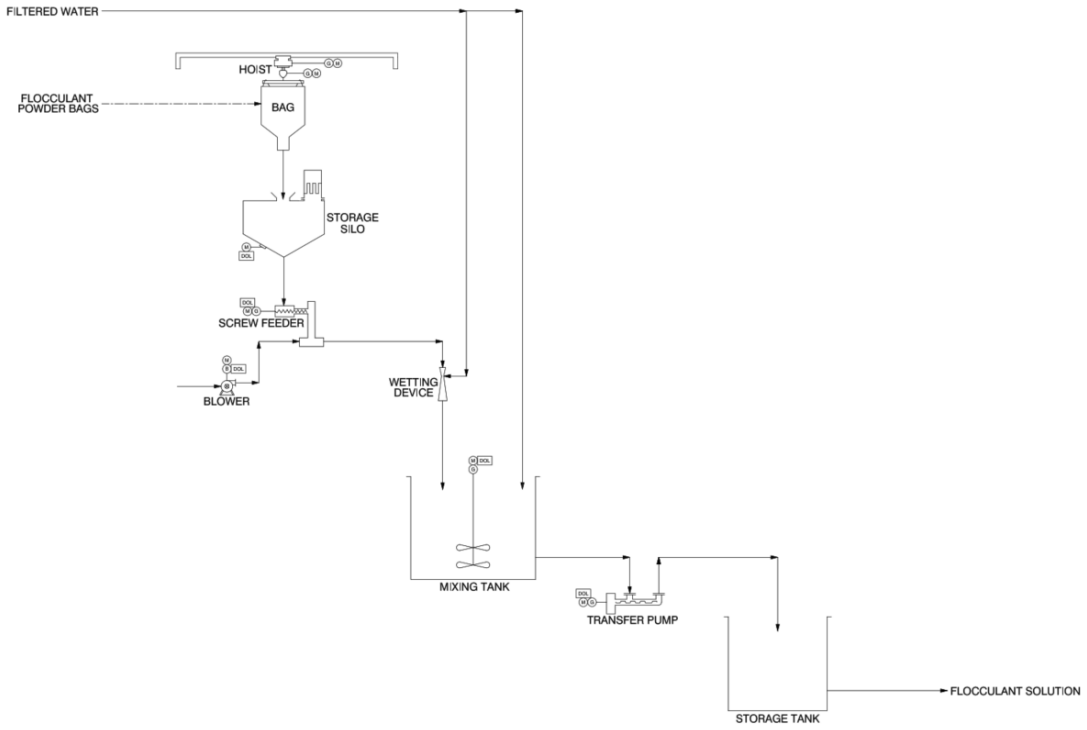

Figure 2. Batch make-up system process flow diagram.

Figure 3 is a snapshot of the two-batch per day make-up plant 3D model. Note the large batch make-up tank (240 m^3) and the storage tank (360 m^3).

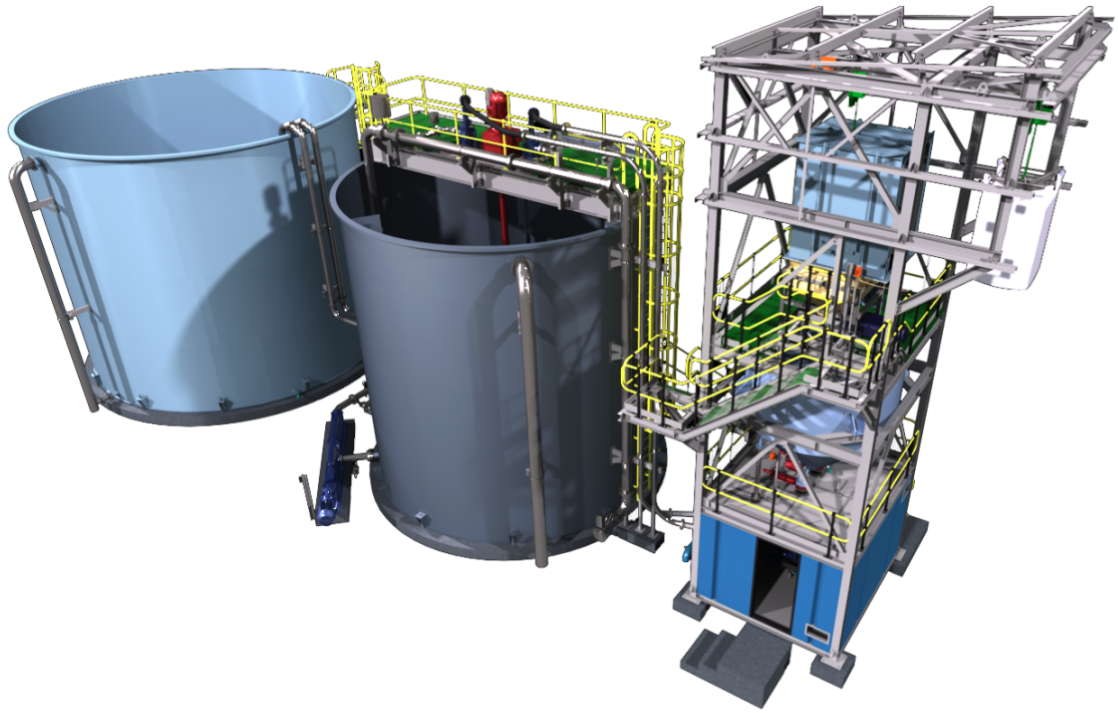

Figure 3. 3D model of the batch make-up system.

The batch preparation sequence was deliberately maximised within the available operating window to minimise the required equipment capacities. Lower initial fill rates, powder feed rates, wetting water flowrates, and transfer rates reduce instantaneous utility demand and equipment sizing but increase the duration of each batch preparation step. The selected equipment specifications and batch cycle times are given in Tables III and IV respectively.

Table III. Case study batch process design

Design parameter	**Unit**	**Value (2-Batch System)**	**Value (4-Batch System)**
Flocculant bulk storage capacity	m^3	5	5
Initial fill water flow rate	m^3/hr	45	60
Powder feed rate	kg/min	4	6
Wetting water to powder ratio	L/kg	125	83
Wetting device water flow rate	m^3/hr	30	30
Solution transfer to storage flow rate	m^3/hr	80	80

Table IV. Batch process cycle time

Process step	**Calculation**	**Time (min) (2-Batch System)**	**Calculation**	**Time (min) (4-Batch System)**
Fill to agitator start level	60 m^3 filled at 45 m^3/hr (25 % tank level)	80	30 m^3 filled at 60 m^3/hr (25 % tank level)	30
Powder feed and wetting	1200 kg dry powder fed at 4 kg/min 150 m^3 filled at 30 m^3/hr (62.5 % tank level)	300	600 kg dry powder fed at 6 kg/min 50 m^3 filled at 30 m^3/hr (41.7 % tank level)	100
Fill to full tank volume	30 m^3 filled at 45 m^3/hr (12.5 % tank level)	40	40 m^3 filled at 60 m^3/hr (33.3 % tank level)	40
Hydration time		90		90
Transfer to storage time	240 m^3 transferred at 80 m^3/hr	180	120 m^3 transferred at 80 m^3/hr	90
Total batch cycle time		690 (11.5 hrs)		350 (5.8 hrs)

Reducing installed tankage requires either higher process rates or increased batch frequency. As the number of batches per day increases, the system progressively approaches quasi-continuous operation but still retains the transient behaviour and sequential control complexity inherent to batch processing.

Process description: continuous modular system

For the continuous make-up system, equipment sizing is governed by the steady-state material balance and the required hydration residence time rather than by a batch preparation cycle. Powder metering, wetting, hydration, and transfer occur continuously at the average process demand rate.

In contrast to the batch system, the continuous make-up system does not require large discrete preparation volumes or intermittent high-capacity transfer operations. Tank volumes and pumping rates are therefore determined directly from the required steady-state throughput and retention time requirements.

A PFD of a typical continuous make-up system is presented in Figure 4.

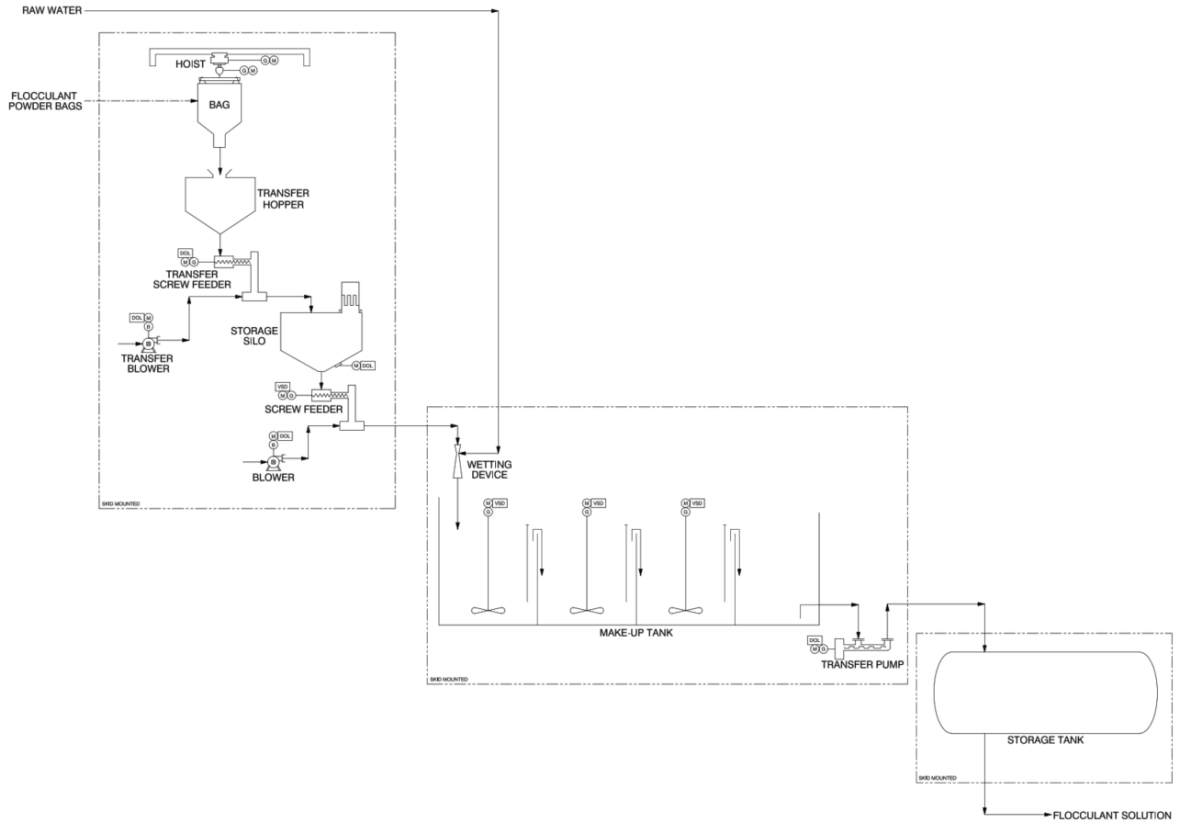

Figure 4. Continuous make-up system process flow diagram.

Figure 5 is a snapshot of the continuous make-up plant 3D model. Note the significantly smaller continuous make-up tank (30 m^3) and the storage tank (80 m^3) when compared to the tanks required for the batch make-up plant.

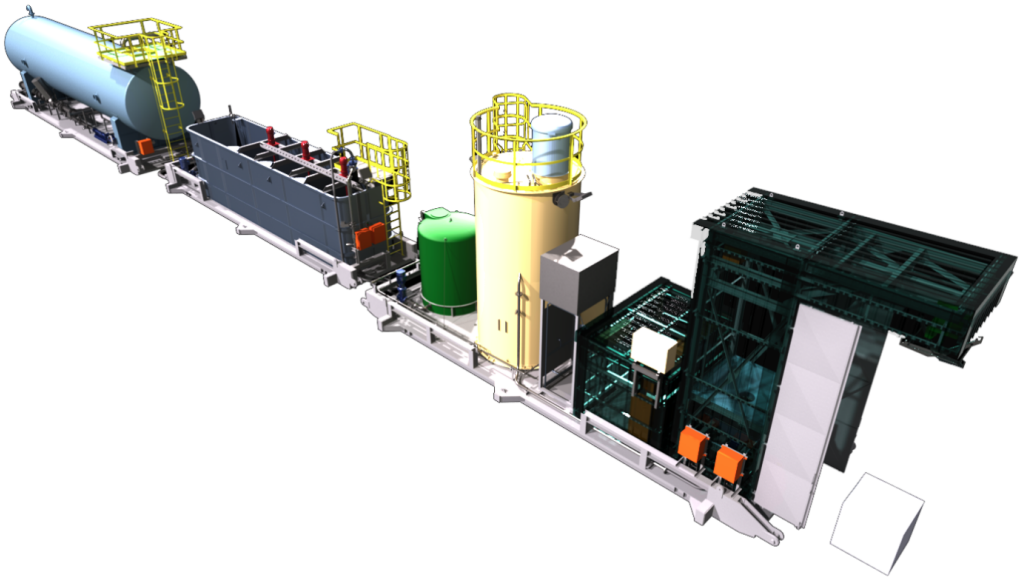

Figure 5. 3D model of the continuous modular make-up system.

In the continuous system, flocculant powder is continuously metered into the wetting device in proportion to the process water flowrate to maintain the required solution concentration. The wetted polymer solution then passes through a series of agitated compartments that provide the required hydration residence time under controlled low-shear conditions. Because the system operates continuously at steady-state conditions, the make-up tank only needs to provide the required hydration residence time rather than storing large batch volumes. The final storage tank provides operational buffer capacity and allows the make-up system to remain decoupled from fluctuations in downstream dosing demand.

The design resulting from the specified design criteria and steady-state material balance is summarised in Table IV.

Table IV. Case study continuous process design

Design parameter	Unit	Value
Flocculant bulk storage capacity	m^3	5
Powder feed rate	kg/min	1.67
Wetting water to powder ratio	L/kg	200
Wetting device water flow rate	m^3/hr	20
Make-up tank volume at 90 min hydration time	m^3	30
Solution transfer to storage flow rate	m^3/hr	20
Storage tank capacity at 4 hr retention time	m^3	80

CASE STUDY: TECHNO-ECONOMIC COMPARISON

The key difference between the batch and continuous systems is that the batch plants are sized around intermittent peak preparation requirements, while the continuous plant is sized around average steady-state demand.

This difference fundamentally affects:

- installed tankage,
- transfer capacities,
- utility demand,
- installed power,
- plant footprint,
- and modularisation suitability.

The techno-economic comparison therefore focuses on how the governing operating philosophy influences equipment sizing and operational complexity.

Capital investment comparison

Table V compares the principal process equipment sizing for the batch and continuous flocculant make-up systems. The 'batch size factor' represents the ratio between the batch equipment size and the corresponding continuous equipment size. This factor represents the ratio between the estimated batch equipment capital cost and the corresponding continuous equipment capital cost.

The comparison shows that the batch systems require substantially larger tankage and higher transfer capacities due to the intermittent nature of batch preparation. In the selected operating philosophy, the batch plants must prepare and transfer large discrete solution volumes within a limited operating window, whereas the continuous plant operates continuously at the average process demand rate.

The bulk bag debagging systems and final dosing systems are excluded from the comparison since these would be common to both configurations for the case study considered.

Table V. Comparison of the batch vs continuous modular process equipment design

Design parameter	Unit	2-Batch System	4-Batch System	Continuous	2-Batch size factor	2-Batch cost factor	4-Batch size factor	4-Batch cost factor
Flocculant bulk storage capacity	m^3	5	5	5	1	1	1	1
Powder feed rate	kg/min	4	6	1.67	2.4	1.95	3.6	1.95
Make-up tank volume	m^3	240	120	30	8	2.65	4	1.67
Solution transfer to storage flow rate	m^3/hr	80	80	20	4	1.72	4	1.72
Storage tank capacity	m^3	360	180	80	4.5	2.84	2.25	1.79
Plant footprint	m x m	29 x 11	-	41 x 4	1.9		-	
	m^2	319	-	164	1.9		-	

The most significant difference between the batch and continuous systems is the installed tankage requirement. The batch systems require a 240 or 120 m^3 make-up tank, and a 360 or 180 m^3 storage tank, compared with only a 30 m^3 hydration tank and an 80 m^3 storage tank for the continuous system.

Although the continuous plant has a greater overall length than the two-batch plant, its narrow skid-based arrangement allows the system to be modularised into transportable sections suitable for standard road freight or containerised transport. The continuous plant therefore remains highly suited to modular off-site fabrication and rapid installation. In contrast, the batch systems are dominated by large diameter tanks with substantially greater individual vessel volumes. These tanks cannot practically be transported as complete assembled modules and therefore require significant site fabrication, lifting, and installation activities.

The comparison therefore highlights an important distinction between overall footprint area and practical modularisation suitability. While the two-batch plant occupies a more compact arrangement in plan view, the continuous plant is substantially more transportable and better aligned with modular construction methodologies.

The batch cost factors shown in Table V are based on estimated relative equipment and installation costs for the two configurations. Final installed project cost would also be influenced by factors such as site location, fabrication strategy, installation methodology, logistics, and local infrastructure availability.

Operating cost comparison

Table VI compares the water and power requirements of the batch and continuous flocculant make-up systems. As previously described, the debagging and final dosing systems are excluded from the comparison since these would be common to all plant configurations. Since all systems ultimately prepare the same quantity of flocculant solution, the total flocculant powder consumption is also identical and is therefore excluded from the operating utility comparison.

Table VI. Comparison of the batch vs continuous modular water and power requirements

Design parameter	Unit	2-Batch System	4-Batch System	Continuous	2-Batch size factor	2-Batch cost factor	4-Batch size factor	4-Batch cost factor
Water								
Wetting device water flow rate	m^3/hr	30	30	20	1.5	1	1.5	1
Fill water flow rate	m^3/hr	45	60	-	-	1	-	1
Power								
Powder blower	kW	11	11	7.5	1.5	0.61	1.5	0.41
Powder screw feeder	kW	0.75	0.75	0.25	3	1.25	3	0.83
Make-up tank agitator	kW	22	15	3 x 0.75	9.8	5.84	6.7	4.26
Solution transfer pump	kW	15	15	5.5	2.7	0.68	2.7	0.68
Total installed power comparison	kW	48.75	41.75	15.5	3.1	1.41	2.7	1.07

Although all systems ultimately consume the same average quantity of water, the batch plants require substantially higher instantaneous water flowrates during rapid filling and wetting operations. The batch systems therefore require larger water supply infrastructure, including larger piping systems, pumps, valves, and associated distribution equipment to accommodate the intermittent peak demand.

The installed power requirement for the batch systems is greater than that of the continuous system, reflecting the significantly larger equipment required to complete intermittent batch preparation within the available operating window.

While certain items within the batch plants operate intermittently rather than continuously, the larger installed equipment and higher instantaneous operating loads still result in an overall operating power cost to be greater than that of the continuous system.

The higher instantaneous utility demand of the batch systems also impacts upstream infrastructure sizing, including water supply systems, piping, pumps, electrical reticulation, motor control centres, structural steelwork, and foundations. These indirect infrastructure impacts become increasingly significant at larger plant throughputs and further favour continuous steady-state operation.

Operational considerations

The process control philosophies of the batch and continuous systems differ fundamentally. Batch systems rely on sequential event-based control requiring repeated initiation and completion of filling, metering, hydration, transfer, and reset operations. Each batch therefore introduces multiple transient operating states and repeated opportunities for variation in process conditions.

As batch frequency increases to reduce installed tankage or increase throughput, the number of process transitions and control events also increases. The system progressively approaches quasi-continuous operation but still retains the transient behaviour and sequencing complexity inherent to batch processing.

Continuous systems instead operate primarily under steady-state feedback and ratio control. Powder feed rate, wetting water flowrate, solution concentration, residence time, and transfer rate are maintained continuously within predefined operating ranges. The reduction in process transitions simplifies control architecture and reduces operational variability.

Consistent flocculant solution quality is inherently easier to achieve in a continuous make-up system

operating under stable steady-state conditions. In contrast, batch preparation introduces repeated opportunities for operator error, inconsistent wetting, variable hydration performance, and fluctuations in solution quality with every batch cycle.

Modern process control systems further enhance continuous operation by maintaining tightly controlled operating conditions throughout operation, ensuring that solution concentration, flowrate, residence time, and hydration performance remain within specification.

From an operational risk perspective, the continuous system also significantly limits the potential impact of process upsets. Should a fault or quality deviation occur within the make-up system, the continuous plant can be isolated rapidly, with a maximum of approximately 30 m^3 of solution potentially requiring rejection. By comparison, a two-batch preparation system may produce an entire off-specification batch before the deviation is identified, potentially resulting in up to 240 m^3 of unusable solution. The operational exposure associated with the batch system is therefore approximately eight times greater than that of the continuous system.

Continuous systems also provide superior operational flexibility. Solution concentration and dosing parameters can be adjusted dynamically during operation, allowing real-time optimisation and rapid correction of process deviations. In batch systems, process adjustments can generally only be implemented between batches, resulting in slower response times and reduced operational agility.

In addition, continuous systems generally impose lower mechanical stress on equipment. Batch systems are subject to repeated start-stop cycles, filling and emptying operations, and fluctuating mechanical loads, all of which contribute to increased wear on pumps, mixers, valves, and drive components. Continuous systems operating under stable loading conditions therefore typically experience reduced mechanical fatigue, lower maintenance requirements, and improved long-term equipment reliability.

CONCLUSION

This paper demonstrates that continuous modular flocculant make-up systems offer significant technical and economic advantages over conventional batch systems for high-throughput minerals processing applications.

The comparison shows that batch systems become increasingly constrained at higher throughputs because equipment sizing is governed by intermittent batch preparation requirements and repeated transient operation. In contrast, continuous systems operate directly at steady-state process demand, enabling substantially lower installed tankage, reduced instantaneous utility demand, smaller equipment sizing, and simplified process control.

The advantages of continuous systems extend beyond equipment reduction alone. Improved process stability, reduced operational variability, lower upset consequence, and improved modularisation suitability make continuous flocculant preparation increasingly aligned with modern mining project execution strategies.

While conventional batch systems remain suitable for smaller or intermittent duties, increasing plant throughput progressively drives batch systems toward higher-frequency operation, increasing process complexity while retaining the transient nature of batch preparation. Continuous systems fundamentally eliminate this scaling limitation through steady-state operation.

The comparison also demonstrates that the governing operating philosophy has a direct impact on modularisation suitability and project execution strategy. Although the continuous system has a greater overall plant length, its narrow skid-based configuration enables transportable modular construction using standard freight and containerised logistics. In contrast, the large tankage associated with low-frequency batch preparation requires significant site fabrication and installation activities, reducing the

practicality of modular deployment.

From an operational perspective, continuous systems further reduce process risk by limiting the volume of solution exposed to process upsets, while also enabling tighter process control, improved operational flexibility, and reduced mechanical stress on equipment.

The advantages identified in this paper are particularly relevant to modern hydrometallurgical operations, including uranium and critical minerals projects, where increasing plant throughput, remote project locations, water management requirements, and modular execution strategies continue to drive demand for compact, transportable, and operationally stable process solutions.

Continuous modular flocculant preparation therefore represents a fundamentally more scalable and operationally robust approach for future high-throughput minerals processing applications.

REFERENCES

Beshr, M., Fourie, A.B., Becker, M., and Gorman, R. 2022. The impacts of high salinity and polymer properties on dewatering and structural characteristics of flocculated high-solids tailings. *Journal of Cleaner Production*, vol. 330.

Bonnier, C., Heath, A., and Fawell, P. 2025. Ensuring efficient tailings treatment: the importance of optimal flocculant dissolution. In: *Proceedings of Paste 2025*.

Castillo, C., Fawell, P., and Costine, A. 2023. Optimising the activity of acrylamide-based polymer solutions used to flocculate mineral processing tailings suspensions – A review. *Chemical Engineering Research and Design*, vol. 199, pp. 654-676.

International Atomic Energy Agency (IAEA). 2005. *Management of Uranium Mine and Mill Wastes*. IAEA Technical Reports Series. Vienna, Austria.

Perry, R.H. and Green, D.W. 2008. *Perry's Chemical Engineers' Handbook*. 8th edn. McGraw-Hill, New York.

Seborg, D.E., Edgar, T.F., Mellichamp, D.A., and Doyle, F.J. 2017. *Process Dynamics and Control*. 4th edn. John Wiley & Sons, Hoboken, New Jersey.

Towler, G. and Sinnott, R. 2022. *Chemical Engineering Design: Principles, Practice and Economics of Plant and Process Design*. 3rd edn. Elsevier, Oxford.

Cara-Mari Klopper

Process Engineering Lead
ProProcess Engineering

My professional career began in the design and application of heat transfer equipment for the mining and food & beverage sectors. I have since transitioned into process design consultancy, where I contribute to diverse projects within the oil & gas and mining industries. This trajectory has allowed me to lead design work across the full project lifecycle—from initial feasibility studies and detailed engineering to final commissioning.

Through these experiences, I have cultivated a versatile technical skillset and a proven ability to implement complex engineering solutions across multiple industrial sectors

Beyond the grade: Structural geology and rock mass characteristics as a first-order control on life-of-mine value

G. Ockhuizen,[1,2], R. Gibson[2], S. Maclennan[2], A. Mungunda[1], I. Simataa[1], Z. Huai Feng[1]

[1]CGNPC Swakop Uranium, Namibia
[2]Witwatersrand University, South Africa

Mine designs are predominantly grade driven. Resource models are constructed around the spatial distribution of mineralisation, and the pit shells, pushbacks and final slope geometries that follow are optimised largely against the ore envelope, with limited regard for structural and geotechnical contributions. Structural and rock-mass data often receive limited attention during the resource definition stage and are incorporated only later during detailed geotechnical design and operations. This sequencing creates a persistent blind spot: significant structures may be recognised only after mining of an area is already underway, resulting in structurally controlled failures, reactive redesign, increased costs and loss of recoverable ore. This study argues that structural and geotechnical inputs is a first order control on life-of-mine (LOM) alongside grade and belong in the front of the workflow together with resource definition. Many large open pits sit in structurally complex, fault-controlled settings (the Husab Uranium deposit among them), yet only a handful of structural and geotechnical drillholes are drilled to inform the design across large area. Structures therefore go unresolved until they intersected the pit, where they generate structurally controlled failures that must be managed reactively, at the expense of cost and recoverable ore. Earlier, purpose-targeted, structural and geotechnical drilling improves pit optimisation and reduces redesigns. The paper proposes a practical framework for embedding structural interpretation and rockmass characterisation into resource domaining from the earliest planning stages, rather than retrofitting it after failures occur. Early characterisation cost little against the LOM value it preserves, and structure-led design transfers readily to other commodities on the Damara Province and comparable settings.

Keywords: Grade; Life of Mine; Exploration, Mining, Structures; Mine design

INTRODUCTION

Every mining project begins by defining the orebody during exploration. As exploration matures, the project advances through order-of-magnitude assessments, scoping studies, feasibility and bankable feasibility studies, and eventually construction (Read & Stacey, 2011). At each stage, drilling is undertaken to define the extent of the orebody, reduce geological uncertainty, and support the conversion of resources to reserves so the deposit can be evaluated economically. In most cases, however, this drilling is primarily designed to distinguish ore from waste and to quantify grade, tonnage, and continuity. Less attention is given to the structural setting, rock mass conditions, and geotechnical variability of material that must safely support the final mine geometry. As a result, while the ore body is progressively being de-risked through these successive stages, the rock mass required to expose and access the orebody often remains under-characterized.

Structural geology and rock mass characterization are commonly deferred to later geotechnical investigations. This sequencing creates a critical blind spot. By the time the structural controls are properly understood, major mine design decisions such as:

- pit shell selection
- pushback geometry
- slope angle domains
- ramp placement
- reserve conversions

may already be made. At Copper Mountain Mine, Canada limited site-specific geotechnical information contributed to multi-bench instability and subsequent slope flattening, unloading and design revision (Gray Hubbard & Huber, 2025). Similarly, at a short-life Australian lithium mine, feasibility drilling was largely directed towards the orebody rather than the proposed pit walls, contributing to poor early understanding of the rock mass and groundwater conditions. Repeated toppling failures subsequently required structural remapping, back-analysis, increased monitoring, depressurisation and reduced slope angles (Weir et al., 2025) At Kansanshi, Zamibia limited early geotechnical data and optimistic assumptions regarding weathering and groundwater resulted in operational instability and late-stage characterisation and depressurisation programmes (More O'Ferrall & Simbile, 2020). These cases demonstrate that delayed characterisation can lead to redesign, additional stripping, ore sterilisation and structurally controlled failures. Husab represents a comparable case and is discussed in this paper.

This paper examines the risks, limitations and project impacts associated with insufficient structural and rock-mass information during early mine design. It reviews the conventional resource-to-reserve workflow and shows how drilling at each study stage is typically aimed at defining grade and tonnage, while structural and rock-mass characterisation is postponed to a later, more limited geotechnical programme. It examines how unresolved structures can affect slope performance, recoverable ore, and LOM value. Finally, it proposes a practical framework to capture structural and rock mass information from exploration and resource drilling programmes so that these inputs can be embedded earlier into the resource domain in pit optimisation and geotechnical design.

PROBLEM STATEMENT

Current mine design workflows are dominated by the economic envelope. Pit shells, push backs, and final slope geometries are optimised primarily against grade stripping ratio; metal price; recovery; mining and processing cost. Structural geology and the rock mass conditions are frequently introduced only later, during geotechnical design or even during operations, when the opportunity to influence the fundamental mine design is already reduced (JORC, 2012; Read & Stacey, 2011; Steffen, 1997; *The South African Code for the Reporting of Exploration Results, Mineral Resources and Mineral Reserves (The SAMREC Code)*, 2016).

This creates a situation where the resource model may be well constrained, but the geotechnical model remains comparatively uncertain. In practice, this means that a pit can be economically optimised around the ore body while underestimating the structural and rock mass controls that determine whether the ore can be safely and economically accessed.

In a structurally complex open pit mine, this limitation is significant. Unknown or poorly constrained faults, shears, foliation domains, weak rock mass zones, and persistent discontinuities may only be identified once mining exposes them. In such a case, the operation is forced to respond reactively through slow pre-design flattening of slope angles and applying additional stripping, Increasing the monitoring fleet, introducing catchment controls; identifying exclusion zones; or even sterilizing the ore in the process.

RESEARCH GAP

Although most mine planning workflows recognise geotechnical design as essential, structural and rock mass information is often not captured early enough, at sufficient spatial resolution or in a format that can influence the resource-modelling, pit optimization, pushback sequencing and reserve conversion. The gap is simply a lack of geotechnical drilling (Gray Hubbard & Huber, 2025; More O'Ferrall & Simbile, 2020; Ockhuizen et al., 2024; Weir et al., 2025). It is also a failure to extract structural and geotechnical value from drilling that has already been undertaken for resource definition. Exploration holes are commonly drilled, logged, sampled, and assayed with a strong focus on grade (JORC, 2012; *The South African Code for the Reporting of Exploration Results, Mineral Resources and Mineral Reserves (The SAMREC Code)*, 2016), while important for geotechnical information such as defect orientation; fracture frequency, rock mass quality, alteration, shear zones, and structural fabric are either not captured, inconsistently captured, or not integrated into mine design workflows.

This becomes evident during the start of mining operations in an area and discover unknown structures which were not previously identified during the drilling processes. By that point, the cost of correcting the design is significantly higher than the cost of collecting and integrating the information earlier.

AIM AND OBJECTIVES

The aim of this paper is to demonstrate that structural geology and rock mass characteristics should be treated as first-order controls on LOM value rather than secondary inputs introduced after grade-driven pit optimization.

Objectives

- Review how resources-to-reserve workflows tend to prioritise grade tonnage over structural and geotechnical uncertainty.
- Identify the limitations created by sparse geotechnical drilling and structural characterization
- Demonstrate how unresolved structures and rock mass variability can affect slope design, recoverable ore, push back geometry and LOM value.
- Show how exploration and resource drilling programmes can be modified to capture early structural and rock mass information
- Propose a practical framework for integrating structural and rock mass data earlier into resource domaining, pit optimisation and geotechnical designs

CONVENTIONAL RESOURCE TO RESERVE WORKFLOW

How each study stage is scoped

The progression of a mining project from a conceptual target to financial operation is governed by a well-defined sequence of study stages as shown in Figure 1 (JORC, 2012; Read & Stacey, 2011). It begins with prospecting or exploration, to establish an order of magnitude to get a conceptual study developed, followed by scoping the extent, then feasibility and, finally, definitive or bankable feasibility. Each succeeding step demands a higher level of confidence and corresponding tighter accuracy bands.

Grade-driven Exploration and Resource Definition

To refine and increase the confidence of a specific resource, the first and main aim of drilling is to try to upgrade the resource classification to allow for possible conversion to ore reserves. Generally, the Exploration Drilling Programme is designed to answer several grade-related questions such as:

- Where is the ore?
    - Holes are mainly targeted and spaced to intersect and constrain mineralisation, so the geometry of the grade shell can be defined.

- What is the grade?
  - Samples are collected at defined downhole intervals, to generate a dense quantitative grade record. This is the primary reason the holes are drilled.

- What is the tonnage?
  - Grade shell geometry combined with the bulk density measurements allows the volume and the tonnage of the resource to be estimated

- Is there any continuity of the ore itself?
  - Variography and hole-to-hole correlation are used to assess whether the grade is spatially predictable. This helps to determine the required drill spacing.

- What is the confidence category?
  - Resource classification systems such as JORC (JORC, 2012)/SAMREC (*The South African Code for the Reporting of Exploration Results, Mineral Resources and Mineral Reserves (The SAMREC Code)*, 2016) are fundamentally statements of geological and grade confidence. Drill density, sampling quality, geological continuity, and estimation confidence are the main controls used to upgrade material from inferred to indicated and measured categories. The data collected, the drill spacing selected, and the classification frameworks are primarily directed toward one objective: defining grade and tonnage at the defensible level of confidence. This process is effective for defining the ore body, and the reporting codes do require an assessment of geological confidence that, in principle, encompasses structural understanding. However, that confidence is operationalised almost entirely through grade and tonnage continuity. The programme is therefore rarely configured to resolve the structural architectures and rock mass conditions of the deposit, even though the same hole passes through and could readily be characterized for both.

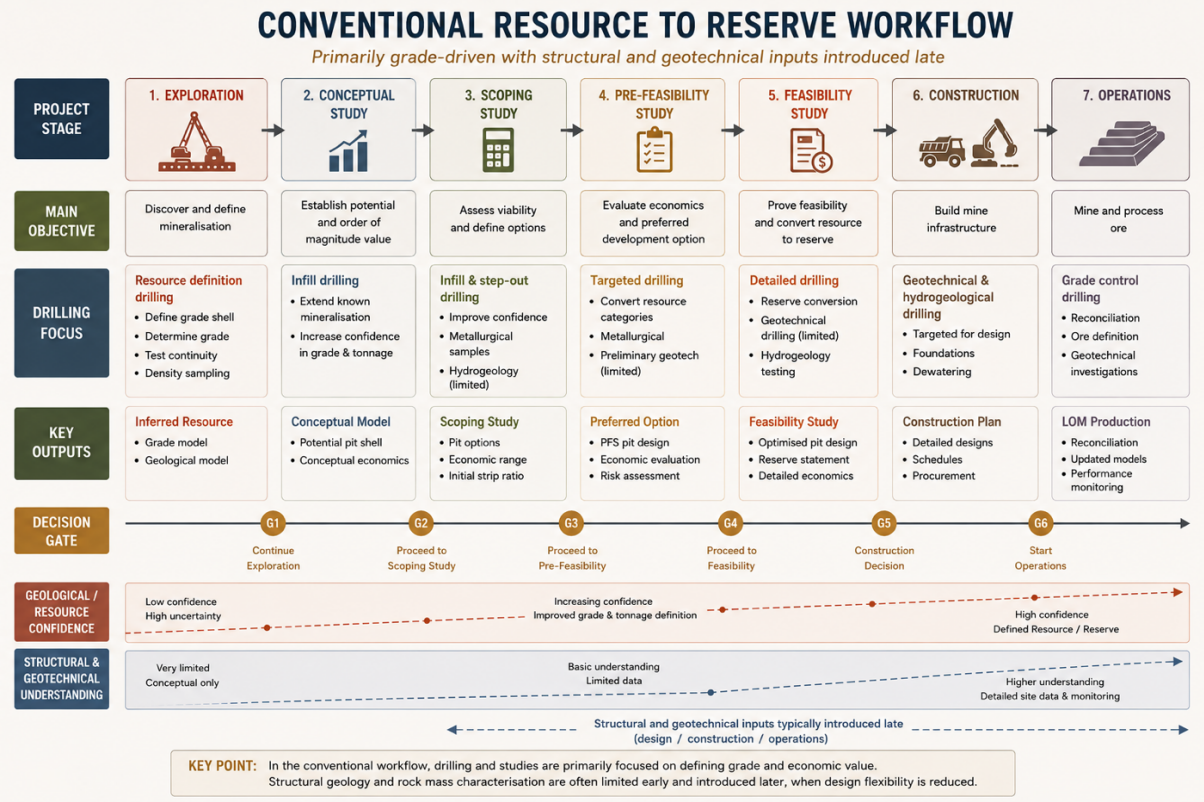

Figure 1. Conventional resource to reserve workflow, which is primarily grade-driven with little regard to structural and geotechnical inputs that are only considered later during feasibility (FS), Definitive feasibility (DFS) or bankable feasibility phases (BFS) (Modified from Read and Stacey, 2011)).

THE STRUCTURAL AND ROCK-MASS DATA GAP IN RESOURCE DRILLING

Why Resource drilling under-captures Structural and Geotechnical Data

Formal structural and geotechnical characterizations typically only enter at the pre-feasibility stage (PFS) or definitive feasibility stage (DFS) when a dedicated geotechnical drilling campaign is commissioned to support the slope design. This campaign is almost always a separate, later and thinner programme than the resource drilling that preceded it, as resource drilling has a formal reporting structures that is required by the formal codes (JORC; SAMREC, NI 43-101), which are audited for company valuation. With fewer holes that are commonly orientated and logged to a different standard in more detail looking at each structure resulting in slower logging, classifying it and aligning it to the orientated line to determine the orientation of the structure subsurface (Hadjigeorgiou, 2012). The holes are targeted at prospective pit walls rather than the ore body itself and often executed by a different team or external consultants (Steffen, 1997). Its output is to define the structural domains, discontinuity sets, the rock mass conditions and the possible slope design angles based on the results from the different parameters (Balideh et al., 2023). This report normally arrives after the resource model has largely been fixed. It is consistently treated as a constraint to be reconciled with a design that has already taken shape around the ore envelope, rather than as inputs that helped shape it.

Resource drilling is optimised for grade, not necessarily for structural interpretation or rock mass characterization (Steffen, 1997). The goals of grade definition and geotechnical characterization can appear to compete because grade drilling is normally designed around mineralized intersections, assay intervals, and resource classification requirements. Structural logging, defect orientation, rock mass characterization, and geotechnical testing are often seen as additional tasks that slow down resource workflow (Hadjigeorgiou, 2012). However, these do not need to be in conflict. Instead of completing a resource drilling campaign first and then conducting a separate geotechnical drilling campaign later, selected resource holes can be designed from the outset to carry both geological and geotechnical value. This can be achieved by applying a defined geotechnical logging suite to selected diamond and RC holes.

The integrated programme may include:

- orientated diamond core and geotechnical core logging;
- optical (OTV) and acoustic (ATV) televiewer surveys;
- full-waveform sonic and fracture-frequency logging;
- weathering, alteration and structural-domain logging;
- selective laboratory testing and early hydrogeological observations.

Most exploration programmes already include downhole surveys to determine hole deviation and orientation. This means that selected additional downhole tools can be incorporated into the same drilling campaign to produce an early, spatially distributed, structural and rock-mass dataset.

The output from such an intervention is an early acquired spatially distributed structural and rock mass dataset that:

a. Identifies the dominant structural sets in the problem domains before a detailed programme is conducted
b. Identifies important targets for the dedicated geotechnical drilling campaign
c. Reduces duplicating geotechnical holes
d. Improves the confidence in designed slope domains
e. Carries structural understanding forward from the start of the project rather than reconstructing it after the first wedge, planar or fault-controlled failure occurs.

STRUCTURAL AND ROCK-MASS PARAMETERS COMMONLY MISSED

Orientation of major structures

A key limitation of resource drilling is that holes are orientated to intersect mineralisation effectively, and not necessarily the structures affecting the ore body. Furthermore, without orientated core, structures may be logged as present, but the true dip and dip direction remain uncertain. This is a major limitation for slope design, where stability depends on how structures are orientated relative to the slope face. Without reliable orientation data, it is difficult to assess whether weak structures are exposed and intersect the slope face, whether wedge failures are kinematically possible, or whether foliation may act as a persistent release plane causing slope failures when area is exposed. Optical and acoustic televiewer surveys can help close this gap by providing oriented images of the subsurface structures to optimised the future pit walls. These tools allow the true dip and dip direction to be measured directly in diamond and RC holes, provided the hole conditions permit.

Persistence and continuity of faults or shears

Implicit modelling tools such as Seequent Leapfrog (Seequent Limited, 2026) can represent faults, shears, veins, and lithological contacts as continuous 3D surfaces, but this continuity is interpretive and depends on data quality, spacing, orientation, and geological consistency. Unlike grade continuity, which is assessed through variography, estimation parameters and resource classification-, structural continuity is rarely quantified with the same level of statistical or design-focused confidence (Steffen, 1997). A modelled shear surface may therefore appear continuous in 3D, but its persistence, defect condition, shear strength, groundwater behaviour, and kinematic relevance to the slope may remain uncertain unless validated by orientated core, televiewer data, pit mapping, and geotechnical testing.

Consistent televiewer interpretation across adjacent holes helps correlate structures where orientations, depths, lithological positions and geotechnical signatures occur; these structures can then be linked and incorporated into a pre-mining 3D structural model. Full-waveform sonic data adds a check by identifying zones of reduced velocity linked to broken, fractured, altered, or sheared rock which can be compared with televiewer picks and core logs to improve confidence in structural continuity.

Rock Mass Quality

Rock mass quality is commonly under-captured in resource drilling because it requires deliberate and consistent geotechnical logging. Parameters such as **Rock Quality Designation (**RQD) (Deere et al., 1967), fracture frequency, weathering, alteration, intact strength, and discontinuity condition may be inconsistently recorded where assay sampling and geological logging are the priority. This is particularly problematic in RC drilling, where chips give limited direct information on the discontinuities, spacing, and core recovery. However, RC holes still provide geotechnical value when paired with suitable downhole tools. Televiewers can provide continuous fracture counts and spacing measurements, which act as a useful proxy for rock mass quality. Full-waveform sonic logging yields P- and S-wave velocity data to estimate the dynamic elastic properties and identify weaker or more fractured zones. These two tools do not replace detailed geotechnical logging of oriented core, but they can significantly improve the spatial coverage of rock mass variability at an early stage.

Defects, spacing, and conditions

Defect spacing, roughness, infill, aperture, wall alteration and surface conditions are critical controls on the shear strength of discontinuities (ISRM, 1978) and directly influence planar, wedge, toppling, and composite failure mechanisms (Read & Stacey, 2011). Because they do not contribute directly to the grade estimation, they may be logged inconsistently or omitted during high-speed resource logging. This creates a major limitation in slope design, as a discontinuity with clay in-fill, polished surfaces, or altered walls may have a very different shear strength from clean, rough, tightly interlocked joints. If these conditions are not captured, slope design assumptions may overestimate rock mass strength. OTV logging resolves spacing, aperture and visible infill or roughness where imaging is clear, while ATV amplitude and travel time distinguish open from healed or tight defects in instances where the optical image is poor due to water clarity or borehole conditions. These observations help prioritise intervals for detailed review, sampling, and laboratory testing.

Structural fabric
Structural fabric including foliations, joints and veins and shear-related fabric elements, is a rock mass property and not a grade property (Dunn & Basson, 2011; Steffen, 1997). In many deposits, this fabric exerts a strong control on slope behaviour, particularly where it is anisotropic and unfavourably oriented relative to the pit wall. Resource models may capture lithological and grade domains, but they do not always capture structural fabric domains, instead producing broad geotechnical domains that may not represent true structural variability of the slope. During the interpretation of the oriented data, stereographic analysis resolves discrete joint, foliation and vein sets and their orientations, allowing fabric to be identified directly from the OTV/ATV log data.

The value of downhole tools is not simply that they provide more data, but they also allow structural and rock-mass information to be captured from holes that have already been drilled. This changes the role of exploration drilling from being purely grade-focused to being a platform for early geotechnical risk reduction.

Table I. Summary of the different parameters and the tools that would help close the gap in resource driven drilling

Data requirement	Gap in resource-driven drilling	Consequence	Tools or methods to close the gap
Orientation of major structures	Structures may be logged pit not oriented	Poor kinematic confidence	Oriented core, OTV, ATV
Fault and shear continuity	Structural continuity not modelled like grade continuity	Persistence poorly constrained	Televiewer correlation, sonic velocity, 3D structural modelling
Rock-mass quality	RQD, fracture frequency, weathering and alteration inconsistently captured	Weak domains missed	Geotechnical core logging, televiewer fracture counts, sonic logging
Defect spacing and condition	Roughness, infill, aperture and wall alteration may be omitted	Shear strength overestimated	OTV, ATV amplitude/travel time, targeted sampling
Structural fabric	Foliation, joint and vein sets not synthesised into domains	Slope-sector risk underestimated	Stereographic analysis, structural domaining, photogrammetry
Hydrogeological indicators	Water strikes and loss zones not always integrated	Pore pressure risk underestimated	Hydrogeological logging, packer testing, piezometers
Weak lithological contacts	Contacts treated as geological boundaries, not mechanical boundaries	Failure surfaces missed	Geotechnical logging, lab testing, model integration

CONSEQUENCES FOR MINE DESIGN AND LOM VALUE

The absence of early structural and rock mass data has direct implications for mine design. For instance, pit optimisation may use slope-angle assumptions that are not adequately supported by structural evidence; and the push-back/stage geometries may be selected without recognising major faults or shear corridors, or may be classified as economically mineable without fully understanding whether the slope geometry required to access it is technically achievable. In this way, structural uncertainty is transferred from exploration into the reserve model and, ultimately, into the operating pit.

Mechanisms of Value Loss

A reserve has practical value only if the slope geometry required to access it can be mined safely and economically. In structural complex slopes, unresolved structural controls can convert economically defined ore into geotechnically constrained or sterilised material. Insufficient structural and rock mass information can reduce the LOM value through several mechanisms (Table II).

Table II Mechanisms by which insufficient early structural and rock mass characterisation reduces life-of-mine value, showing each mechanism, its physical description, and its associated value impact.

Mechanism	Description	Value impact
Slope flattening	Original slope angles cannot be achieved safely	Increased stripping
Pushback redesign	Additional cutbacks required to regain stable geometry	Higher cost and schedule delay
Ore sterilisation	Ore left behind due to unsafe access	Reduced recoverable reserve
Failure remediation	Clean-up, buttressing, catch berms, exclusion zones	Direct cost and lost productivity
Delayed ore access	Instability affects mining sequence	Deferred revenue
Increased monitoring and controls	Additional radar, prisms, inspections, TARPs	Higher operating cost
Reduced mining flexibility	Equipment access or ramp positions constrained	Lower productivity

CASE STUDY: HUSAB URANIUM

The CGNPC Swakop Uranium Husab Mine is one of the world's largest uranium operations. The mine is located in the Erongo Region of Namibia, 60 km northeast of Swakopmund and ~8 km from the well-established Rössing Uranium Mine. It currently consists of 2 operating open pits on the mining lease - Zone 1 in the north and Zone 2 on the south. The deposit was initially owned by Extract Resources, which sold it to CGNPC in 2012. The mine development has been undertaken by CGNPC Swakop Uranium ever since.

Husab Mine is situated within structurally complex Damara Supergroup lithologies in the south-Central Zone of the Damara Belt, where deformation is expressed through foliation development, faulting, folding and shearing (Goscombe et al., 2022; Longridge, 2012; Longridge et al., 2009). Prior to mining, the effects of these features, together with lithological contacts, on slope integrity was poorly understood.

Design stage data limitations

The initial slope designs were developed from a limited number of dedicated geotechnical holes relative to the scale and structural complexity of the open pit. For the initial 2012 design, only 11 geotechnical holes were available for the two pits (6 in Zone 1 North pit and 5 for Zone 2 south pit). These holes formed the basis for defining the initial slope design sectors and associated mining stages. Given the

envisaged size of the pit and the structural complexity and variability expected in a folded and fault-controlled geological setting such as this, the spatial coverage is very limited.

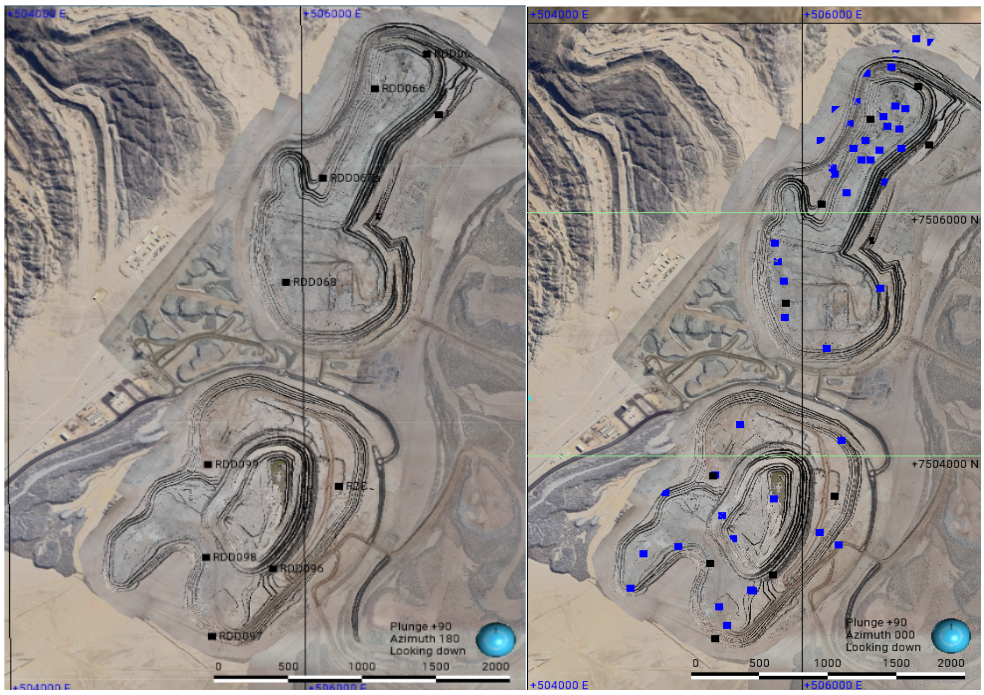

Figure 2: April 2026 aerial image of the Husab Mine showing the Zone 1 (north) and Zone 2 (south) pits. (left) The black squares indicate the drillholes completed during the initial drilling campaign at the start of the project in 2012 (right) black is the geotechnical drillholes of before the mine started and blue square indicate all the geotechnical drillholes that have been drilled during the operational phase of the mine from 2012 to 2025.

Mining commenced in 2013 and, as the phases/stages of the open pits were exposed, structurally controlled instabilities began to occur. These failures highlighted the limitation of the original data coverage. The exposed pit walls provided new structural information that had not been fully resolved by the initial drilling, including discontinuities, weak zones and pervasive structural fabrics that influenced the local slope behaviour. As a result, the early operational phase became an important period of model reconciliation where the design assumptions could be compared against actual slope exposures and performance. In response to the sparse nature of the original geotechnical dataset, an additional drilling campaign was undertaken in 2016-2017. This campaign added seven additional geotechnical holes, consisting of four in the western wall and three in the eastern wall. Given that this additional data was collected after mining had already started and after operational exposures had begun to reveal structural controls on the slope behaviour, this drilling constitutes a reactive improvement to the geotechnical model rather than a fully front-loaded input into the original mine design.

A further effort was made during 2019-2020 to improve the understanding of foliation and other structural controls. Selected Reverse Circulation (RC) holes were drilled and surveyed using optical and acoustic televiewer methods to determine the orientation of geo-discontinuities intersecting the boreholes. The objective was to obtain reliable dip and dip direction data for foliation, jointing, shears, and other structural features that could influence slope behaviour. This was particularly important because foliation orientation relative to the slope face is the key control on planar wedge and composite failure mechanisms.

The 2019-2020 phase of work has demonstrated the value of using downhole tools to extract structural information from holes that are not necessarily drilled as full geotechnical boreholes. It also confirms the central argument of this paper, that structural understanding can be improved significantly when

targeted tools are introduced earlier into the drilling workflow. However, because this work occurred several years after mining commenced, it also highlights the cost of late structural characterization. The same type of information, if collected during the original resource feasibility drilling program, could have provided earlier constraints to slope design, structural risks, and design assumptions.

Operational consequences of late structural recognition

The effect of limited structural characterization became more apparent as mining progressed and the pit walls were progressively exposed. In 2021, a three-bench failure occurred on the Zone 1 northwest, removing a portion of the permanent ramp. That the failure occurred in close proximity to a previous bench-scale failure that was observed above the ramp indicates that the instability was not an isolated, localised event but part of a broader, structurally controlled, slope behaviour pattern. The failure had direct operational consequences - access through the affected area was reduced to one-way traffic, creating a constraint on mining flexibility and increasing the operational significance of the unstable slope sector. A strategy was devised to regain dual access by means of installing a catch fence on the ramp itself, reducing the footprint that the sand berm occupied, as well as mining out the failed material and re-establishing the ramp with waste material (Ockhuizen et al., 2024, 2025).

This event demonstrates how unresolved structural controls can affect not only the slope stability but also the practical operation of the mine. The impact was not limited to the failed volume itself. It affected the ramp access, traffic management, mining sequence, and the ability to maintain normal operational flexibility. In the context of LOM value, such events represent the direct pathway by which structural uncertainty can convert into cost, delay and potential loss of recoverable ore.

Design response and LOM value implications

The affected Zone 1 western wall sector was initially designed at an interim angle of approximately 56°(Figure 3 a on the timeline). Subsequent exposures and structural investigation showed that this geometry was steeper than the controlling foliation fabric, which contributed to the development of structurally controlled failures. Following several design iterations, the inter-ramp slope angle was reduced to approximately 36° (Figure 3 e on the timeline), below the observed foliation dip variability of around 45°-60°. This provides a more conservative geometry relative to the controlling fabric and reduces the potential for larger structurally controlled instabilities.

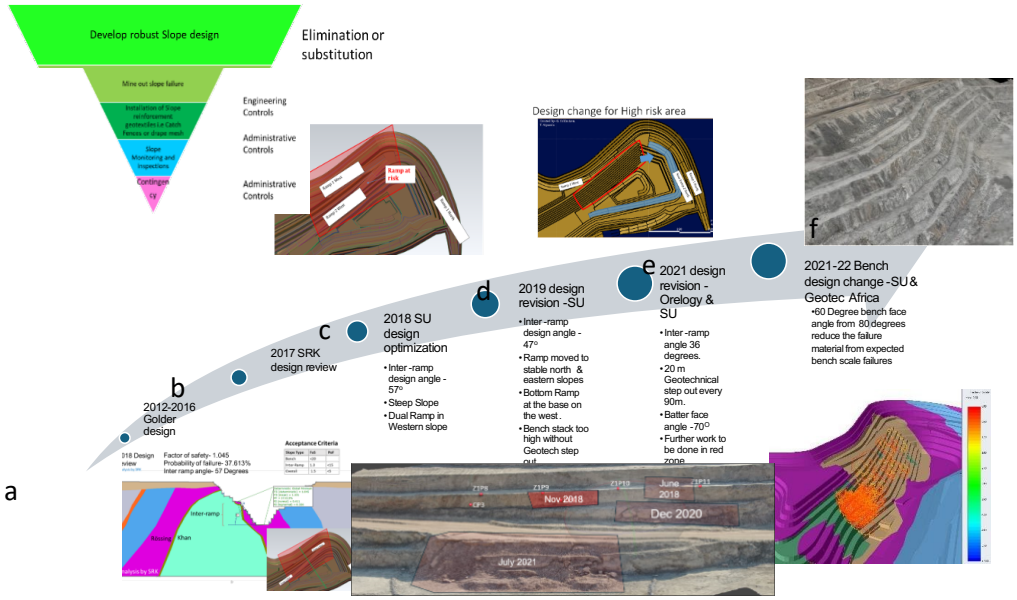

Figure 3. the design evolution timeline of the northern pit (Zone 1) mining design from 2012 to current design (2025) as more structural and geotechnical data was gathered to improve the safety and stability of the western wall that has been causing stability issues since 2018 with several instabilities and bench scale failures illustrated in the centre bottom. Based on the hierarchy of controls (top left) developing a robust slope design can eliminate hazards by applying learnings to the designs.

The 2022 design update also included a reduction of batter angle within the affected domain, from approximately 80° to 60° (Figure 3 f on the timeline). This was intended to reduce the volume of bench-scale failures and allow for the failures to break back to foliation in a more controlled manner. The intervention produced positive operational results, with a significant reduction in the scale of bench failures. However, these design changes created an important mine-planning consequence: flattening the inter-ramp slope angle and reducing the batter angle require additional space in the pit. Where this space is not available, flatter slope designs can increase stripping, sterilise or trap ore behind the revised slope geometry. In this specific case, an important advantage was that the ramp systems were located on the weak western wall of Zone 1 and these ramps could be repositioned towards the northern and eastern parts of the pit, allowing the space previously occupied by the western wall ramp system to be used to accommodate a flatter design. This flexibility reduced the amount of ore lost because of design changes. However, some of the ore remained trapped at the base of the stepped-out area. If the original design had been more aggressive, or if the ramp system could not have been relocated, the required slope flattening would have resulted in greater ore loss. This case therefore demonstrates that late recognition of structural controls can directly affect recoverable value by forcing changes to slope geometry, ramp configuration, stripping requirements and ore recovery.

DISCUSSION

This case study demonstrates that structural uncertainty has a cost beyond investigation and redesign. The larger cost is the loss of design flexibility. Once mining has advanced, the ability to flatten slopes to relocate ramps, revise push-backs, or preserve ore recover becomes increasingly constrained. In the Zone 1 western wall, late recognition of foliation-controlled instability required a reduction in inter-ramp slope angle from approximately 56° to approximately 36°, and a reduction of batter angle from approximately 80° to 60° in the affected domain. These design changes improved slope performance and significantly reduced the scale of bench failures, but it also required additional space within the pit.

The operational impact was partially mitigated because the ramp systems located on the weak western wall could be repositioned toward the northern and eastern parts of the pit. This created the space required to accommodate the flatter design. However, some ore remains trapped at the base of the step-out area. The case therefore shows that the value loss was not caused by the flat slope itself, but by the late recognition of structural conditions that required the slope to be flattened after mining is already advanced.

The late recognition of structures affecting the Husab Mine Zone 1 pit resource has an important implication for reserve confidence. A reserve has practical value only if the slope geometry required to access it allows it to be mined safely and economically. A well-defined grade model may support reserve conversion but, if the structural controls on the axis are poorly constrained, part of that reserve may later become too technically constrained, delayed, or sterilised . In structurally complex open pits, recoverable value is controlled not only by grade, tonnage, price, and cost, but also by the orientation, persistent strength, and continuity of the rock mass fabric.

Early structural and rock mass characterization will not remove all geological uncertainty. Mining will always require reconciliation through pit mapping, monitoring, back analysis, and model updates. However, earlier data improves the timing of key design decisions. If adverse foliation domains, weak rock mass zones, persistent shears, and structurally controlled slope sectors are identified before pit optimisation and pushback designs are finalized, the mine has more options to adjust slope sectors, ramp positions, pushback geometries, and ore recovery strategies. Therefore, the value of early structural data lies not only in improved prediction but also in preservation of design optionality.

The case of the Husab Mine Zone 1 pit indicates that structural and rock mass data should not be treated as late-stage geotechnical inputs in structurally complex mining areas. They should be captured progressively from the resource definition stage and integrated into the design workflows. Selected resource holes can be used to collect:

- Oriented structural data

- Televiewer information
- Sonic logs
- Geotechnical drillcore
- And early hydrogeological indicators

The data should be incorporated into structural domains, geotechnical domains, pit optimisation assumptions, slope angle sensitivity cases and LOM planning. Structural data only protects value when it changes the design decisions.

CONCLUSIONS

This paper has argued that mine design cannot be driven by grade alone. Grade, tonnage, strip ratio, and economic assumptions define the opportunity, but structural geology and rock mass characteristics determine whether the opportunity can be safely and economically recovered. The conventional resource to reserve workflow is effective at progressively de-risking the ore body, but it does not always de-risk the rock mass at the same rate, producing a timing mismatch in which the ability to influence the mine design is highest precisely when structural knowledge is lowest.

The Husab case study demonstrates the consequence of this mismatch. Slope designs founded on sparse early geotechnical data were overtaken by structurally controlled failures; the corrective characterizations - in-fill drilling, RC drillholes with ATV and OTV surveys, and later diamond drilling - only arrived after mining had exposed the controlling foliation fabric. The resulting design changes produced positive operational results by reducing the scale of bench failures and improving the slope performance. However, the revised design also required additional space within the pit. Although ramp reallocation helped accommodate the flatter slope geometry, some ore was trapped at the base of the stepped-out area. The lesson is not that conservative designs destroy value, but that recognising the need for it late does.

Reserve confidence therefore cannot be separated from geotechnical confidence. In structurally complex open pits, the orientation, persistence, condition, rock mass conditions, and continuity of fault shears and foliation within a weak rock mass domain must be considered before optimisation and pushback designs are fixed. Early structural and rock mass characterization will not eliminate uncertainty and will always require reconciliation through pit mapping, monitoring, back analysis, and design updates as mining progresses, but it preserves the design optionality and allows slope geometry, ramp placement, pushback design, and ore recovery to be considered together. Structural geology and rock mass characteristics should be treated as first-order inputs into resource modelling, pit optimization, slope design, and life-of-mine planning.

CREDIT AUTHORSHIP CONTRIBUTION STATEMENT

G. Ockhuizen -Writing – review & editing, Writing – original draft, conceptualisation, Visualization, Investigation, Data curation; **R.Gibson** Supervision. Writing – review & editing; **S. Maclennan** Supervision, Writing – review & editing; **A. Mungunda** Writing – review & editing, validation; **I. Simataa** Resources, validation **Z. Huai Feng** Resources, validation

ACKNOWLEDGEMENTS

The authors gratefully acknowledge the management of Swakop Uranium for their support in enabling the preparation and submission of this paper. The authors further acknowledge the author's university supervisors for their guidance, constructive review, and academic support during the development of the manuscript. The contributions, technical input, and collaboration of the co-authors are also sincerely appreciated.

REFERENCES

Balideh, S., Hilchey, A., Gilma, T., & Kruse, S. (2023). What happened to the structural model? A review of current open pit design practices and the development of structural models. *SSIM 2023: Third International Slope Stability in Mining Conference*, 409–420. https://doi.org/10.36487/ACG_repo/2335_25

Deere, D. U., Hendron, A. J., Patton, F. D., & Cording, E. J. (1967). Design of surface and near-surface construction in rock. *American Institute of Mining, Metallurgical and Petroleum Engineers, Failure and Breakage of Rock: Proceedings of the 8th US Symposium on Rock Mechanics*, 237–302.

Dunn, M., & Basson, F. (2011). Geotechnical data – a strategic or tactical issue? *Proceedings of the Fourth International Seminar on Strategic versus Tactical Approaches in Mining*, 21–30. https://doi.org/10.36487/ACG_rep/1108_03_Dunn

Goscombe, B., Foster, D. A., Kelsey, D., Wade, B., Gray, D., Mulrooney, L., Jiang, P., Haseler, M., & Marsellos, A. (2022). Episodic intra-continental reactivation during collapse of a collisional orogen: The Damara Belt, Namibia. *Gondwana Research*, *109*, 285–375. https://doi.org/10.1016/j.gr.2022.05.003

Gray Hubbard, A., & Huber, J. (2025). Copper Mountain Mine North Pit stabilisation: Observational approach. *SSIM 2025: Fourth International Slope Stability in Mining Conference*, 1–14. https://doi.org/10.36487/ACG_repo/2535_20

Hadjigeorgiou, J. (2012). *Where do the data come from?* 259–277. https://doi.org/10.36487/ACG_rep/1201_19_hadjigeorgiou

ISRM. (1978). Suggested methods for the quantitative description of discontinuities in rock masses. *International Journal of Rock Mechanics and Mining Sciences & Geomechanics Abstracts*, *15*(6), 319–368. https://doi.org/10.1016/0148-9062(78)91472-9

JORC. (2012). *Australasian Code for Reporting of Exploration Results, Mineral Resources and Ore Reserves (The JORC Code)*. AusIMM Publications Department. http://www.jorc.org

Longridge, L. (2012). *Tectonothermal Evolution of the southwestern Central Zone, Damara Belt, Namibia* [PHD]. University of the Witwatersrand.

Longridge, L., Gibson, R. L., & Kinnaird, J. A. (2009). *Dome formation mechanisms in the southwestern Central Zone of the Damara Orogen, Namibia*. *29*, 440–444.

More O'Ferrall, G., & Simbile, N. (2020). Addressing pit wall instabilities in Africa's largest open pit copper mine. *Proceedings of the 2020 International Symposium on Slope Stability in Open Pit Mining and Civil Engineering*, 1507–1520. https://doi.org/10.36487/ACG_repo/2025_104

Ockhuizen, G., Armstrong, R., Maclennan, S., & Yang, X. L. (2025). Integrating Monitoring Technologies to Understand Slope Deformation in Open-Pit Mines: A Case Study from Swakop Uranium Mine. *Pioneering Progress: The Future of Rock Engineering*, 161–178.

Ockhuizen, G., Maduray, C., & Armstrong, R. (2024, April 14). The importance of geological understanding in the development of a geotechnical model and its impact on slope design. *Proceedings of the 2024 International Slope Stability Conference*. International slope stability conference.

Read, J., & Stacey, P. (Eds). (2011). *Guidelines for open pit slope design* (Reprint. with corr). CSIRO Publications.

Seequent Limited. (2026). *Leapfrog Geo* (Version 2026.1.2) [Computer software]. Seequent Limited. https://www.seequent.com/products-solutions/leapfrog-geo/

Steffen, O. K. H. (1997). *Planning of open pit mines on a risk basis.*

The South African Code for the Reporting of Exploration Results, Mineral Resources and Mineral Reserves (The SAMREC Code) (2016th edn). (2016). [Resource Standard]. www.samcode.co.za

Weir, F., Gazi, J., & Duran, A. (2025). To topple or not to topple: Managing failures at a case study site. *SSIM 2025: Fourth International Slope Stability in Mining Conference*, 1–13. https://doi.org/10.36487/ACG_repo/2535_19

Grantham Ockhuizen
Superintendent: Geotechnical
CGNPC Swakop Uranium

Grantham Ockhuizen is a highly experienced Engineering Geologist with 17 years in the mining industry. Professionally registered with SACNASP, he serves as Superintendent - Geotechnical at Husab Mine, Namibia, where he leads the geotechnical team in managing operational risks, slope design, and executing monitoring programs aligned with medium- and long-term mine plans. His role includes the continuous improvement of departmental systems to enhance efficiency and effectiveness in support of production targets. He supports operations and projects by implementing best-practice geotechnical standards in mapping, logging, structural analysis, groundwater assessment, and slope stability interpretation.

Beyond his operational responsibilities, Grantham served as Chairman of the SAIMM Namibian branch from 2013 to 2017 and remains an active affiliate member, demonstrating his strong commitment to professional excellence and industry advancement. Grantham is currently doing post graduate studies focused on structural complexities and deformation mechanisms in large open-pit mines, with research centred on the Husab Mine and the broader Damara Orogen at the School of Geosciences, University of the Witwatersrand.